Disruption of p54nrb's gene regulatory function by caspase-2 exhibits a multifaceted role in tumor cell death susceptibility

Dissertation

zur Erlangung des Doktorgrades

der Naturwissenschaften

Vorgelegt beim Fachbereich 14 Biochemie, Chemie und Pharmazie

der Johann Wolfgang Goethe-Universität

in Frankfurt am Main

von

Madeleine Eichler

aus Frankfurt am Main

Frankfurt am Main

2023

D30

Vom Fachbereich 14 Biochemie, Chemie und Pharmazie

der Johann Wolfgang Goethe-Universität

als Dissertation angenommen.

Dekan:	Prof. Dr. Clemens Glaubitz	
Gutachter:	Erstgutachter:	Prof. Dr. Volker Dötsch
	Zweitgutachter:	Prof. Dr. Josef M. Pfeilschifter
Projektbetreuung:	Dr. Gergely Imre	
Prüfungskommission:	Vorsitz:	Prof. Dr. Dieter Steinhilber
	Protokoll:	Prof. Dr. Eugen Proschak
Datum der Disputation:	23.06.2023	

List of Contents

List of Figures

List of Tables

List of Abbreviations

Abbreviation	Definition
AKT/PKB	Protein kinase B
Apaf-1	Apoptosis protease activating factor-1 protein
Apo3L/TNFSF12	Apo 3 ligand/Tumor necrosis factor ligand superfamily member 12
APS	Ammonium persulfate
ATP	Adenosine triphosphate
BAK	Bcl-2 homologous antagonist/killer 1 protein
BAX	Bcl-2 associated X protein
Bcl-2	B-cell lymphoma 2
Bcl-xL	B-cell lymphoma extra large
BH3	Bcl-2 homology domain 3
BH3-only	Bcl-2 homology 3-only protein
BH4	Bcl-2 homology domain 4
Bid	BH3 interacting domain death agonist protein
bp	Base pairs
BSA	Bovine serum albumin
$CaCl_2$	Calcium chloride
CARD	Caspase activation and recruitment domain
CCND1	Cyclin D1
CD95L/FasL	Cluster of differentiation 95 ligand/Fas ligand
CDK4	Cyclin dependent kinase 4
CDK6	Cyclin dependent kinase 6
CDKN2A	Cyclin-dependent kinase inhibitor 2 A
CED-3	*Caenorhabditis elegans* death gene-3 protein
c_{end}	Final concentration
cFLIP	Cellulare FLICE -like inhibitory protein
CHAPS	3-[3-Cholamidopropyl]-dimethylammonio]-1-propane-sulfonate
ChIP	Chromatin immunoprecipitation
CO_2	Carbon dioxide
CRISPR	Clustered regularly interspaced short palindromic repeats
DBD	DNA binding site
DBHS	Drosophila behaviour/human splicing
DD	Death domain
dd-H_2O	Double distilled water
DDT	Dithiothreitol
DED	Death effector domain
DEPC	Diethyl pyrocarbonate
DIA	Data independent acquisition
DISC	Death inducing singling complex
DMSO	Dimethylsulfoxide
DNA	Desoxyribonucleic acid
dNTPs	Desoxynucleotidetriphosphates
Doxo	Doxorubicin
DPBS	Dulbecco's phosphate buffered saline
DPI-ELISA	DNA-protein-interaction enzyme-linked immunosorbent assay
DR	Death receptor

DTT	1,4-Dithiothreitol
ECL	Enhanced chemiluminescence
EDTA	Ethylenediaminetetraacetic acid
EGTA	Ethylene glycol-bis (β-aminoethyl ether)-N,N,N',N'-tetra acetic acid
EMSA	Electrophoretic mobility shift
EMT	Epithelial-mesenchymal transition
ER	Endoplasmic reticulum
Eto	Etoposide
FADD	Fas-associated protein with death domain protein
FASP	Filter-aided sample preparation
FBS	Fetal bovine serum
FDR	False discovery rate
FLICE	FADD-like ICE / Caspase-8
GEMM	Genetically engineered mouse model
HCl	Hydrogen chloride
HEPES	4-(2-hydroxyethyl)-1-piperazineethanesulfonic acid
HRP	Horseradish peroxidase
IAA	Iodoacetamide
IAP	Inhibitor of apoptosis protein
ICAD	Inhibitor of caspase-activated DNase
ICE	Interleukin-1 beta-converting enzyme
ICH-1	ICE and CED-3 homolog 1
IL-18	Interleukin 18
IL-1β	Interleukin-1 beta
IMS	Ion mobility separation
IPE	IAP proximal enhancer
KCl	Potassium chloride
kDa	Kilodalton
LC-MS	Liquid chromatography–mass spectrometry
LDHA	Lactate dehydrogenase A
Mcl-1	Induced myeloid leukemia cell differentiation protein Mcl-1
MDM2	Mouse double minute 2 homolog/ E3 ubiquitin-protein ligase
$MgCl_2$	Magnesium chloride
miRNA	Micro RNA
MMP2	Matrix metallo proteinase 2
MOI	Multiplicity of infection
MOMP	Mitochondrial outer membrane permeabilisation
MPT	Mitochondrial permeability transition
mRNA	Messenger ribonucleic acid
mTOR	Mammalian target of rapamycin
Na_3VO_4	Sodium orthovanadate
NaCl	Sodium chloride
NaF	Sodium fluoride
NaOAc	Sodium acetate
NEDD-2	Neuronally expressed developmentally downregulated gene 2
NETs	Neutrophil extracellular traps
NF-κB	Nuclear factor kappa-light-chain-enhancer of activated B-cells
NH_4HCO_3	Ammonium bicarbonate
NLS	Nuclear localisation signal

Noc	Nocodazole
NonA	Protein no-on-transient A
NonO	Non POU (Pituitary-specific factor, octamer transcription factor, neural un-coordinated-86) domain-containing octamer-binding protein
NOPS	NonA (protein no-on-transient A)/paraspeckle domain
NP40	Nonyl phenoxypolyethoxylethanol
NQO1	NAD(P)H: quinone oxidoreductase 1
p54nrb	54 kDa nuclear RNA-binding protein
PAGE	Polyacrylamide gel electrophoresis
PARP	Poly (ADP-Ribose)-Polymerase 1 protein
PCD	Programmed cell death
PCR	Polymerase chain reaction
PEG 800	Polyethylenglycol 800
Pen-Strep	Penicillin/Streptomycin
PI	Propidium-iodide
PIDD	p53 inducible protein along with a death domain
PIM	Protease-inhibitor-cocktail/mix
PLGS	Protein Lynx Global Server
PSPC1/PSP1	Paraspeckle protein component 1 protein
Puro	Puromycin
RAIDD	Receptor-interacting protein-associated ICH-1 homologous with a death domain
RIP	Ribonucleoprotein immunoprecipitation
RIP1/RIPK1	Receptor-interacting serine/threonine-protein kinase 1
RIP3/RIPK3	Receptor interacting serine/threonine protein kinase 3
ROS	Reactive oxygen species
rpm	Rounds per minute
RRM	RNA recognition motif
SDS	Sodium dodecyl sulfate
SFPQ/PSF	Splicing factor proline/glutamine rich protein
sgRNA	Subgenomic messenger ribonucleic acid
shRNA	Small hairpin ribonucleic acid
siRNA	Small interfering ribonucleic acid
SIRT6	Sirtuin 6
Smac	Second mitochondria derived activator of caspases/direct IAP binding protein with low PI
STS	Staurosporine
tBid	Truncated Bid
TEMED	Tetramethylethylenediamine
TFA	Trifluoroacetic acid
TL1A/TNFSF15	TNF-like 1A/Tumor necrosis factor superfamily member 15
TNF	Tumor necrosis factor
TNFR	Tumor necrosis factor receptor
TPD52	Tumor protein D52
TRADD	Tumor necrosis factor receptor type 1-associated death domain protein
TRAF2	TNF receptor-associated factor 2
TRAIL/Apo2L	TNF-related apoptosis-inducing ligand/Apoptosis ligand 2

Tris	Tris-hydroxymethyl-aminomethane
WGA	Wheat germ agglutinin
XIAP	X-linked inhibitor of apoptosis protein
z-VAD-fmk	Carbobenzoxy-valyl-alanyl-aspartyl-[O-methyl]- fluoromethylketone
z-VDVAD-fmk	Methyl (3S)-5-fluoro-3-[[(2S)-2-[[(2S)-2-[[(2S)-4-methoxy-2-[[(2S)-3-methyl-2-(phenyl methoxy carbonyl amino) butanoyl] amino]-4-oxobutanoyl] amino]-3-methylbutanoyl] amino] propanoyl] amino]-4-oxopentanoate

1 Introduction

1.1 Programmed cell death

In multicellular organisms, cell death is the result of the natural process to remove unrequired, injured, or malfunctioning cells, which will be in turn replaced by new ones. Cell death can occur in non-physiological processes, passively caused by external factors, such as trauma or infection, which exceed the cell's repair capacity. This form of cell death is called necrosis and is characterised by swelling of the organelles and rupture of the plasma membrane (Kerr et al., 1972; Walker et al., 1988; Chen et al., 2018).

In contrast to necrosis exists another form of cell death, termed programmed cell death (PCD). PCD, also called cell suicide, takes place upon regulated processes inside of a cell leading to the cell's self-determined death. PCD plays an essential role in embryonic development (Saunders, 1966) and in the elimination of defective cells to maintain tissue homeostasis (Kerr et al., 1972). Additionally, PCD is an indispensable mechanism for the development of the nervous system, as 50 % of the developing neurons get removed by PCD (Dekkers et al., 2013), and it also has a role in protection from infections (Perez et al., 1998; Aachoui et al., 2013). A malfunctioning regulation of PCD is associated with a variety of pathological conditions. Hyperregulation can cause neurodegenerative diseases, such as Alzheimer's and Parkinson's disease, whereas insufficient PCD can lead to cancer and autoimmune disorders (Fadeel et al., 1999; Vigneswara & Ahmed, 2020).

Initially, apoptosis (Chapter 1.2) was discussed as the only cell death modality of PCD (Kerr et al., 1972). However, in recent years, the number of newly discovered PCD mechanisms increased, of which some are still not sufficiently studied. Therefore, their classification is still under debate. Additional ambiguity is caused by various crosstalks between different PCD pathways (Vanden Berghe et al., 2015). Here, one of the most recent classification systems, based on Yan et al. (2020), is briefly represented (Figure 1). This system majorly differentiates between apoptotic PCD, which is dependent on the enzyme family called caspases, and non-apoptotic PCD, which shares some hallmarks of apoptosis or necrosis, but is regulated independently of caspases, hence it is also termed "apoptosis- or necrosis-like" (Leist & Jaattela, 2001; Kroemer & Martin, 2005).

Several mechanisms belong to the class of non-apoptotic PCD, which can be subgrouped based on their signal-dependency and molecular mechanisms. These include necroptosis, which is a

form of programmed necrosis, hence a pro inflammatory cell death. This RIPK1/3-dependent cell death signalling pathway is known to act as a backup pathway, when caspases are inhibited, as for example during viral infections (Holler et al., 2000; Chan et al., 2003; Degterev et al., 2005; Feng et al., 2007; Cho et al., 2009; Nailwal & Chan, 2019).

Another group of non-apoptotic PCD is linked to the function of the immune system. Member of this category is the cell death pathway termed NETosis, a process, in which neutrophils build up NETs (Neutrophil extracellular traps) in a ROS (Reactive oxygen species) dependent manner within the cell, followed by breakage of the membrane (Brinkmann et al., 2004; Fuchs et al., 2007). Whereas the other member of this group, the pyroptosis pathway, is characterised by the formation of the inflammasome complex, that leads to the activation of inflammatory caspases and gasdermin-D mediated pore formation (Cookson & Brennan, 2001; Shi et al., 2017).

Another group is the iron-linked non-apoptotic PCD, termed ferroptosis, which is initiated upon an iron-dependent accumulation of oxidised lipids (Dixon et al., 2012).

Also discussed is a non-apoptotic PCD group, with a characteristic link to mitochondria, like the cell death termed parthanatos, which is defined by PARP1 hyperactivation (David et al., 2009). Whereas, MPT-driven regulated necrosis, also called mitoptosis, takes place through permeabilisation of the mitochondrial membrane (Skulachev, 1999; Chaabane et al., 2013).

Another group of non-apoptotic PCD is phenotypically associated with vacuole formation. Among them, cell death termed paraptosis, which is featured by cytoplasmic vacuolation (Sperandio et al., 2000). But also, the pathway of methuosis, which is characterised by a massive accumulation of macropinosome derived vacuoles (Chi et al., 1999; Maltese & Overmeyer, 2014). Entotic cell death is an actomyosin-dependent cell-in-cell internalisation (Entosis) via lysosomes (Overholtzer et al., 2007). But also, autophagy, which is a cathepsin-dependent self-cannibalisation mechanism and mainly important to dispose cellular debris and misfolded proteins through double-membrane vesicles, called autophagosomes, is a form of PCD (Nikoletopoulou et al., 2013; Tiwari et al., 2014). Besides a cytoprotective function, autophagy can also serve pro-death functions during normal development (Mizushima & Levine, 2010).

The class of apoptotic PCD consists of apoptosis, which is further described in chapter 1.2, and cell death termed anoikis. Anoikis is a special version of apoptosis and takes place when adhesive cells lose the cell-matrix interaction. The activating mechanism of anoikis is still unknown (Frisch & Francis, 1994).

As previously mentioned, the general aim of PCD is the clearance of malfunctioning cells without harming surrounding tissue and its dysregulation is the cause of many pathologic conditions. Therefore, it is not surprising that the research on PCD mechanisms, which can be utilised for clinical therapies is steadily increasing, as further described in chapter 1.2.1.

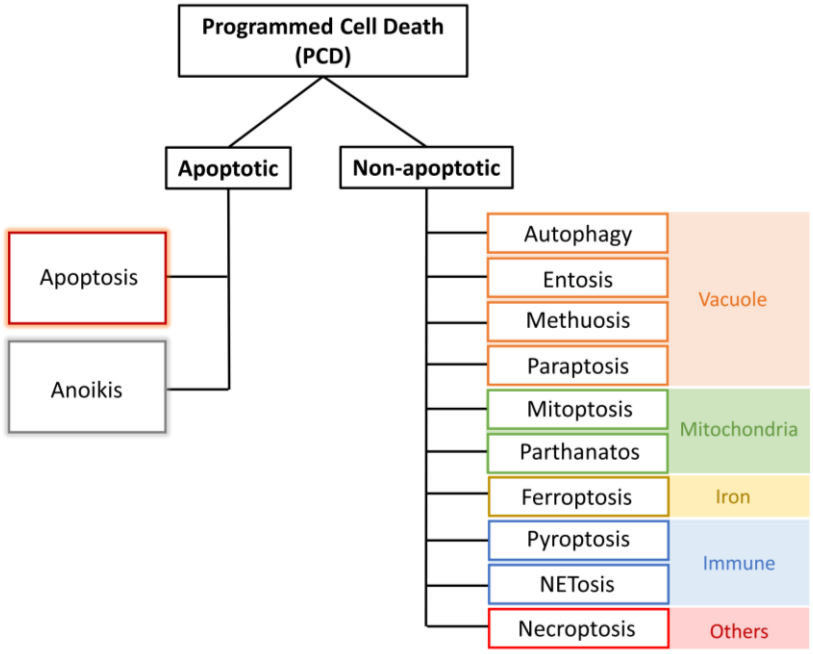

Figure 1. Classification of programmed cell death.
Categorisation of programmed cell death (PCD) pathways, based on morphological properties, signal-dependency, and molecular mechanisms (Maniam & Maniam, 2021).

1.2 Apoptosis

Apoptosis is an evolutionary highly conserved form of PCD, which occurs in multicellular organisms. Morphologically it is characterised by shrinkage of the cell, DNA fragmentation, nuclear fragmentation, and membrane blebbing (Kerr et al., 1972; Hacker, 2000). In contrast to necrosis, apoptosis leads to the formation of cell fragments, called apoptotic bodies, which are presenting phosphatidylserine on their outer plasma membrane (Verhoven et al., 1995), a signal for initiation of phagocytosis. This helps to avoid harming of surrounding cells with the cell content as through lysis, which would cause inflammation as it does under necrosis.

Activation of apoptosis can be mediated via two pathways, called the extrinsic or death receptor-dependent pathway and the intrinsic or mitochondria-dependent pathway (Figure 2).

The intrinsic pathway is triggered by intracellular stress signals, like hypoxia, free radicals, high cytosolic concentrations of calcium, toxins, DNA damage, and deficiency of growth factors (Orrenius et al., 2003; Roos & Kaina, 2006; Elmore, 2007). All these stimuli can lead to the activation of Bcl-2 associated X protein (BAX) and Bcl-2 homologous antagonist/killer 1 proteins (BAK) by Bcl-2 homology 3-only proteins (BH3-only), which subsequently causes mitochondrial outer membrane permeability (MOMP) and thereby the release of cytochrome-C from the intermembrane space of mitochondria (Lindsten et al., 2000; Wei et al., 2001; Dadsena et al., 2021). Cytochrome-C binds apoptosis protease activating factor-1 (Apaf-1), ATP, and pro-caspase-9, thus creating a complex called apoptosome, which converts the initiator caspase-9 into its active state (P. Li et al., 1997; Zou et al., 1999; Green & Llambi, 2015).

The extrinsic pathway is stimulated by external death ligands binding to death receptors (DRs) on the cell surface. The DRs contain an extracellular cysteine-rich subdomain for specific recognition of their corresponding ligands. To date, six DRs are known: DR1 (TNFR1/CD120a/p55) binds TNF and lymphotoxin alpha, DR2 (alias Fas/CD95/Apo1) binds CD95L/FasL, DR3 (alias Apo3/TRAMP/LARD) binds Apo3L and TL1A, DR4 (alias Apo2/TRAILR1) and DR5 (alias TRAILR2/TRICK2/KILLER) bind TRAIL/Apo2L, whereas DR6 is not yet well characterised (Mahmood & Shukla, 2010). The DRs bear a homologous intracellular cysteine-rich domain termed death domain (DD), relevant for transmitting the death signal via protein-protein interaction (Tartaglia et al., 1993; Nagata, 1997). The proteins which bind intracellularly to the receptors carry a DD themselves, like Fas-associated protein with death domain (FADD) (Grimm et al., 1996; Chaudhary et al., 1997) and tumor necrosis factor receptor type 1-associated death domain protein (TRADD) (Hsu et al., 1995). Their recruitment further leads to the binding of pro-caspase-8 or -10 which results in the formation of the so called death-inducing signalling complex (DISC) and ultimately to the activation of initiator caspase-8 or -10 (Kischkel et al., 1995; Kischkel et al., 2001).

Following the activation of initiator caspases, effector caspase-3, -6, or -7 get cleaved by the active initiator caspases and thereby get activated. At this point, the intrinsic and extrinsic pathway converge. Active effector caspases proteolytically cleave specific intracellular proteins, which leads to a gradual decomposition of the cell, determining its death. A prominent substrate of effector caspases is Poly (ADP-Ribose)-Polymerase 1 (PARP) (Kaufmann et al., 1993) or the inhibitor of caspase-activated DNAse (ICAD) (Sakahira et al., 1998), each relevant for DNA cleavage. Both apoptotic pathways can also act simultaneously. For example, caspase-8 can

additionally process Bid (BH3 interacting domain death agonist) to t-Bid, which subsequently activates the intrinsic pathway through initiating MOMP (Plati et al., 2008; Kiraz et al., 2016).

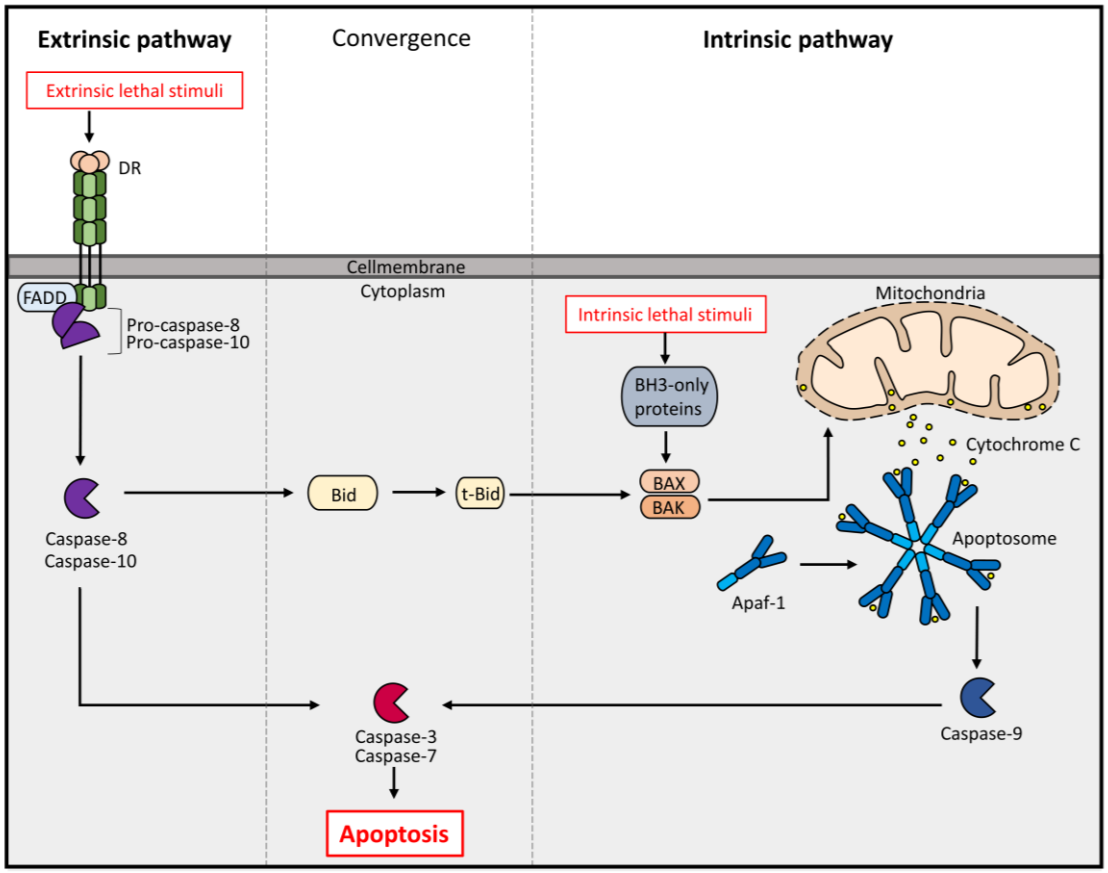

Figure 2. Schematic illustration of the apoptotic pathways.
The extrinsic pathway starts with an external death inducing ligand, which binds to the death receptor (DR). Recruitment of Fas-associated protein with death domain (FADD) and pro-caspase-8/-10 leads to the formation of the death inducing signalling complex (DISC) and the subsequent caspase-8/-10 activation. The Intrinsic pathway follows BH3-only protein (Bcl-2 homology 3 only proteins) and BAX/BAK (Bcl-2 associated X protein/Bcl-2 homologous antagonist/killer 1) activation. These proteins are inducing mitochondrial outer membrane permeabilisation (MOMP), resulting in cytochrome-C release. Cytochrome-C, apoptosis protease activating factor-1 (Apaf-1), and pro-caspase-9 form the apoptosome resulting in caspase-9 activation. Active initiator caspase-8/-10/-9 can eventually converge the pathways by activating caspase-3/-7, which in turn cleave apoptotic substrates, resulting in the decomposition of the cell. The extrinsic and intrinsic pathways are also connectable via the BH3 interacting domain death agonist (Bid), which can be cleaved by caspase-8/-10, leading to BAX/BAK activation.

1.2.1 Therapeutic utilisation of the apoptotic machinery in cancer treatment

As previously mentioned, malfunctioning PCD causes pathological conditions. Dysregulation of apoptosis often leads to uncontrollable proliferation and insufficient cell death, which can subsequently result in cancer development. Many oncologic cases are described, where

components of the apoptotic pathway are affected. Therefore, targeting apoptotic proteins is of great interest to restore the defects in the apoptotic pathway (Figure 3). However, harnessing apoptotic processes for therapy needs caution, since on the one side healthy surrounding tissue should not be collaterally damaged, but on the other side, an inefficient treatment can lead to a rapid development of resistant cells (Fadeel et al., 1999). In order to find new targets, to optimise current treatments, and to overcome tumor resistance, additional research is required.

Hereinafter, a simplified list of apoptotic dysregulations in cancer and the equivalent therapeutic options, which are currently in pre-clinical or clinical trials, are briefly described.

For addressing the extrinsic, receptor-inducing apoptotic pathway, one of the therapeutic strategies is to target the tumor marker cFLIP, which is the negative regulator of caspase-8 (Irmler et al., 1997). Since cFLIP is overexpressed in many different tumor types, downregulation of cFLIP with metabolic inhibitors, as well as enhancing caspase-8 activity with interferon are feasible strategies to activate receptor-induced apoptosis in tumors (Fulda & Debatin, 2002; Shirley & Micheau, 2013).

Another death receptor-inducing therapeutical strategy is the usage of the ligand TRAIL to induce apoptotic signalling. However, since TRAIL shows a preferential effect in tumor cells, soluble recombinant TRAIL derivates were developed (Amarante-Mendes & Griffith, 2015). Also promising is CaspPro, a small molecule, which supports the activation of caspase-8 upon TRAIL stimulation (Bucur et al., 2015). However, therapeutics inducing TRAIL mediated apoptosis, which have passed the pre-clinical phase, did not prove a good clinical efficacy so far (Carneiro & El-Deiry, 2020).

As for the intrinsic apoptotic pathway, several drugs, which inhibit anti-apoptotic proteins, like Bcl-2, Bcl-xL, and Mcl-1, are under development and in clinical trials. Such inhibitors target for example the BH3 or BH4 domain of the Bcl-proteins by mimicking pro-apoptotic BH3-only proteins (Oltersdorf et al., 2005; Kang & Reynolds, 2009; Albershardt et al., 2011; Carneiro & El-Deiry, 2020).

IAPs (Inhibitor of apoptosis protein) are at high level in various cancers and function as the intrinsic inhibitors of caspases. For therapeutical downregulation of IAPs, siRNA and antisense oligonucleotides are in development and pre-clinical trials. Their administration in combination with chemotherapy or radiation showed a sensitisation towards apoptosis in some therapy resistant tumors (Sasaki et al., 2000; Amantana et al., 2004; Wong, 2011; Tekedereli et al., 2013; Pistritto et al., 2016; Carneiro & El-Deiry, 2020). For example, targeting the IAP protein survivin,

which directly binds and suppresses caspase-3, -7, and -9 activity is of great interest. Effects could be shown by the administration of survivin anti-sense, siRNA (Wong, 2011), and a small molecule suppressant (Nakahara et al., 2007).

The protein Smac/DIABLO (second mitochondria derived activator of caspases/direct IAP binding protein with low PI) antagonises the activity of IAPs and high level of Smac in cancer patients is associated with longer overall survival. Some mimetics of Smac were shown to induce apoptosis and have a sensitising effect in combination with cytotoxic treatment, by blocking the IAP mediated inhibition of caspases (Sun et al., 2010; Fulda, 2015; Maniam & Maniam, 2021).

Another promising option is a direct intervention on effector caspase level by caspase-3 gene-therapy or small caspase activating molecules, which could show enhanced apoptosis, drug sensitivity, and reduced tumor growth (Philchenkov et al., 2004; Wong, 2011).

The tumor suppressor and transcription factor p53 is the most studied protein involved in cell cycle arrest and apoptosis (Vousden & Lane, 2007). Wildtype p53 is activated upon genotoxic stress and does transcriptionally regulate the level of TNFR, pro-survival proteins, and pro-apoptotic proteins of the Bcl-2 family. In 50 % of tumor types p53 is mutated, deleted, or affected by other regulatory proteins, making p53 a challenging target for therapy (Pistritto et al., 2016). Recently, a novel compound named APR-246, which directly interacts and thereby restores the p53 activity, entered the clinical phase (Q. Zhang et al., 2018). Besides other approaches for p53 restoration, as by immuno- and gene-therapy (Wong, 2011), there are ongoing clinical trials to specifically address the tumor suppressor function of p53 indirectly by targeting its antagonist MDM2 (Carneiro & El-Deiry, 2020).

The E3 ligase MDM2 binds to p53 and thereby initiates its proteasomal degradation. Many tumor types have a high level of MDM2 (Momand et al., 2000). It could be demonstrated that inhibition of MDM2 leads to an increased sensitivity of tumors towards apoptosis (Shangary & Wang, 2008). Furthermore, the induction of p53 activity with doxorubicin can be elevated by the administration of zinc ions, which interfere with the negative regulation of MDM2 on p53 (Garufi et al., 2015).

MicroRNAs (miRNAs) also have a significant role in the posttranscriptional regulation of many apoptosis regulating proteins. The list of apoptosis regulating miRNAs is long and covers the regulation of mRNA translation of death receptors, ligands, and Bcl-proteins. Some miRNAs regulate and are regulated by p53, and consequently are affected by p53 mutations (Lima et al., 2011; Garibaldi et al., 2016). Therefore, the number of developed synthetic miRNAs for cancer

treatment is increasing and a few have already reached clinical application status, like MRX34 and TargomiRs (Pistritto et al., 2016).

Finally, there are compounds, like the viral death effector protein apoptin, which can induce p53- and Bcl-2-independently apoptosis and shows promising effects in the induction of apoptosis, specifically in cancer cells (Rohn & Noteborn, 2004; Malla et al., 2020).

In summary, divers strategies for therapeutical cancer treatment have been discovered and are currently under optimisation (Figure 3). However, many promising therapeutical compounds do not pass the pre-clinical or the clinical stage (Mullard, 2016), which means continuous research on cell death signalling for successful cancer treatment is mandatory.

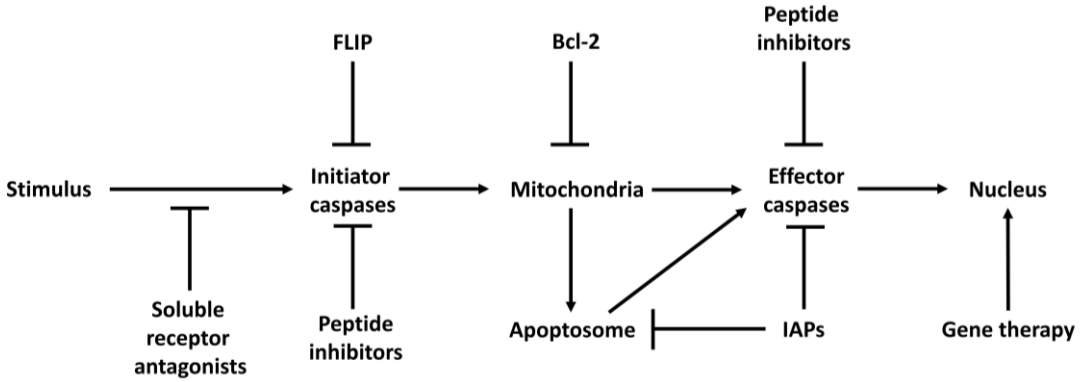

Figure 3. Strategies for therapeutical modulations of apoptosis.
Intervention options in the apoptotic pathway, based on observed dysregulations in diseases (Fadeel et al., 1999).

1.2.2 Caspases

Caspases are cysteine-dependent endoproteases, which recognise certain tetrapeptide motifs and cleave after a specific aspartic residue (Thornberry et al., 1997; Lamkanfi et al., 2002). Caspases have conserved structures in diverse organisms, and likewise their molecular mechanisms are conserved across species (Sakamaki & Satou, 2009). They take place in different cellular functions, such as initiating and executing cell death, but are also involved in the control of inflammation by processing proinflammatory mediators, like IL-1β and IL-18 (Nicholson, 1999; Martinon & Tschopp, 2007; Van Opdenbosch & Lamkanfi, 2019). Therefore, caspases are divided into three functional categories (Figure 4). Group 1 is summarised as the inflammatory caspases (Caspase-1, -4, -5, and -11 (the mouse homologue of caspase-4 and -5)). Group 2 are the initiator

caspases (Caspase-8, -9, -10) and group 3 are the effector caspases (Caspase-3, -6, -7) (Van Opdenbosch & Lamkanfi, 2019). Caspase-2, -12, and -14 are more complex in their function and therefore difficult to clearly assign to one of the mentioned groups (Figure 4). Caspase-2 will be discussed in detail in the next section (Chapter 1.3). Caspase-12 often gets phylogenetically classified as an inflammatory caspase, although its function remains unclear (Van Opdenbosch & Lamkanfi, 2019), and the deviating caspase-14 has a very particular localisation and is functionally linked to PCD in the process of cornification (Markiewicz et al., 2021).

All caspases exist first as inactive zymogens, which require activation through proteolytic processing. Initiator caspases, structurally characterised by containing a long pro-domain, like the caspase recruitment domain (CARD) or the death effector domain (DED) (Muzio et al., 1996; Hofmann et al., 1997), are processed after being recruited to an adaptor protein. The through dimerisation induced proximity leads hereby to its autocleavage (Pop & Salvesen, 2009). In contrast, effector caspases have a short pro-domain and are cleaved by active initiator caspases, which leads to their activation (Pop & Salvesen, 2009).

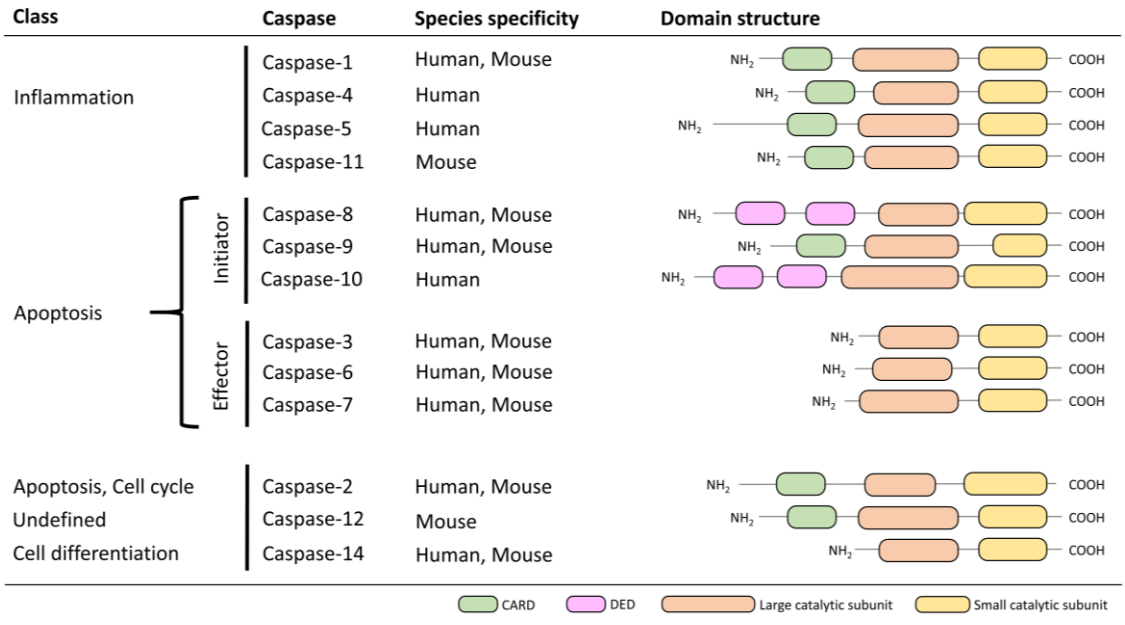

Figure 4. Structure and functional classification of mammalian caspases.
Caspase-1, -4, -5, and -11, are inflammatory caspases, caspase-8, -9, and -10 are apoptotic initiator caspases, whereas caspase-3, -6, and -7 are apoptotic effector caspases. The functional classification of caspase-2, -12, and -14 are indicated. Abbreviations: Caspase recruitment domain (CARD); death effector domain (DED); large and small catalytic subunit (Van Opdenbosch & Lamkanfi, 2019).

1.3 Caspase-2

Caspase-2 received its name by being the second mammalian caspase, which was historically characterised. Initially, caspase-2 was identified by a hybridisation screen for mouse genes that are highly expressed in neural precursors cells and was named NEDD-2 (neuronally expressed developmentally downregulated gene 2), since the mRNA level of this gene was downregulated during brain development. The human NEDD-2 homolog was observed to be genetically related to the *Caenorhabditis elegans* death gene-3 (CED-3) and the interleukin-1 beta-converting enzyme (ICE) and therefore originally has been termed ICH-1 (ICE and CED-3 homolog 1) (Kumar et al., 1994; Wang et al., 1994; Kumar et al., 1995), which later was renamed to caspase-2.

Caspase-2 is the evolutionary most conserved member of the caspases (Lamkanfi et al., 2002). Two isoforms of caspase-2 exist, due to differential splicing of the pro-caspase-2 encoding mRNA (Droin et al., 2000). Caspase-2 contains a long N-terminal pro-domain (CARD), similar to the initiator caspase-9, and C-terminally a catalytic domain consisting of a large (p19) and a small (p12) subunit (Figure 4). Unlike other caspases, caspase-2 has a nuclear localisation signal (NLS), which is responsible for its predominant localisation in the nucleus (Kumar, 2009). But caspase-2 also resides in the nucleolus (Ando et al., 2017), the Endoplasmic reticulum (ER) (Cheung et al., 2006), the mitochondria (Zhivotovsky et al., 1999), and the Golgi apparatus (Mancini et al., 2000), leading to the implication of a localisation specific function. Interestingly, caspase-2 acts also as an effector caspase since it can selectively cleave protein substrates, similar to caspase-3 and -7 (Wejda et al., 2012; Brown-Suedel & Bouchier-Hayes, 2020).

1.3.1 Activation of caspase-2

Induction of caspase-2 activation has been observed in the extrinsic, as well as in the intrinsic pathway. The experimentally best-known extrinsic inducers of caspase-2 include TNF, CD95L, and TRAIL. As for the intrinsic induction, caspase-2 activation was observed under genotoxic stress, metabolic stress, endoplasmic reticulum (ER) stress, reactive oxygen species (ROS), heat shock, and deprivation of neurotrophic factors (Vigneswara & Ahmed, 2020). Also, stimulation with the pore-forming alpha-toxin, which induces potassium efflux, led to the activation of caspase-2 (Imre et al., 2012).

Regarding the mechanistic enzyme activation, caspase-2 structurally resembles initiator caspases, which principally transform from their inactive monomeric zymogen state into the

active state by homodimerisation via their pro-domains (Butt et al., 1998). Caspase-2 also needs the proximity of two pro-caspase molecules, which induces a two-stage proteolytic cleavage process, whereby the large and small subunits are separated, and the pro-domain is removed. The cleaved fragments form a fully active heterotetramer (Baliga et al., 2004). However, linker cleavage is not essential for the catalytic activity of caspase-2, since mutated caspase-2 retains 20 % activity, even as a dimer (Baliga et al., 2004).

As previously described, initiator caspases get activated via induced proximity. The initiator caspase-9 achieves proximity by recruitment to the apoptosome complex, and caspase-8 by recruitment to the DISC complex. Caspase-2 also can be recruited to a high molecular weight activating platform, which is called PIDDosome. This complex consists of PIDD (p53 inducible protein along with a death domain) and RAIDD (receptor-interacting protein-associated ICH-1 homologous with a death domain) (Duan & Dixit, 1997; Lin et al., 2000; Read et al., 2002; Tinel & Tschopp, 2004).

On the other hand, activation of caspase-2 was also detected PIDD independently, suggesting that alternative modes of caspase-2 activation do exist (Kim et al., 2009; Manzl et al., 2009; Imre et al., 2012; Imre et al., 2017). A PIDD independent caspase-2 recruitment to TNFR1 via RAIDD, TRAF2, and RIP1 was observed and might act as an alternative and localisation dependent pathway. However, the catalytic activity of caspase-2 is not required for further signalling by this complex (Vigneswara & Ahmed, 2020). Caspase-2 activation can also occur through the receptor complexes TRAILR and CD95 DISC formation (Brown-Suedel & Bouchier-Hayes, 2020), and another PIDD independent and RAIDD mediated activation of caspase-2 was observed with the anticancer drug LBH589, which induces the intrinsic pathway (Hasegawa et al., 2011; Vigneswara & Ahmed, 2020).

Surprisingly, sole ectopic overexpression of caspase-2 leads to proximity-driven autocatalytic activation without additional stimulation (H. Li et al., 1997; Baliga et al., 2004). However, the relevance of this mechanism *in vivo* remains questionable.

Effector caspases can be activated through proteolytic transactivation by other caspases. Caspase-2 transactivation was observed to happen by caspase-3, -7, -8, and -9, whereas caspase-2 itself does not process other pro-caspases (Vigneswara & Ahmed, 2020). Activation of caspase-2 downstream of effector caspases was shown to be dispensable for cell death signalling, thus implicating that auto-processing might be the more prominent activation mode for caspase-2 (Brown-Suedel & Bouchier-Hayes, 2020). It is obvious, that more investigation is required to understand, whether the cleavage by other caspases between the subunits of

caspase-2 may serve as a mechanism of activity enhancement or is specifically related to caspase-2 isoform transactivation (Baliga et al., 2004; Vigneswara & Ahmed, 2020).

Although caspase-2 structurally resembles the initiator caspases, its known activation mechanisms differ and are context dependent. In summary, the current experimental data cannot precisely explain the physiological activation of caspase-2 (Figure 5).

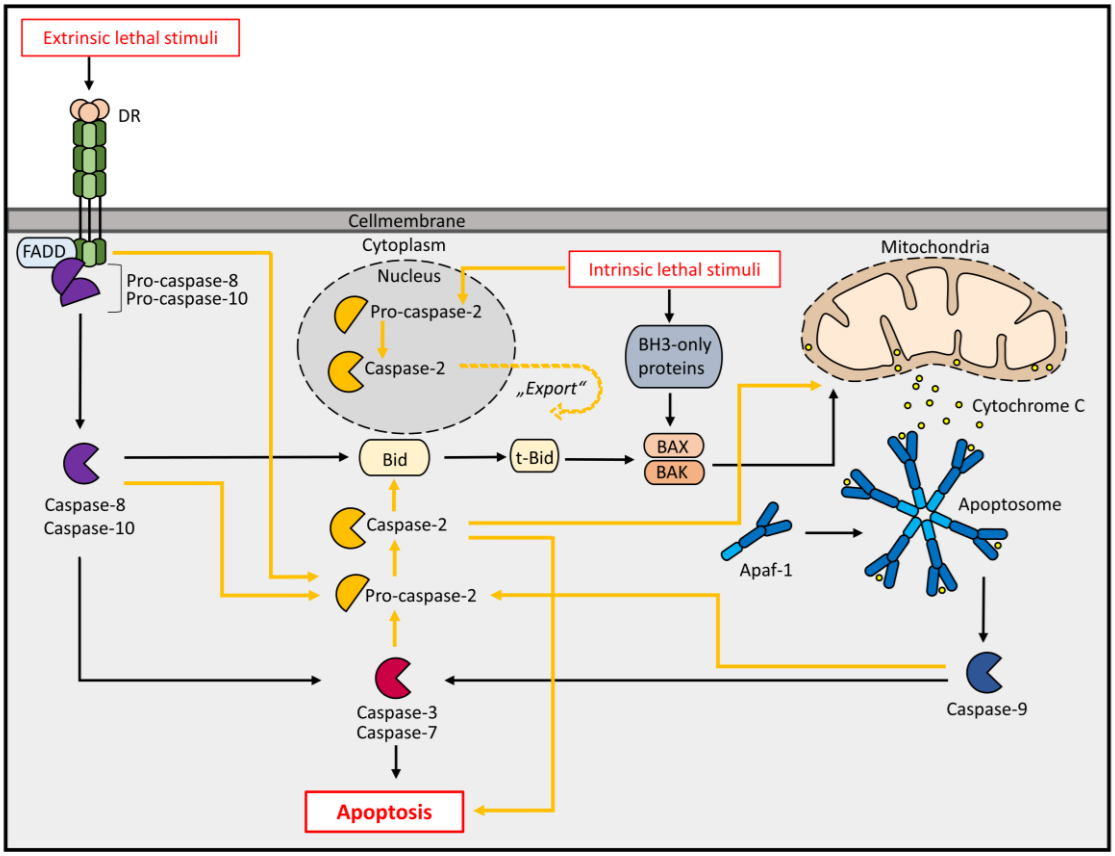

Figure 5. The enigmatic pathway of caspase-2 in apoptosis.
A schematic illustration, representing the current understanding of caspase-2 signalling, which is strongly dependent on the activating signal, the localisation of caspase-2 in the cell, and the cellular conditions. Abbreviations: Death receptor (DR), Fas-associated protein with death domain (FADD), Bcl-2 homology 3 only proteins (BH3-only proteins), Bcl-2 associated X protein (BAX), Bcl-2 homologous antagonist/killer 1 (BAK), apoptosis protease activating factor-1 (Apaf-1), and BH3 interacting domain death agonist (Bid) and its truncated version tBid.

1.3.2 Functional role and substrates of caspase-2

Initially, caspase-2 was postulated as an initiator caspase due to its structure and implicated role in apoptotic cell death, which was based on the observations of cell death induction by caspase-2 overexpression (Kumar et al., 1994). Meanwhile, many further studies have been

conducted by employing different death stimuli resulting in caspase-2 activation (Puccini, Dorstyn, et al., 2013; Vigneswara & Ahmed, 2020).

The observation that caspase-2 depletion does not generally protect from cell death undermines its unified role in apoptosis (Bouchier-Hayes & Green, 2012). Furthermore, caspase-2 knockout mice are missing a concrete phenotype, thus indicating caspase-2 as redundant (Bergeron et al., 1998). The lack of identification of caspase-2 specific substrates and the missing adequate technologies to investigate the functional role of caspase-2 resulted in caspase-3 getting into the spotlight, mainly due to its catalytic efficiency and its high abundance, whereas research on caspase-2 got impeded (Vakifahmetoglu-Norberg & Zhivotovsky, 2010; Olsson et al., 2015; Vigneswara & Ahmed, 2020). The following challenge in caspase-2 research was to confirm its role as an apoptotic initiator or as an amplifier by mediating pro-apoptotic feedback loops. Further complicating this attempt, caspase-2 activation can take place up- and downstream of effector caspases, depending on the stimulus and the investigated context (Krumschnabel et al., 2009; Vigneswara & Ahmed, 2020).

Contrary to its apparently subordinate role in apoptosis, caspase-2 shows several proofs of non-apoptotic functions. For example, the splice variants of caspase-2 can exert opposing functions. Whereas the caspase-2L isoform acts pro-apoptotic, has the caspase-2S isoform an anti-apoptotic role (Droin et al., 2000; Iwanaga et al., 2005; Han et al., 2013). Another non-apoptotic function of caspase-2 is mediated via its recruitment to the TNFR, thus conditionally leading to apoptotic or anti-apoptotic signalling via NF-κB activation, which even happens independent of caspase-2's catalytic activity (Lamkanfi et al., 2006; Vigneswara & Ahmed, 2020). Furthermore, phosphorylation of caspase-2 was shown to influence its function. For example, serine phosphorylation promotes to cell cycle arrest and DNA repair, whereas dephosphorylated caspase-2 promotes apoptosis under genotoxic stress (Nutt et al., 2005; Andersen et al., 2009; Shi et al., 2009; Lim, De Bellis, et al., 2021).

Moreover, caspase-2 got postulated as a potential tumor suppressor. Several oncogene-driven mice and cancer models in combination with caspase-2 depletion showed increased proliferation, tumorigenicity, and poorer overall survival. Notably, caspase-2 depletion singularly was unable to cause carcinogenesis (Ho et al., 2009; Parsons et al., 2013; Puccini, Shalini, et al., 2013; Terry et al., 2015; Shalini et al., 2016). In line with that, caspase-2 is downregulated in some human cancer types (Fava et al., 2012). Additionally, it was observed, that genomic instabilities and aneuploidy take place under caspase-2 deficiency, indicating a loss of cell cycle control and a potential role of caspase-2 mediated cell death upon genomic

aberrations (Parsons et al., 2013; Puccini, Shalini, et al., 2013; Dawar et al., 2017; Lopez-Garcia et al., 2017). In accordance with that, a connection of caspase-2 with the p53 tumor suppressor has been observed (Lim, Dorstyn, et al., 2021). Cells oscillate their p53 level via autoregulative feedback loops. P53 transcriptionally upregulates MDM2, which then degrades p53. On the other hand, under genotoxic stress, p53 regulates PIDD expression and subsequent PIDDosome formation which leads to an activation of caspase 2. In consequence, caspase-2 cleaves MDM2, leading to stabilisation of p53 and resulting in a turnover from cell cycle arrest to apoptosis. Notably, caspase-2 activation and cell cycle arrest were also found to occur p53-independently (Sidi et al., 2008; Vigneswara & Ahmed, 2020; Lim, Dorstyn, et al., 2021).

Caspase-2 also seems to be involved in senescence, since depletion affects ageing related metabolic changes, like the ROS (Reactive oxygen species) defence in mice (Zhang et al., 2007; Dorstyn et al., 2012). Along with it, caspase-2 is also involved in DNA damage sensing. It was shown that the PIDDosome formation varies in response to the intensity of DNA damage. Mild damage leads to a different PIDD processing and signals survival, whereas severe damage mediates caspase-2 dependent apoptosis (Tinel et al., 2007; Ando et al., 2012; McCoy et al., 2012).

Caspase-2's subcellular localisation is confirmed in the nucleus, nucleolus, cytoplasm, mitochondria, endoplasmic reticulum (ER), and Golgi apparatus, which implies a role in exerting compartment specific functions via access to compartment specific substrates (Vigneswara & Ahmed, 2020). To date, roughly 250 substrates of caspase-2 were identified which is approximately half the number of known caspase-3 substrates. Notably, only a dozen of them are confirmed experimentally (Brown-Suedel & Bouchier-Hayes, 2020). In accordance with the localisation based function, the majority of experimentally identified substrates correlate with the exclusive localisation of caspase-2 (Brown-Suedel & Bouchier-Hayes, 2020). For example, cleavage of golgin-160 by caspase-2 in the Golgi apparatus leads to Golgi body dissolution during apoptosis (Tinel & Tschopp, 2004) and cleavage of MDM2 (Mouse double minute 2 homolog) in the nucleus affects cell cycle control by p53 (Brown-Suedel & Bouchier-Hayes, 2020). Furthermore, caspase-2 was shown to act upstream of effector caspases by cleaving Bid, resulting in MOMP, and subsequently in the activation of apoptosis (Guo et al., 2002; Bonzon et al., 2006).

It is to be emphasised, that in recent times, caspase-2 finally gets its rightful attention, since its functional role turned out to be much more complex and versatile than initially assumed (Figure 6). The elucidation of various roles in both, apoptotic and non-apoptotic functions sets caspase-2

into a new perspective. The current experimental revelations indicate that the function of caspase-2 is strongly dependent on the cell type and the context. For a profound understanding of the role and mechanisms of caspase-2, more investigations are needed. This further includes the revelation of novel caspase-2 specific substrates (Vigneswara & Ahmed, 2020).

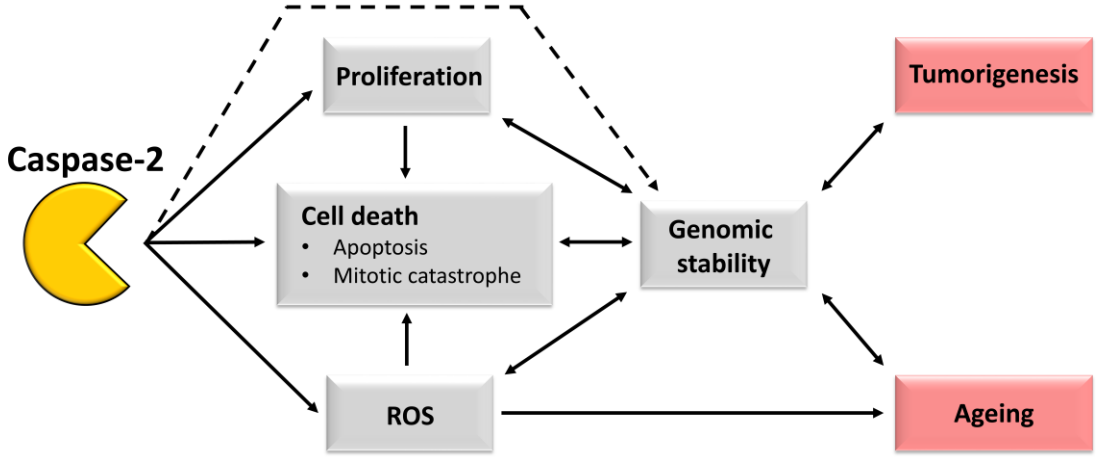

Figure 6. Map of functional interrelations of caspase-2.
Systemic illustration of the functional connections and interrelations of caspase-2 in cellular processes directly and indirectly. Abbreviations: ROS (Reactive oxygen species). (Olsson et al., 2015).

1.4 The protein p54nrb/NonO

The human protein p54nrb (54 kDa nuclear RNA-binding protein) and the equivalent mouse protein NonO (Non POU [Pituitary-specific factor, octamer transcription factor, neural un-coordinated-86] domain-containing octamer-binding protein) are ubiquitously expressed (Yang et al., 1993). P54nrb belongs to the DBHS (Drosophila behaviour/human splicing) protein family, exclusively found in vertebrates and invertebrates, with multipurpose mediating functions (Knott, Bond, et al., 2016). Vertebrate DBHS family proteins include splicing factor proline/glutamine rich (SFPQ or PSF), paraspeckle protein component 1 (PSPC1 or PSP1), and p54nrb/NonO. Invertebrate members of the DBHS family include protein no-on-transient A (NonA) and NonA-like in *Drosophila melanogaster*, and NonO-1 in *Caenorhabditis elegans* (Knott, Bond, et al., 2016) (Figure 7 A).

The DBHS proteins have a highly conserved core structure of roughly 300 amino acids, consisting of two RNA recognition motifs (RRMs), which are N-terminally positioned, a NonA (protein no-on-transient A)/paraspeckle domain (NOPS), and a coiled-coil domain is found at the C-terminus

(Dong et al., 1993), followed by a nuclear localisation signal (NLS) (Zhang & Carmichael, 2001) (Figure 7 A).

Besides the conserved core elements, DBHS family proteins vary in length and sequence complexity. The protein p54nrb/NonO (Figure 7 A and B) bears a N-terminal histidine, proline, and glutamine rich region (HPQ), and C-terminally a helix-turn-helix, a basic/acidic charged stretch (+/-), and a glutamine and proline rich region (GP) (Shav-Tal & Zipori, 2002; Knott, Bond, et al., 2016). As indicated by the NLS, p54nrb is localised in the nucleus (Andersen et al., 2002), but is also part of a specific nuclear substructure termed paraspeckles (Fox et al., 2002).

The structural features of the DBHS protein domains allow its binding to different interaction partners. This and different post-translational modifications facilitate the multifunctional characteristics of p54nrb/NonO, which are described in detail in the following sections.

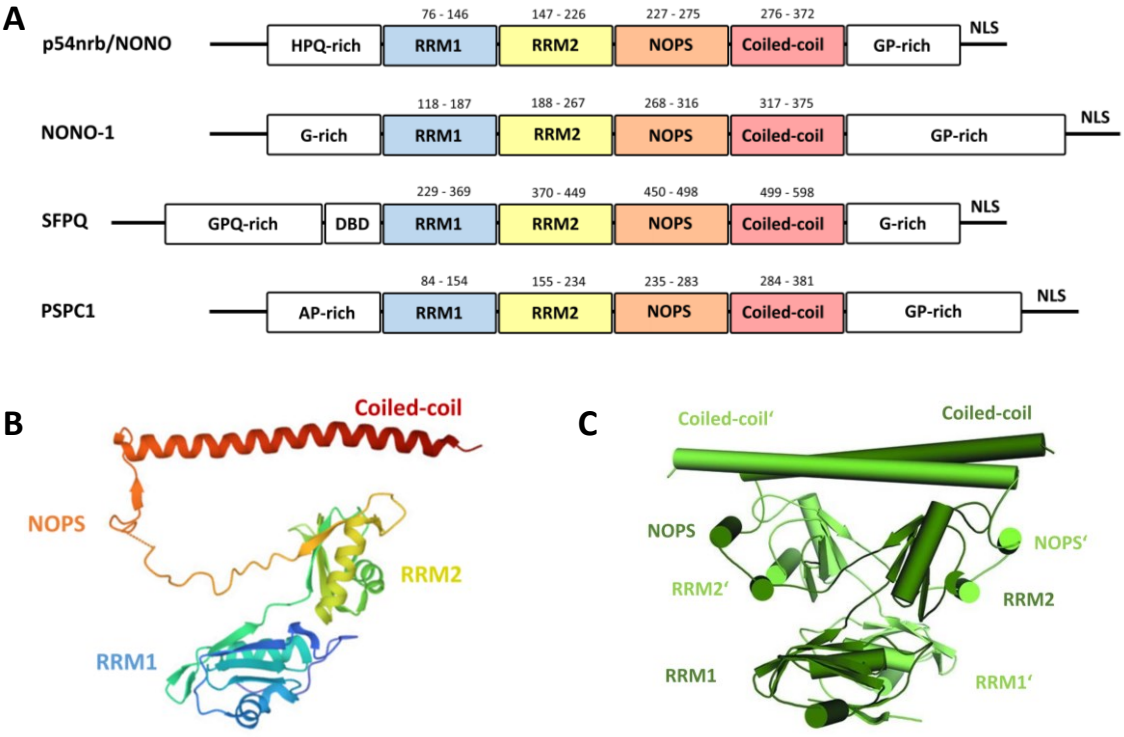

Figure 7. Structure of the DBHS protein p54nrb/NonO.
(A) Schematic model of the DBHS protein domains with the RNA recognition motifs (RRM) RRM1 and RRM2, the NonA/paraspeckle (NOPS) domain, and the coiled-coil domain, as well as the aminoacid-boundraries (HPQ-, GP-, G-, GPQ-, HP-rich), and the uncharacterised DNA-binding domain (DBD) as indicated of NonO, SFPQ, and PSPC1 from *Homo sapiens*, and NonO-1 from *Caenorhabditis elegans* (Knott, Bond, et al. (2016). Representative protein structure models of (B) a p54nrb monomer (www.wwpdb.org) and (C) a p54nrb dimer (Knott, Panjikar, et al., 2016).

1.4.1 The interaction and modification modes of p54nrb

As previously described, p54nrb consists of several conserved structural core elements, equally found in all DBHS proteins, which mediate interactions. The RRM1 domain contains aromatic residues, which can stack with RNA nucleotides, combined with an attachment through charged side chains. The RRM2, in contrast, by bearing several conserved salt bridges is rather similar to a typical double stranded DNA/RNA recognition motif. The NOPS domain is the dimerisation platform. It allows contact with the RRM2 and coiled-coil domain of a partner protein through hydrophobic residues (Figure 7 C). Some basic residues in the NOPS domain resemble parts in the RRM2 and thereby may be involved in nucleic acid binding (Knott et al., 2015). The C-terminal helix-turn-helix motif in combination with the charged stretch is suggested to act as a DNA binding site (DBD). The proline and glutamine rich regions are supposed to be relevant for interaction with other proteins (Yang et al., 1993).

It has been described that DBHS proteins can interact reciprocally (Dong et al., 1993). Dimerisation of p54nrb with PSPC1 was shown by co-purification and X-ray crystallography (Fox et al., 2005; Passon et al., 2011), but also with SFPQ (Dong et al., 1993), as well as a p54nrb homodimerisation (Figure 7 C) (Knott, Panjikar, et al., 2016).

Besides the different interaction sites of p54nrb, it is known that post-translational modifications can affect its function. For example, p54nrb gets phosphorylated in the coiled-coil domain during mitosis, influencing its binding ability (Proteau et al., 2005; Bruelle et al., 2011). Also, dephosphorylation by protein phosphatase-1 was shown to deactivate p54nrb's transcriptional repressor function (Liu et al., 2011). The phosphorylation of p54nrb further seems to influence the localisation of p54nrb, as described by Otto et al. (2001). Likewise, a methylation can affect p54nrb's interactions. For instance, methylation of arginine in the coiled-coil domain disrupts p54nrb's binding to mRNA (Hu et al., 2015).

1.4.2 The functional diversity of p54nrb

Since the interaction partners of p54nrb have been reported to affect its function, the operation field of p54nrb is likewise very divers. Through its ability to bind proteins, DNA, and RNA, it was early on apparent that p54nrb may be involved in the fields of transcription, splicing, or translation. Indeed, p54nrb was shown to act in transcriptional regulation, in both modes, co-activation and co-repression (Hallier et al., 1996; Basu et al., 1997; Yang et al., 1997; Ishitani

et al., 2003; Yadav et al., 2014). In addition, p54nrb also shows a role in post-transcriptional processing (Emili et al., 2002; Peng et al., 2002; Kameoka et al., 2004; Liang & Lutz, 2006; Hall-Pogar et al., 2007; Kaneko et al., 2007; Lu & Sewer, 2015). Later, after the detection of a binding to DNA-topoisomerase I (Straub et al., 1998), Bladen et al. (2005) and Li et al. (2009) could confirm a role of p54nrb in DNA double strand repair.

The discovery of p54nrb's localisation in the subnuclear bodies within the nucleus, termed paraspeckles, gave a new idea about the execution of p54nrb's divers activities (Fox et al., 2002; Fox et al., 2005). Paraspeckles primarily accommodate mature mRNA for retention (Zhang & Carmichael, 2001; Chen & Carmichael, 2009). In this regard, the location of p54nrb matters for its functional role.

Another reported role of p54nrb is the participation in the circadian oscillator mechanism by acting as a transcriptional cofactor (Kowalska et al., 2012). Following this investigation, evidence was found, that p54nrb is likewise a regulator of the cell-cycle G1-S checkpoint (Kowalska et al., 2013).

Further research revealed, that p54nrb is also of clinical relevance. Raghavendra et al. (2010) detected a p54nrb binding to pre-integration complexes from HIV-1 and Cao et al. (2015) discovered a binding of a noncoding lytic transcript from Epstein-Barr virus to p54nrb. Besides, p54nrb is also relevant in some human diseases. P54nrb mutation leads to syndromic intellectual disability (Mircsof et al., 2015), intron 4 mutation of p54nrb causes a cardiac phenotype (Scott et al., 2017; Sun et al., 2020), and decreased expression of p54nrb can also lead to aortic dissection (Ren et al., 2014). In rheumatoid arthritis progression, p54nrb acts as a transcriptional regulator (Q. Li et al., 2017).

Recently, more indications of a role of p54nrb in cancer have been assembled. P54nrb is frequently overexpressed in tumorous tissues. For instance, in prostate cancer (Ishiguro et al., 2003), neuroblastoma (Liu et al., 2014), as well as in breast cancer cells. In the latter case, p54nrb is involved in the regulation of the lipid metabolism (Zhu et al., 2016). P54nrb also plays a role in insulinomas (Kharade et al., 2018) and malignant pleural mesothelioma (Vavougios et al., 2015). In malignant melanoma, p54nrb is regulated by MIA (Melanoma Inhibitory Activity), a protein which drives tumor progression (Schiffner et al., 2011). P54nrb is also overexpressed in colorectal cancer, where p54nrb expression correlates with a reduced overall survival (Nelson et al., 2012) and with increased chemotherapeutic resistance (Tsofack et al., 2011).

P54nrb's multifunctionality and its developing clinical significance, yet limited understanding of its mechanical complexity makes it a fascinating and adequate research object.

1.5 Aim of the thesis

Apoptosis mediating proteins have been of interest as therapeutical targets since the discovery of diseases being caused by malfunctioning apoptotic signalling. The enigmatic enzyme caspase-2 was shown to take place in the execution of apoptosis, although caspase-2 knockout does not universally inhibit apoptotic signalling. On the other hand, caspase-2 was also suggested as a tumor suppressor, by means exerting non-apoptotic functions. However, the underlying mechanisms of caspase-2's function are still not completely understood.

This study aimed to unveil the mechanistic relations by which caspase-2 accomplishes its tumor suppressor function. Since only a few caspase-2 substrates are known so far, an important part of this investigation was to experimentally identify novel caspase-2 specific substrates. Because caspase-2, uniquely among other members of the caspase family, resides prominently in the nucleus, compartment specific substrates to mediate its specific functional role seem apparent.

To experimentally confirm new caspase-2 substrates, apoptosis inducing compounds in combination with a caspase-2 inhibitor, as well as gain of function and loss of function approaches of caspase-2, and immunoprecipitation assays, were employed.

P54nrb is a nuclear protein, able to bind RNA and DNA, and is involved in divers cellular processes. Since p54nrb is overexpressed in several human tumor types, its role as an oncogenic factor seems apparent. The aim of this study was the investigation of the underlying regulatory mechanism of p54nrb in cancer cells. Therefore, the cell viability of three tumor cell types was measured with flow cytometry, and tumor growth behaviour was analysed with a 3D anchorage-independent growth assay of p54nrb depleted cells. Furthermore, since p54nrb is known to be involved in transcriptional regulation, mass-spectrometric analyses were performed to unveil p54nrb regulated proteins, which can exert tumorigenic functions.

In summary, this study aimed to elucidate the mechanism of caspase-2's tumor suppressor function through the regulatory protein p54nrb. Data from this study may open novel therapeutic avenues to improve current cancer therapies.

2 Materials and Methods

In the following subsections, the used materials and methods are described and listed.

2.1 Materials

2.1.1 Cell lines

In Table 1 the used cell lines are presented. Additionally, the corresponding media are listed.

Table 1. List of cell lines

Cell line	Culture medium	Identifier
DLD-1 (Human colon cancer cells, p53 mutation)	DMEM 10 % (v/v) FBS 1 % (V/V) Pen-Strep	ATCC CCL-221
DLD1 CRISPR-caspase-2	DMEM 10 % (v/v) FBS 1 % (V/V) Pen-Strep	Generated in this project
DLD1 CRISPR-control	DMEM 10 % (v/v) FBS 1 % (V/V) Pen-Strep	Generated in this project
DLD1 shRNA-control	DMEM 10 % (v/v) FBS 1 % (V/V) Pen-Strep	Generated in this project
DLD1 shRNA-p54nrb	DMEM 10 % (v/v) FBS 1 % (V/V) Pen-Strep	Generated in this project
HEK-293T (Human embryonic kidney cells)	DMEM 10 % (v/v) FBS 1 % (V/V) Pen-Strep	ATCC CRL-11268
HeLa (Human Cervix Carcinoma)	RPMI 10 % (v/v) FBS 1 % (V/V) Pen-Strep	ATCC CCL-2
HeLa shRNA-caspase2	RPMI 10 % (v/v) FBS 1 % (V/V) Pen-Strep	Generated in this project
HeLa shRNA-control	RPMI 10 % (v/v) FBS 1 % (V/V) Pen-Strep	Generated in this project

HeLa shRNA-p54nrb	RPMI 10 % (v/v) FBS 1 % (V/V) Pen-Strep	Generated in this project
RKO (Human colon cancer cells, p53 wild type)	DMEM 10 % (v/v) FBS 1 % (V/V) Pen-Strep	LGC-Promochem (Wiesbaden, Germany)
SK-MEL shRNA-control	DMEM 10 % (v/v) FBS 1 % (V/V) Pen-Strep	Generated in this project
SK-MEL shRNA-p54nrb	DMEM 10 % (v/v) FBS 1 % (V/V) Pen-Strep	Generated in this project
SK-MEL-28 (Human Melanoma)	DMEM 10 % (v/v) FBS 1 % (V/V) Pen-Strep	ATCC HTB-72

2.1.2 Small RNAs

In this section the used small RNAs (Table 2, Table 3, Table 4) for gene knockdowns are listed.

Table 2. List of siRNAs

siRNA	Company	Identifier
siRNA-control	Qiagen GmbH (Hilden, Germany)	#1027310
siRNA-p54nrb#2	Qiagen GmbH (Hilden, Germany)	#2999579

Table 3. List of shRNAs

shRNA	Sequence	Company	Identifier
shRNA-caspase-2	CCGGGATATGTTGCTCACCACC CTTCTCGAGAAGGGTGGTGAG CAACATATCTTTTT	Sigma-Aldrich Chemie GmbH (Taufkirchen, Germany)	TRCN-0000003508
shRNA-control	Non-target shRNA sequence	Sigma-Aldrich Chemie GmbH (Taufkirchen, Germany)	SHC016-1EA

shRNA-p54nrb#1	CCGGGCCAGAATTCTACCCTGGAAACTCGAGTTTCCAGGGTAGAATTCTGGCTTTTTG	Sigma-Aldrich Chemie GmbH (Taufkirchen, Germany)	TRCN-0000286693
shRNA-p54nrb#3	CCGGGCAGGCGAAGTCTTCATTCATCTCGAGATGAATGAAGACTTCGCCTGCTTTTTG	Sigma-Aldrich Chemie GmbH (Taufkirchen, Germany)	TRCN-0000074560

Table 4. List of sgRNAs

sgRNA	Sequence
No.1-Forward	CACCGAGTCACGGACTCCTGCATCG
No.1-Reverse	AAACCGATGCAGGAGTCCGTGACTC
No.2-Forward	CACCGAACTCTAAAAAAGAACCGAG
No.2-Reverse	AAACCTCGGTTCTTTTTTAGAGTTC
No.3-Forward	CACCGAATTCTCACCTGTCGACAGG
No.3-Reverse	AAACCCTGTCGACAGGTGAGAATTC

2.1.3 Plasmids

The used plasmids are listed below (Table 5). Additionally, a short description of their properties are given.

Table 5. List of plasmids

Plasmids	Properties	Identifier
pcDNA3-caspase-2-C303A-Flag	6895 bp, ampicillin bacterial resistance, CMV-promoter, caspase-2 with C303A mutation, C-terminal Flag-tag	#11812, Addgene, Watertown, MA USA
pcDNA3-caspase-2-Flag	6750 bp, ampicillin bacterial resistance, CMV-promoter, C-terminal Flag-tag	#11811, Addgene, Watertown, MA USA

pcDNA3-caspase-3-C163A-myc	6303 bp, ampicillin bacterial resistance, CMV-promoter, caspase-3 with C163A mutation, C-terminal Myc-tag	#11814, Addgene, Watertown, MA USA
pcDNA3-caspase-3-myc	6350 bp, ampicillin bacterial resistance, CMV-promoter, C-terminal Myc-tag	#11813, Addgene, Watertown, MA USA
pcDNA3-caspase-7-Flag	6446 bp, ampicillin bacterial resistance, CMV-promoter, C-terminal Flag-tag	#11815, Addgene, Watertown, MA USA
pcDNA3-Flag-HA-1436	5505 bp, ampicillin bacterial resistance, CMV-promoter, N-terminal HA/Flag-tag	#10792, Addgene, Watertown, MA USA
pFlag-p54nrb	6831 bp, ampicillin bacterial resistance, CMV-promoter, N-terminal Flag-tag	#35379, Addgene, Watertown, MA USA
pLentiCRISPRv2	14877 bp, ampicillin bacterial resistance, EF-1a promoter	#98290, Addgene, Watertown, MA USA
psPAX2	10709 bp, ampicillin bacterial resistance	#12260, Addgene, Watertown, MA USA
pMD2.G	5822 bp, ampicillin bacterial resistance, CMV-promoter	#12259, Addgene, Watertown, MA USA
pcDNA3.1-p54nrb-D422N-Flag	6831 bp, ampicillin bacterial resistance, CMV-promoter, p54nrb with D422N mutation, N-terminal Flag-tag	Generated in this project in cooperation with Dr. Koraljka Husnjak
pcDNA3.1-p54nrb-D58N-Flag	6831 bp, ampicillin bacterial resistance, CMV-promoter, p54nrb with DN mutation, N-terminal Flag-tag	Generated in this project in cooperation with Dr. Koraljka Husnjak

2.1.4 Chemicals, reagents, and kits

In this section the used chemicals, reagents (Table 6), and kits (Table 7) are presented.

Table 6. List of chemicals and reagents

Chemicals and reagents	Company	Identifier
1 kb DNA Ladder RTU	Nippon Genetics EUROPE GmbH (Düren, Germany)	#MWD1
1,4-Dithiothreitol (DTT)	Carl Roth GmbH & Co. KG (Karlsruhe, Germany)	#6908.1
2-[(3,4-Dichlorophenyl) amino]-1,4-dihydro-6-nitro-4-oxo-*N*-2-propenyl-8-quinazolinecarboxamide; AQZ-1 (Caspase-3 selective non-peptide inhibitor)	Tocris Bioscience (Bristol, UK)	#2172
3-[3-Cholamidopropyl]-dimethylammonio]-1-propanesulfonate (CHAPS)	Carl Roth GmbH & Co. KG (Karlsruhe, Germany)	#1479.1
4-(2-hydroxyethyl)-1-piperazineethanesulfonic acid (HEPES)	Sigma-Aldrich Chemie GmbH (Taufkirchen, Germany)	#3375
Agarose, SeaKem®LE	Lonza Biosciences (Basel, Switzerland)	#50004
Alpha-toxin (*Staphylococcus aureus*)	Merck KGaA (Darmstadt, Germany)	#H9395
Ammoniumperoxodisulfat (APS)	Carl Roth GmbH & Co. KG (Karlsruhe, Germany)	#9592.2
BlueStar Prestained Protein Marker	Nippon Genetics EUROPE GmbH (Düren, Germany)	#MWP03
Boric acid	Merck KGaA (Darmstadt, Germany)	#1.00165
Bovine Serum Albumin (BSA)	Sigma-Aldrich Chemie GmbH (Taufkirchen, Germany)	#A2153
Bromphenol blue	Sigma-Aldrich Chemie GmbH (Taufkirchen, Germany)	#114405

Calcium chloride ($CaCl_2$)	Carl Roth GmbH & Co. KG (Karlsruhe, Germany)	#5239.1
Chloroform	Sigma-Aldrich Chemie GmbH (Taufkirchen, Germany)	#C2432
Crystal violet	Sigma-Aldrich Chemie GmbH (Taufkirchen, Germany)	#V5265
Desoxynucleotidetriphosphates (dNTPs)	Thermo Fisher Scientific (Pittsburgh, USA)	#R0191
Diethylpyrocarbonat (DEPC)	Sigma-Aldrich Chemie GmbH (Taufkirchen, Germany)	#D5758
Dimethylsulfoxide (DMSO)	Sigma-Aldrich Chemie GmbH (Taufkirchen, Germany)	#D8418
DMEM (1x) + GlutaMAX™-I	Gibco® Thermo Fischer Scientific (Waltham, USA)	#61965-026
Doxorubicin (hydrochloride)	Cayman Chemical Company (Michigan, USA)	#15007
Dulbecco's Phosphate Buffered Saline (DPBS)	Gibco® Thermo Fischer Scientific (Waltham, USA)	#14190-094
Ethanol	Sigma-Aldrich Chemie GmbH (Taufkirchen, Germany)	#32221-M
Ethylene glycol-bis (β-aminoethyl ether)-N,N,N',N'-tetraacetic acid (EGTA)	AppliChem GmbH (Darmstadt, Germany)	#A0878
Ethylenediaminetetraacetic acid (EDTA)	AppliChem GmbH (Darmstadt, Germany)	#A1103
Etoposide	Sigma-Aldrich Chemie GmbH (Taufkirchen, Germany)	#E1383
FASTGene 100bp DNA Ladder	Nippon Genetics EUROPE GmbH (Düren, Germany)	#MWD100
Fetal Bovine Serum (FBS)	Sigma-Aldrich Chemie GmbH (Taufkirchen, Germany)	#F7524
GeneJuice®Transfection Reagent	Merck Millipore (Burlington, USA)	#70967

Glycerol	Carl Roth GmbH & Co. KG (Karlsruhe, Germany)	#3783.1
Glycine	Carl Roth GmbH & Co. KG (Karlsruhe, Germany)	#0079.4
GlycoBlue™ Coprecipitant	Invitrogen, Thermo Fisher (Pittsburgh, USA)	#AM9515
HiPerFect Transfection Reagent	Qiagen GmbH (Hilden, Germany)	#301705
Isopropanol	Sigma-Aldrich Chemie GmbH (Taufkirchen, Germany)	#33539-M
Magnesium chloride ($MgCl_2$)	AppliChem GmbH (Darmstadt, Germany)	#A3618
Methanol	VWR International GmbH (Darmstadt, Germany)	#83638.320
Midori-green Advance	Biozym Scientific GmbH (Hessisch Oldenburg, Germany)	#617004
OPTI-MEM®I (1x)	Gibco® Thermo Fischer Scientific (Waltham, USA)	#31985-062
Penicillin/Streptomycin (Pen-Strep)	Gibco® Thermo Fischer Scientific (Waltham, USA)	#11548876
Phenol-chloroform	Sigma-Aldrich Chemie GmbH (Taufkirchen, Germany)	#P3803
Polybrene Infection /Transfection Reagent	Sigma-Aldrich Chemie GmbH (Taufkirchen, Germany)	#TR-1003-G
Polyethylenglycol 800 (PEG 800)	New England Biolabs GmbH (Frankfurt, Germany)	#B1004A
Poly-L-lysine	Sigma-Aldrich Chemie GmbH (Taufkirchen, Germany)	#P4707
Potassium chloride (KCl)	AppliChem GmbH (Darmstadt, Germany)	#A1362
Propidium-iodide	Sigma-Aldrich Chemie GmbH (Taufkirchen, Germany)	#P4864
Protease-inhibitor-cocktail Complete® (PIM)	Roche Biochemicals (München, Germany)	#04693132001
Protein G Sepharose™ 4 Fast Flow	GE Healthcare (München, Germany)	#17-0618-01

Proteinase K	Merck Millipore (Burlington, USA)	#CS203218
Puromycin	neoLab Migge GmbH (Heidelberg, Germany)	#1299
RiboLock Rnase inhibitor	Thermo Scientific, Fermentas (Dreieich, Germany)	#11581505
Rotiphorese®Gel 30 (37; 5:1) Acrylamid/Bisacrylamid	Carl Roth GmbH & Co. KG (Karlsruhe, Germany)	#3029.2
RPMI Medium 1640 (1x) + GlutaMAX™-I	Gibco® Thermo Fischer Scientific (Waltham, USA)	#61870-010
SeaPlaque™-Agarose	Lonza Biosciences (Basel, Switzerland)	#50101
Skim Milk	Carl Roth GmbH & Co. KG (Karlsruhe, Germany)	#T145.2
Sodium acetate (NaOAc)	Sigma-Aldrich Chemie GmbH (Taufkirchen, Germany)	#W302406
Sodium chloride (NaCl)	Sigma-Aldrich Chemie GmbH (Taufkirchen, Germany)	#31434-M
Sodium fluoride (NaF)	Sigma-Aldrich Chemie GmbH (Taufkirchen, Germany)	#201154
Sodium orthovanadate (Na_3VO_4)	Sigma-Aldrich Chemie GmbH (Taufkirchen, Germany)	#450243
Sodiumdodecylsulfat (SDS)	Carl Roth GmbH & Co. KG (Karlsruhe, Germany)	#CN30.3
Staurosporine	Tocris Biosciences (Bristol, UK)	#1285
SYTOX™ Blue dead cell stain	Invitrogen, Thermo Fisher (Pittsburgh, USA)	#S34857
Taxol/Paclitaxel	Sigma-Aldrich Chemie GmbH (Taufkirchen, Germany)	#T7402
Tetramethylethylenediamine (TEMED)	Carl Roth GmbH & Co. KG (Karlsruhe, Germany)	#2367.3
TRAIL	PeproTech, Thermo Fisher Scientific (Hamburg, Germany)	#310-04
Tris-hydroxymethyl-aminomethane (Tris)	Carl Roth GmbH & Co. KG (Karlsruhe, Germany)	#4855.2

Triton X-100	Carl Roth GmbH & Co. KG (Karlsruhe, Germany)	#3051.2
Trizol/TRI-Reagent	Sigma-Aldrich Chemie GmbH (Taufkirchen, Germany)	#T9424
Trypsin/EDTA, 0.05 % (1x)	Gibco® Thermo Fischer Scientific (Waltham, USA)	#25300-054
Tween-20/Polysorbate-20	AppliChem GmbH (Darmstadt, Germany)	#A4974
z-VAD-fmk (Carbobenzoxy-valyl-alanyl-aspartyl-[O-methyl]-fluoromethylketone)	Tocris Biosciences (Bristol, UK)	#2163
z-VDVAD-fmk (Methyl (3S)-5-fluoro-3-[[(2S)-2-[[(2S)-2-[[(2S)-4-methoxy-2-[[(2S)-3-methyl-2-(phenyl methoxy carbonyl amino) butanoyl] amino]-4-oxobutanoyl] amino]-3-methylbutanoyl] amino] propanoyl] amino]-4-oxopentanoate)	APExBIO (Houston, USA)	#A1922

Table 7. List of kits

Kits	**Source**	**Identifier**
Annexin V-EGFP Apoptosis Detection Kit	ENZO Life Science GmbH (Lörrach, Germany)	#ALX-850-253-KI02
Green GoTaq G2 DNA Polymerase Kit	Promega GmbH (Walldorf, Germany)	#M7841
Micro BCA protein assay kit	Thermo Fisher Scientific (Pittsburgh, USA)	#23235
Pierce™ ECL Western Blotting Substrate	Thermo Fisher Scientific (Pittsburgh, USA)	#32106

Quickchange II site directed mutagenesis kit	Agilent (Santa Clara, USA)	#200523
RevertAid cDNA Synthesis kit	Thermo Fisher Scientific (Pittsburgh, USA)	#K1622

2.1.5 Enzymes and proteins

Used recombinant proteins and enzymes are listed in Table 8.

Table 8. List of enzymes and proteins

Enzymes and proteins	Source	Identifier
Recombinant active caspase-2	ENZO Life Science GmbH (Lörrach, Germany)	#ALX-201-057
Recombinant active caspase-3	ENZO Life Science GmbH (Lörrach, Germany)	#ALX-201-059
Recombinant p54nrb	OriGene Technologies Inc. (Rockville, USA)	#TP326567
RNase A	Qiagen GmbH (Hilden, Germany)	#19101

2.1.6 Antibodies

In Table 9 the used primary and secondary antibodies are listed. Their species source, detectable size, and used dilution are mentioned.

Table 9. List of antibodies

Antibody	Species	Size (kDa)	Dilution	Company	Identifier
Alexa Fluor 488 Anti-Rabbit	Goat	-	1:1000	Invitrogen, Thermo Fisher (Pittsburgh, USA)	#A32731

Alexa Fluor 647 Anti-Mouse	Goat	-	1:1000	Invitrogen, Thermo Fisher (Pittsburgh, USA)	#A21235
Beta-Actin	Mouse	42	1:5000 in 5 % Milk-TBST	Sigma-Aldrich Chemie GmbH (Taufkirchen, Germany)	#A5441
Caspase-2	Rat	48, 32, 14	1:2000 in 5 % Milk-TBST	Merck Millipore (Burlington, USA)	#MAB3507
Caspase-3	Rabbit	35	1:1000 in 5 % Milk-TBST	Cell Signaling Technology (Danvers, USA)	#9662
Caspase-3 cleaved	Rabbit	17	1:1000 in 5 % Milk-TBST	Cell Signaling Technology (Danvers, USA)	#9664
Caspase-7	Rabbit	35, 20	1:1000 in 5 % Milk-TBST	Cell Signaling Technology (Danvers, USA)	#9492
Cathepsin-Z	Rabbit	35	1:5000 in 5 % Milk-TBST	Abcam (Cambridge, UK)	#Ab182575
CDKN2A/ p16INK4a	Rabbit	17	1:2000 in 5 % Milk-TBST	Abcam (Cambridge, UK)	#Ab108349
Flag M2-Peroxidase	Mouse	-	1:400 in 5 % Milk-TBST	Sigma-Aldrich Chemie GmbH (Taufkirchen, Germany)	#A8592
Gelsolin	Rabbit	83	1:1000 in 5 % Milk-TBST	Cell Signaling Technology (Danvers, USA)	#12953
Mouse IgG HRP	Rabbit	-	1:5000 in 5 % Milk-TBST	Cell Signaling Technology (Danvers, USA)	#58802
NQO1	Mouse	30	1:200 in 5 % Milk-TBST	Invitrogen, Thermo Fisher (Pittsburgh, USA)	#39-3700

P54nrb	Rabbit	54, 51, 48	1:2000 in 5 % Milk-TBST	Biomol GmbH/Bethyl Lab (Hamburg, Germany)	#A300-587A
Rabbit IgG Peroxidase	Goat	-	1:5000 in 5 % Milk-TBST	Sigma-Aldrich Chemie GmbH (Taufkirchen, Germany)	#A0545
Rat IgG HRP	Goat	-	1:5000 in 5 % Milk-TBST	ENZO Life Science GmbH (Lörrach, Germany)	#01281513
TPD52	Rabbit	25	1:5000 in 5 % Milk-TBST	Abcam (Cambridge, UK)	#Ab182578
Wheat-germ-agglutinin Alexa Fluor350 (WGA)	Wheat germ	-	1:1000	Thermo Fisher Scientific (Pittsburgh, USA)	#W11263

2.1.7 Oligonucleotides

Table 10 lists the oligonucleotides used for PCR reactions, ordered from Sigma-Aldrich Chemie GmbH.

Table 10. List of oligonucleotides

Oligonucleotide	**Sequence (5'-3')**
Cathepsin-Z Forward	CTCATGTTAAACATTAACCAAG
Cathepsin-Z Reverse	CTTCCCATCCTTATAGGTG
Gelsolin Forward	GCCAGTCTAATGAGATATACAC
Gelsolin Reverse	CTTATTTTCACCATTTATCTATATG

2.1.8 Instruments

Table 11 lists the instruments used during this study.

Table 11. List of instruments

Instrument	Company
Agfa CP 1000 Developer	Agfa (Mortsel, Belgium)
BD FACS Canto™ II	BD Biosciences (Heidelberg, Germany)
CO_2 Incubator HERAcell™ VIOS 160i	Thermo Fisher Scientific (Washington, USA)
Dual Monochromator Spectramax M5e ELISA-reader	Molecular Devices (Ismaning, Germany)
Heat block Thermomixer compact	Eppendorf (Hamburg, Germany)
Heraeus Microfuge Fresco 21	Thermo Fisher Scientific (Washington, USA)
Heraeus Multifuge 1S-R	Thermo Fisher Scientific (Washington, USA)
Herasafe Steril bank	Thermo Fisher Scientific (Washington, USA)
Laser Scanning Microscope LSM 510 META	Carl Zeiss (Jena, Germany)
Mini-PROTEAN Tetra Vertical Electrophoresis Cell	BIO-RAD Laboratories Inc. (München, Germany)
MS2 Minishaker	IKA (Köln, Germany)
Nanodrop ND-1000 spectrophotometer	Thermo Fisher Scientific (Washington, USA)
PCR Thermocycler GeneAmp 9700	Applied Biosystems (Forster City, USA)
pH-Meter PB-11	Sartorius AG (Göttingen, Germany)
PowerPac Universal™ Power Supply	BIO-RAD Laboratories Inc. (München, Germany)
Rotating Mixer	Rettberg (Göttingen, Germany)
Semidry Blotter Trans-Blot Turbo	BIO-RAD Laboratories Inc. (München, Germany)
UV Gel camera GelDoc 1000	BIO-RAD Laboratories Inc. (München, Germany)
Zeiss Axioskop 2	Carl Zeiss (Jena, Germany)

2.1.9 General materials

General materials which were used are listed in Table 12.

Table 12. List of general materials

Material	Company	Identifier
µ-slide 8-well uncoated	Ibidi GmbH (Gräfelfing, Germany)	#80821
Amersham Hypercassette	Cytica (Amersham, UK)	#10499404
Blotting paper (3 mm)	neoLab Migge GmbH (Heidelberg, Germany)	#2-4323
Cell Culture Flask (175 cm^2)	Greiner Bio-One GmbH (Frickenhausen, Germany)	#660160
Cell Culture Petri dish (10 cm)	Greiner Bio-One GmbH (Frickenhausen, Germany)	#P7612
Cell Culture Plate (6, 12, 96-well)	Greiner Bio-One GmbH (Frickenhausen, Germany)	-
Cell scraper	Sarstedt AF & Co. KG (Nuürnbrecht, Germany)	#83.3951
Cryogenic Storage Vials	Greiner Bio-One GmbH (Frickenhausen, Germany)	#126261
Cytiva Amersham™ Hperfilm™ MP	GE Healthcare (München, Germany)	#28906844
Inject Syringe (10 ml)	B. Braun SE (Melsungen, Germany)	#12742637
Microtiter plate	Greiner Bio-One GmbH (Frickenhausen, Germany)	#655101
Nitrocellulose membrane 0.45 µm	BIO-RAD Laboratories GmbH (München, Germany)	#1620115
ROTILABO PVDF Filter 0.45 µm	Carl Roth GmbH & Co. KG (Karlsruhe, Germany)	#P667.1
Safe-Lock Tubes (1.5, 2 ml)	Eppendorf SE (Hamburg, Germany)	-
Steril Conical Tube (15 ml)	Greiner Bio-One GmbH (Frickenhausen, Germany)	#GB188261-N
Steril Conical Tube (50 ml)	Greiner Bio-One GmbH (Frickenhausen, Germany)	#GB210270

2.1.10 Softwares

All utilised softwares are listed in Table 13.

Table 13. List of softwares

Software	Utilisation	Company
FACS Diva™ Software	Flow Cytometry	BD Biosciences (Heidelberg, Germany)
GraphPad Prism 9	Statistics and Graphics	GraphPad Software Inc.
ImageJ 1.41	Quantification	Wayne Rasband (NIH)
Office Excel 2010	Statistics	Microsoft (Redmond, USA)
Office Powerpoint 2010	Graphics	Microsoft (Redmond, USA)
Office Word 2010	Text	Microsoft (Redmond, USA)
Quantity One 4.6.5	Agarosegel visualisation	BIO-RAD Laboratories GmbH (München, Germany)
QuickChange Primer Design	Primer design	Agilent (Santa Clara, USA)
SoftMax Pro Software 4.6.5	ELISA-Reader	Molecular Devices (Ismaning, Germany)
Zeiss Zen Imaging Software 2008	Fluorescence microscopy	Carl Zeiss (Jena, Germany)

2.2 Methods

2.2.1 Cell culture

All works on cell lines were done in sterile conditions under a laminar flow hood. Cells were cultured in 175 cm^2 culture flasks at 37 °C with 5 % CO_2. For splitting of confluent cells, the supernatant was discarded, the cells were washed with 5 ml DPBS and subsequently washed with 3.5 ml Trypsin/EDTA (0.05 %) and incubated for 5 minutes. The cells were detached by gentle resuspending in 10 ml complete medium and then diluted in a ratio of 1:5.

2.2.2 Long term storage of cells and thawing

To store cell lines long term, a confluent culture flask was trypsinised and the resuspension centrifugated at 2000 rpm for 4 minutes. The cell pellet was resuspended in 3 ml medium with 10 % DMSO and 1 ml aliquots were frozen at -80 °C for 24 hours before transferring them into liquid nitrogen for long term storage.

To thaw cells, the cryogenic aliquot was thawed in a 37 °C water bath for 90 seconds and added to 10 ml prewarmed medium. After 4 minutes of centrifugation at 1000 rpm, the supernatant was discarded, the cells resuspended in fresh medium, and transferred to a culture flask. Cells were split at least one time before using for experiments.

2.2.3 Cell transfection with siRNA

For transient knockdown, cells were cultured until 70-80 % confluency. 100 µl/ml OptiMEM, 9 µl/ml Hiperfect and 3 µl/ml siRNA (20 µM siRNA-Control (Qiagen, #1027310) or siRNA-p54nrb#2 (Qiagen, #2999579)) were mixed, incubated for 15 minutes at room temperature, and added dropwise to the cells. Then the cells were incubated in the incubator with 5 % CO_2 at 37 °C.

2.2.4 shRNA lentiviral knockdown

To produce shRNA lentiviral transduction particles, HEK-293T cells were seeded in 6-well plates. At 70-80 % confluency, the cells were transfected with 4 packaging vectors (each 0.25 µg/ml)

and pLenti-shRNA (pLKO.1) target-vector (1 µg/ml) using GeneJuice. The supernatant was harvested after 24 hours, refilled with medium, and after further 24 hours harvested a second time. The collected supernatants were pooled and filtered using a 0.45 µm pore size filter.

To generate shRNA knockdown, 30.000 cells/100 µL were seeded in a 96-well plate. The next day, the filtered viral supernatants (100 µl/well) or ready-to-use viral particles (Sigma-Aldrich) (MOI=5.6) and 8 µg/ml polybrene were added to the cells. After 24 hours, the medium was changed and 2.5 µg/ml puromycin was added for selection. After reaching 90-100 % confluency, the cells were transferred to a 12-well plate. Again, after reaching 90-100 % confluency, the cells were transferred to a 6-well plate. And finally, the cells were transferred to a cell culture flask, while samples were taken for knockdown validation.

2.2.5 CRSIPR-Cas9 gene editing

To generate CRISPR-Cas9 directed gene deletion of caspase-2, sgRNA sequences targeting caspase-2 were designed using rule set 2 (PMID: 26780180). The sgRNA sequences targeting caspase-2 were cloned into the pLentiCRISPRv2 by employing BsmBI restriction digestion and ligation based on the protocol from Wegner et al. (2019).

To produce infectious lentiviral CRISPR particles, HEK-293T cells were seeded in 6-well plates to 70-80 % confluency and then transfected with 1.35 µg/ml psPAX2 and 0.5 µg/ml pMD2.G packaging vectors, and a mix of pLentiCRISPRv2 vectors harbouring three different sgRNA sequences (1.65 µg/ml) using GeneJuice. The supernatant was harvested at 24 hours, refilled with fresh complete medium, and after further 24 hours incubation, harvested a second time. The collected supernatants were pooled and filtered using a 0.45 µm pore size filter.

To generate CRISPR knockout cells, 30.000 cells/100 µl were seeded in a 96-well plate. On the next day, the filtered viral supernatants (200 µl/well) and 8 µg/ml polybrene were added to the cells. After 24 hours, the medium was changed, and 2.5 µg/ml puromycin was added for selection. After reaching 90-100 % confluency, the cells were transferred to a 12-well plate. After reaching 90-100 % confluency, the cells were transferred to a 6-well plate. And finally, the cells were transferred to a cell culture flask, while samples were taken for knockout validation.

2.2.6 In vitro site-directed mutagenesis

The site directed mutagenesis was performed in cooperation with Dr. Koralika Husnjak. In the Flag-p54nrb vector, Aspartate D58 and D422 were exchanged for asparagine (N). The point-mutations were achieved by employing the Quickchange II site directed mutagenesis kit following the manufacturer´s instructions. The primers harbouring the mutated sequences were designed by using the primer design software from Agilent. The mutations in the corresponding sequence were validated by employing standard DNA sequencing services (Microsynth SeqLab GmbH).

2.2.7 Cell transfection with plasmids

For ectopic expression of proteins, cells were cultured until 70-80 % confluency. Then, 100 µl/ml OptiMEM was mixed with GeneJuice (Ratio of 1 µg DNA: 3 µl GeneJuice) and incubated at room temperature for 5 minutes. Then 1 µg plasmid per 1 ml volume of 1 well was added, mixed, and incubated for further 15 minutes. The mix was dropwise slowly added to the cells and then incubated in 5 % CO_2 at 37 °C.

2.2.8 Cell harvest and protein measurement

For harvesting cell samples, the cells were detached by use of a cell scraper and centrifuged at 2000 rpm for 4 minutes. The cell pellet was washed with 1 ml DPBS and the cell pellet was then lysed by giving freshly prepared lysis buffer. For samples of one well of a 12-well plate 50 µl lysis buffer was given, per well of a 6-well plate 80 µl, and per 10 cm Petri dish 100 µl were given respectively. Lysis buffer was prepared freshly by mixing 1 ml total protein buffer (137 mM NaCl, 20 mM Tris-HCl pH 8, 5 mM EDTA pH 8, 10 % Glycerol, 1 % Triton X-100) with 40 µl 25x Protease-Inhibitor-Mix, 10 µl Na_3VO_4 (c_{end}= 1 mM), and 1 µl NaF (c_{end}= 1 mM). After resuspension in the lysis buffer, the cells were frozen five times in liquid nitrogen and thawed at 30 °C in a heat block, followed by 30 minutes of centrifugation at 13.000 rpm at 4 °C. The supernatant was transferred to a new vessel and the protein concentration was determined in duplicates with a Pierce BCA protein assay kit. Therefore, in a 96-well plate 149 µl double-distilled water (dd-H_2O) was pipetted, 1 µl lysate sample was added, followed by 150 µl working reagent (25 parts of reagent A, 24 parts of reagent B and 1 part of reagent C). For quantitative evaluation, a standard curve

was established by using BSA in concentrations from 2.5 to 200 µg/ml. The plate was covered to protect it from light and incubated at 60 °C for 45 minutes. The absorbance was measured at 562 nm on a microplate Elisa-reader using SoftMax Pro software.

2.2.9 Western blot analysis

2.2.9.1 SDS gel electrophoresis

To separate proteins according to their molecular weight, Sodium dodecyl sulfate-polyacrylamide gel electrophoresis (SDS-PAGE) was used. The gel was cast in two phases (Table 14). The lower phase, called resolving gel, was prepared first, and covered by isopropanol to even the surface border. After polymerisation, the isopropanol was discarded and the upper phase with the well comb, called stacking gel, was prepared.

Table 14. SDS-PAGE recipe

Ingredients	**Resolving gel**		**Stacking gel**
	10 % gel	**12 % gel**	
dd-H_2O	10.4 ml	8.8 ml	7.9 ml
3 M Tris pH 9	2.5 ml		-
1 M Tris pH 6.8	-		1.5 ml
20 % SDS	100 µl		50 µl
10 % APS	200 µl		100 µl
30 % Bis-acrylamide	6.7 ml	8.3 ml	1.46 ml
TEMED	20 µl		10 µl

A lysate with a content of 40 µg protein was mixed with 4x Laemmli buffer (40 % Glycerol, 10 % SDS, 125 mM Tris-HCl pH 6.8, 50 mM DTT, 0.01 % Bromphenol blue) and dd-H_2O to the final volume of 18 µl. The samples were heated for 5 minutes at 95 °C and the complete volume was subjected to an SDS-PAGE. Additionally, 5 µl of page ruler prestained protein ladder was loaded as a molecular weight marker.

Protein separation on the SDS-PAGE was carried out in a gel chamber filled with SDS-running buffer (25 mM Tris-base, 192 mM Glycine, 0,1 % SDS) at 50 mA.

2.2.9.2 Protein transfer to a nitrocellulose membrane

The protein transfer from SDS-PAGE to a nitrocellulose membrane (0.45 µm) was performed by using a blotting chamber. Two sheets of blotting paper were wet with Towbin transfer buffer (25 mM Tris-base, 192 mM Glycine, 20 % Isopropanol). On top of the paper was put, likewise wet with Towbin buffer, a nitrocellulose membrane, followed by the SDS-PAGE gel, which was washed in Towbin buffer. The gel was covered with further two wet sheets of blotting paper. The transfer was carried out at 70 mA for 80 minutes.

2.2.9.3 Immunodetection of proteins

The nitrocellulose membrane was blocked for 1 hour with 5 % milk in TBST (20 mM Tris-HCl pH 7.5, 150 mM NaCl, 0.1 % Tween) at room temperature, washed three times for 5 minutes with TBST and then incubated with the indicated primary antibody in 5 % milk in TBST overnight at 4 °C. The next day, the membrane was washed three times for 5 minutes with TBST, incubated with the corresponding HRP-conjugated secondary antibody for 1 hour at room temperature and washed again three times for 5 minutes. Finally, the membrane was incubated with ECL solution for 5 minutes and luminescence was detected using a light sensitive X-ray film.

2.2.10 Endogenous Immunoprecipitation

For an endogenous immunoprecipitation, 1 mg of protein lysate was incubated with 30 µl protein-G sepharose beads for 2 hours at 4 °C under rotation to preclean the lysate of unspecific binding. After a short centrifugation at 2000 rpm for 1 minute, the supernatant was transferred into a new vessel and adjusted to 1 ml with lysis buffer. 50 µl of FBS and 1 µg antibody (same amount and species of IgG for control) were added and incubated at 4 °C under rotation overnight. The next day, 70 µl protein-G sepharose beads, which were pre-washed 3 times with 500 µl ice-cold lysis buffer and supplemented with protease and phosphatase inhibitor, were added to the overnight reaction, and incubated for 2 hours at 4 °C under rotation. The reaction was centrifuged at 10.000 rpm for 1 minute at 4 °C and washed as described in the following methods: ChIP (Chapter 2.2.11) and RIP (Chapter 2.2.12).

2.2.11 Chromatin Immunoprecipitation (ChIP)

After endogenous immunoprecipitation as described (Chapter 2.2.10), the supernatant was discarded and the beads were washed four times for 20 minutes with 500 µl RIPA buffer (50 mM Tris-HCl pH8, NaCl, 1 % Triton-X100, 0.1 % SDS) at 4 °C under rotation. After the last repetition, all liquid was removed from the beads. Next, the immunoprecipitation was validated by western blot analysis and the isolation of DNA was performed.

For DNA isolation, the beads were resuspended in 200 µl elution buffer A (1 % SDS, Tris-EDTA pH 8) and incubated for 10 minutes at 62 °C and 500 rpm rotation. After centrifugation at 13.000 rpm for 2 minutes the supernatant was collected in a new vessel. The beads were now resuspended in 200 µl elution buffer B (0.67 % SDS, Tris-EDTA pH 8), incubated at 62 °C and 500 rpm rotation for 10 minutes, centrifuged and pooled with the previous batch. To the pooled supernatant, 365 µl water, 4 µl 5 M NaCl, and 1 µl RNase A were added and incubated at 65 °C for 4 hours. Subsequently, 2 µl Protein K, 2 µl 0.5 M EDTA pH 8, and 2 µl 1M Tris-HCl pH 6.5 were added and incubated for 2 hours at 42 °C. Then, samples were mixed with 400 µl basic phenol-chloroform and centrifuged at 13.000 rpm for 15 minutes at 4 °C. The upper layer was transferred to a new vessel and supplemented with 1 ml Ethanol, 40 µl 3 M NaOAc pH 5.2, and 4 µl Glycoblue. DNA was precipitated overnight at -20 °C. The next day, the samples were centrifuged at 13.000 rpm at 4°C for 15 minutes and the supernatant was removed. The pellet was washed with 1 ml 70 % ice-cold ethanol and centrifuged again. After carefully removing the supernatant, the pellet was dried at 37 °C for 4 minutes and then resuspended in 20 µl dd-H_2O. The DNA content was measured with a Nanodrop spectrophotometer.

2.2.12 Ribonucleoprotein Immunoprecipitation (RIP)

After endogenous immunoprecipitation as described (Chapter 2.2.10), the supernatant was discarded and the beads were washed under rotation three times for 20 minutes at 4 °C with 500 µl of low salt wash buffer (100 mM NaCl, 50 mM Tris-HCl pH 7.4, 2 mM EDTA pH 8, 2 mM EGTA pH 8, 0.1 % SDS, 0.2 % Tween) and also under same conditions three times with high salt wash buffer (350 mM NaCl, 50 mM Tris-HCl pH 7.4, 2 mM EDTA pH 8, 2 mM EGTA pH 8, 0.1 % SDS, 0.2 % Tween). After the last step, all liquid was removed from the beads. Next, the immunoprecipitation was validated by western blot analysis and the isolation of RNA was performed.

For RNA isolation, 1 ml Trizol was added to the dried beads and mixed with 200 µl chloroform thoroughly mixed for 10 seconds. Samples were centrifuged for 15 minutes at 13.000 rpm at 4 °C and upper aqueous phase was carefully transferred to a new RNase-free vessel. 800 µl isopropanol and 3.5 ml Glycoblue was added and incubated overnight at -20 °C. Samples were centrifuged at 13.000 rpm for 20 minutes at 4 °C and the supernatant was carefully removed. The RNA pellet was washed with 500 µl ice-cold 70 % ethanol and then dried for 5 minutes at 37 °C. The pellet was resuspended in 15 µl DEPC-treated water for 10 minutes at 65 °C. The RNA content was measured with a Nanodrop spectrophotometer.

2.2.13 In vitro immunoprecipitation assay

For the *in vitro* p54nrb/DNA binding assay, 0.5 µg human recombinant p54nrb (Origene, Rockville, MD USA) and 100 ng plasmid containing the coding sequence of gelsolin (Ch-gelsolin) [#37262] [Addgene]) were incubated at 37 °C for 18 hours. Immunoprecipitation was performed by employing either 1 µg p54nrb antibody or the same amount and species of IgG as the control (Chapter 2.2.10). Next, DNA was isolated as described (Chapter 2.2.11). P54nrb precipitation was confirmed by immunoblot detection. The DNA content of the isolates was measured by nanodrop, and equal amounts were added to the PCR reaction (Chapter 2.2.15), employing gelsolin-specific primers. Amplification was confirmed by agarose gel electrophoresis.

2.2.14 Reverse Transcriptase (RT) reaction

To synthesis cDNA from RNA, a RT reaction was performed as described in the following. For one RT reaction was mixed: 1 µl Random Hexamer Primer, 4 µl 5x RT-PCR reaction buffer, 2 µl 10 mM dNTP-mix, 1 µl RNase inhibitor 40 U/µl, 1 µl Revert-Aid Reverse Transcriptase 200 U/µL, 1 µg RNA and adjusted to 20 µl with dd-H_2O. The sample run in a PCR thermocycler with the program of 25 °C for 5 minutes, followed by 60 minutes at 37 °C, and terminated with 5 minutes at 70 °C.

2.2.15 Polymerase Chain Reaction (PCR)

For DNA amplification by PCR, the following components were mixed per sample: 3 µl 5x Green GoTaq buffer, 1 µl 50 µM Primer forward, 1 µl 50 µM Primer reverse, 2 µl 10 mM dNTP-mix, 0.15 µl GoTaq G2 DNA Polymerase 5 U/µl, 3 µl 25 mM $MgCl_2$, and 200 ng DNA-template and adjusted to 25.15 µl with dd-H_2O.

The reaction-mix run in a PCR thermocycler with the program of 94 °C for 4 minutes, followed by 35-40 cycles of 30 seconds at 94 °C, 45 seconds at 55 °C, and 45 seconds at 72 °C, and a single final step for 5 minutes at 72 °C. PCR amplifications were analysed with agarose gel electrophoresis. Therefore, next to 5 µl 100 bp-DNA-ladder, whole PCR sample volumes were loaded onto a 2 % (w/v) Agarose-TBE gel (TBE buffer: 90 mM Tris-HCl, 80 mM Boric acid, 2 mM EDTA pH 8.3) with 5 µl/100 ml Midori-green and run at 50 V for 1-2 hour. DNA separation was visualised under a UV transilluminator and documented by using Gel Doc software.

2.2.16 Subcellular fractioning

For the isolation of the subcellular fractions, nucleus and cytoplasm, cells were seeded in a 10 cm petri dish. After reaching 90 % confluency the cells were harvested by scratching in ice-cold DPBS with 0.5 mM EDTA. After 5 minutes centrifugation at 6000 rpm and 4° C, the cell pellet was resuspended in 70 µl hypotonic buffer A (10 mM HEPES pH 7.9, 10 mM KCl, 0.1 mM EDTA, 0.1 mM EGTA; before use freshly added: 1x Protease inhibitor mix, 1 mM Na_3VO_4, 1 mM NaF). After incubation on ice for 10 minutes, 4.7 µl 10 % NP40 were added and mixed thoroughly and further centrifuged at 10.000 rpm and 4° C for 3 minutes. The supernatant was separated as the “cytoplasmic fraction” into a new vessel and stored at -20° C.

The remaining pellet was resuspended in 70 µl ice-cold high salt buffer C (20 mM HEPES pH 7.9, 25 % glycerol, 0.4 M NaCl, 1 mM EDTA, 1 mM EGTA; before use freshly added: 1x Protease inhibitor mix, 1 mM Na_3VO_4, 1 mM NaF) and thoroughly mixed for 30 min on a shaker machine at 4° C. Then, the sample was centrifuged at 13.000 rpm and 4° C for 30 minutes and the supernatant was separated as the “nuclear fraction” and stored at -20° C.

2.2.17 Liquid Chromatography-Mass Spectrometry (LC-MS) analysis and label-free quantification analysis

LC-MS analysis was performed in cooperation with the working group of Prof. Stefan Tenzer from the university of Mainz.

Proteins were extracted and digested using filter-aided sample preparation (FASP), as described in detail before (Wisniewski et al., 2009; Distler et al., 2016). In brief, samples (corresponding to 20 µg of total protein) were loaded onto spin filter columns (Nanosep centrifugal devices, 30 kDa MWCO; Pall, Port Washington, NY). After washing the samples three times with a buffer containing 8 M urea, proteins were reduced and alkylated using dithiothreitol (DDT) and iodoacetamide (IAA), respectively. Excess IAA was quenched by the addition of DTT. Afterwards, the membrane was washed three times with 50 mM NH_4HCO_3 and proteins were digested overnight at 37 °C using trypsin (Trypsin Gold, Promega, Madison, WI) at an enzyme-to-protein ratio of 1:50 (w/w). After proteolytic digestion, peptides were recovered by centrifugation. Samples were subsequently acidified with trifluoroacetic acid (TFA) to a final concentration of 1 % (v/v) TFA. After lyophilisation, purified peptides were reconstituted in 0.1 % (v/v) formic acid (FA) for LC-MS analysis.

Tryptic peptides were analysed as detailed before using a NanoAQUITY UPLC system (Waters Corporation, Milford, MA) coupled online to a Synapt G2-S high definition mass spectrometer (Waters Corporation, Milford, MA) (Distler et al., 2014; Distler et al., 2016). In brief, peptides were loaded directly onto an HSS-T3 C18 1.8 µm, 75 µm × 250 mm reversed-phase analytical column (Waters Corporation) running a gradient 5 to 40 % (v/v) mobile phase B (0.1 % (v/v) FA and 3 % (v/v) DMSO in ACN) at a flow rate of 300 nL/min over 90 min. Mobile phase A was 0.1 % (v/v) FA and 3 % (v/v) DMSO in water. MS analysis of eluting peptides was performed by ion-mobility separation (IMS) enhanced data-independent acquisition (DIA) in $UDMS^E$ mode as described in detail before (Distler et al., 2014; Distler et al., 2016).

The LC-MS raw data was processed in ProteinLynx Global Server (PLGS, ver.3.0.2, Waters Corporation). Data were searched against a custom compiled human proteome database (UniProtKB human reference proteome release 2020) which contained a list of common contaminants. For database search, the following parameters were applied: i) trypsin as enzyme for digestion, ii) up to two missed cleavages per peptide, and iii) peptides had to have a length of at least six amino acids. Carbamidomethyl cysteine was set as fixed, and methionine oxidation as variable modification. The false discovery rate (FDR) for peptide and protein identification

was assessed using the target-decoy strategy by searching a reverse database and was set to 0.01 for database search in PLGS.

Postprocessing of data and label-free quantification analysis was performed using the software tool ISOQuant ver.1.8 as detailed before (Distler et al., 2014; Distler et al., 2016). An FDR of 0.01 at the peptide-level was applied for cluster annotation in ISOQuant. Proteins were only reported if they had been identified by at least two peptides with a minimum length of six amino acids, a minimum PLGS score of 5.5 and no missed cleavages. For each protein, absolute in-sample amounts were calculated using TOP3 quantification (Silva et al., 2006). To identify significantly regulated proteins ($p < 0.01$), a two tailed t-test was performed and corrected for multiple-hypothesis testing using Benjamini-Hochberg correction. To be included in the final list of significantly regulated proteins, proteins had to be additionally identified in all biological replicates and display a log_2-ratio of >0.5 or <-0.5 as compared to the control group.

2.2.18 Cell death detection by flow cytometry

For cell death analysis, flow cytometry was employed. Therefore, $0.5x10^6$ cells were seeded and treated in a 12-well plate. The samples were harvested by collecting the supernatant, washing with 150 µl DPBS, incubating for 5 minutes with 150 µl Trypsin-EDTA and collecting the detached cells. 300 µl of cell suspension was incubated for 30 minutes in the dark with the staining solution (10 µl resuspension buffer (ENZO), 0.75 µl 1 M $CaCl_2$, 3 µl propidium iodide (PI) (ENZO) or 0.3 µl Sytox-Blue (Life Technologies GmbH), and 3 µl Annexin-V-EGFP (ENZO)). The measurement was held on FACS Canto-II flow cytometer (BD Bioscience) by using the software FACS Diva. 10.000 events in total were measured. Thereby first, cell debris (population exhibiting low FSC/SSC intensity) were excluded from the analysis by employing the FSC/SSC dot-plot. Cell death was measured by employing the PI/FL2 channel (488 nm blue laser/585 nm band-pass filter) or Sytox-Blue/FL1 channel (405 nm violet laser/450 nm band-pass filter) and the annexin-V-EGFP/FL1 channel (488 nm blue laser/530 nm band-pass filter). The resulting cell populations were gated accordingly upon the negative cell control and the cell death and viability share were evaluated in percentage of measured events.

2.2.19 3D soft agar tumor growth assay

Anchorage independent growth was monitored by employing a 3D soft agar assay. Thereby cells get cast in an agarose solidified medium. Like this, metastatic-like growth can be monitored. To prepare the assay, 1.5 ml/well agar-base (0.75 % (w/v) SeaPlaque-Agarose (Lonza) - DMEM) was poured and solidified in a 6-well plate. Then, 1000 cells/well in 1.5 ml agar-topper (0.45 % (w/v) SeaPlaque-Agarose - DMEM) were poured and hardened on top of the agar-base. The plate was cultured at 37 °C with 5 % CO_2 for 3 weeks, while adding 200 µl DMEM medium every four days to keep the plate from drying out. For quantitative analysis cell colonies were stained with 0.1 % crystal violet for 3 hours, then washed three times with 1 ml dd-H_2O for 1 hour each. Images of the plates were taken, and cell colonies were quantified by employing ImageJ.

2.2.20 In vitro caspase cleavage assay

For validation of caspase-2 cleavage *in vitro*, 0.7 µg recombinant p54nrb and 1-4 U recombinant active caspase-2 or recombinant active caspase-3 were mixed with caspase-buffer (0.1 M HEPES pH 7, 10 % PEG, 0.1 % CHAPS, 10 mM DTT). The samples were incubated for 6 hours at 37 °C. Next, the samples were mixed with 4x Laemmli and used for western blot detection.

2.2.21 Immunologic staining for fluorescence microscopy

For fluorescence microscopical detections in cells, a µ-slide 8-well was coated with 300 µl poly-L-lysine for 1 hour at 37 °C. After washing two times with DPBS, 50.000 cells/well were seeded and incubated for 48 hours in 5 % CO_2 at 37 °C. The plate was kept on ice, washed two times with DPBS, and 200 µl ice cold methanol was pipetted on the slides for 4 minutes, then once again washed two times with DPBS. Then, the samples were incubated in 5 % Milk-PBS for 1 hour at room temperature. After washing two times with DPBS, the primary antibody (2 ng/µl) in 0.1 % BSA-DPBS was added to the samples for 1 hour at room temperature. After two times washing with DPBS, the secondary antibody was added (1:1000) in 0.1 % BSA-DPBS and incubated for 1 hour at room temperature in the dark. After two times washing with DPBS, 5 µg/ml WGA and 1 µg/ml propidium-iodide in DPBS were added for 10 minutes at 37 °C. Finally, the samples were washed three times with DPBS. Afterwards, fluorescence was detected with laser scanning microscopy.

3 Results

3.1 P54nrb has a role in the regulation of key tumorigenic features of tumor cells

P54nrb is reported to be overexpressed in various cancer types and is even seen as a potential independent prognostic marker for some cancers (Feng et al., 2020). Despite its functional characterisation as a multipurpose scaffold and observations of a tumorigenic role in cancers, the underlying mechanisms still need to be revealed and are addressed in this study.

3.1.1 P54nrb is overexpressed in tumor cells

First, the p54nrb expression level in different tumor cells was validated. By using the online data mining tool oncomine.org, the p54nrb mRNA level of tissue samples, derived from patients with solid tumors of cervix carcinoma, colon carcinoma, and melanoma, were evaluated *in silico*. The p54nrb mRNA level was significantly elevated in all three tumor tissue types in comparison to the equivalent healthy tissue types. The mRNA level of p54nrb in cervix carcinoma cells is 1.63-fold upregulated (Figure 8 A), in colon carcinoma cells by 2.32-fold (Figure 8 B), and in melanoma cells by 1.54-fold (Figure 8 C).

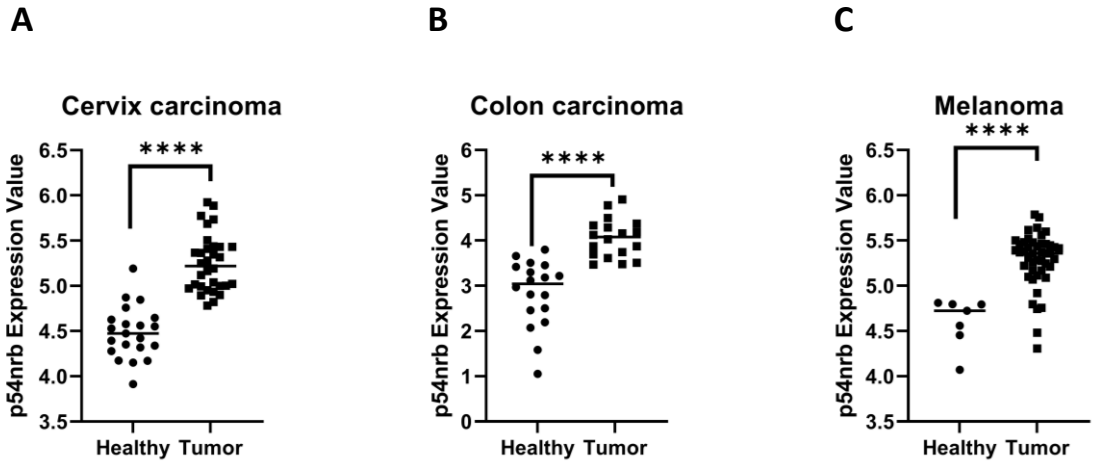

Figure 8. Expression level of p54nrb mRNA in human tissue.
Healthy versus tumor tissue samples from patients were analysed and evaluated *in silico* based on the p54nrb mRNA level. The mRNA expression values (Log2 median centred intensity) were obtained from the oncomine.org database with the criteria of a threshold of p<1E-6 and a fold change of >1.5. Student's t-test was performed for significance with ****p<0.0001. Tissues of (A) Cervix squamous epithelium (21 samples) and cervical squamous cell carcinoma (32 samples) (Scotto et al., 2008), (B) Colon and colon adenocarcinoma (each 18 samples) (Notterman et al., 2001), and (C) Skin tissue (7 samples) and cutaneous melanoma (45 samples) (Talantov et al., 2005), were evaluated (Eichler et al., 2022).

To experimentally analyse the functional role of p54nrb's overexpression in tumor cells, stable depletion of p54nrb by lentiviral shRNA knockdown was performed in HeLa cervix carcinoma, DLD-1 colon carcinoma, and SK-MEL melanoma cells. The efficiency of the knockdown of p54nrb in these cell lines was evaluated by western blot analysis (Figure 9).

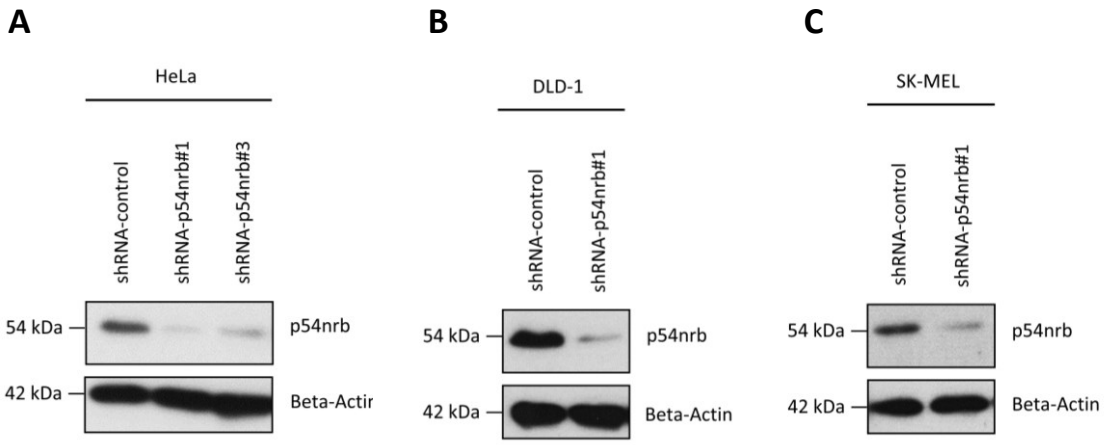

Figure 9. Generation of p54nrb knockdown cells.
(A) Immunoblot of the p54nrb-level in HeLa shRNA-control, shRNA-p54nrb#1, and shRNA-p54nrb#3 cells. (B) Immunoblot of the p54nrb-level in DLD-1 shRNA-control and shRNA-p54nrb#1 cells. (C) Immunoblot of the p54nrb-level in SK-MEL shRNA-control and shRNA-p54nrb#1 cells. Figures from Eichler et al. (2022), except A.

3.1.2 Depletion of p54nrb affects anchorage independent growth

To investigate the impact of p54nrb on tumorigenic traits of the cells, the generated p54nrb knockdown cells in comparison to the control cells were assessed in a 3D soft agar growth assay. This assay serves as a model for metastatic growth by monitoring colony formation and long-term survival capacity of cells under anchorage independency. To this end, cells are poured into agarose medium and after the end of 21 days of incubation, the grown colonies are dyed and quantified.

The growth assay of HeLa cervix carcinoma cells did not show a significant effect in growth behaviour between p54nrb knockdown and control cells (Figure 10 A). However, DLD-1 colon carcinoma cells (Figure 10 B) showed a 1.5-fold reduction in the number of grown colonies under p54nrb depletion. SK-MEL melanoma cells (Figure 10 C) showed a significant 4-fold reduction in both, size, and number of the grown colonies with p54nrb knockdown in comparison to the

control cells. Thus, the p54nrb protein level affects anchorage independent growth in DLD-1 and SK-MEL cells.

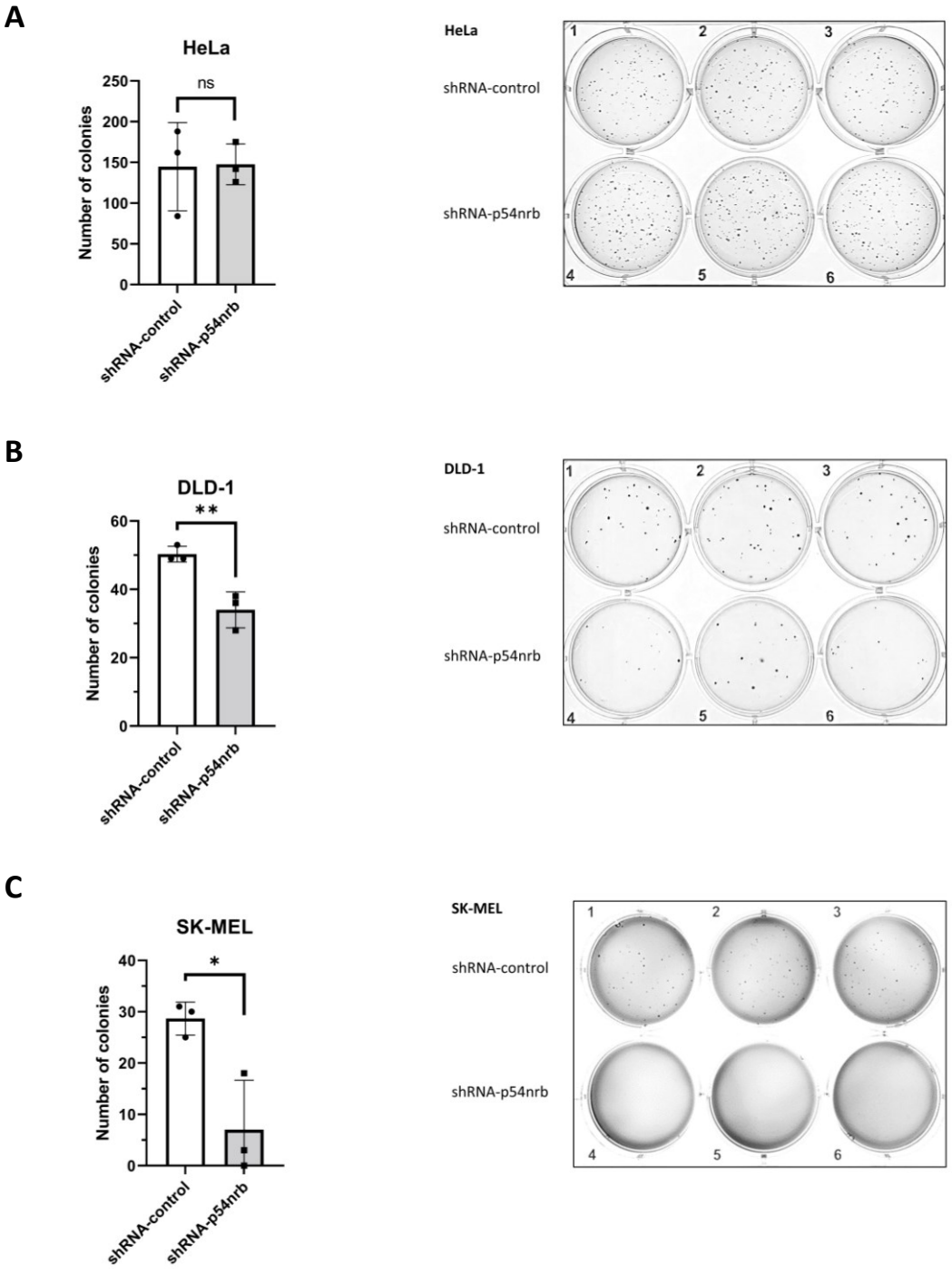

Figure 10. Anchorage independent growth of p54nrb depleted cells.
3D soft agar tumor growth assay of (A) HeLa, (B) DLD-1, and (C) SK-MEL cells with counts of colonies (left) and a photography of one representative experiment (right) with three technical replicates of each, shRNA-Control (upper three wells) and shRNA-p54nrb cells (lower three wells). 1000 cells/well were seeded and grown for 3 weeks and stained with 0.1 % crystal-violet. Student´s t test was employed to test significance. Non-significant (ns), *p<0.05, **p<0.01, n=3. Figures from Eichler et al. (2022), except photography C.

3.1.3 Depletion of p54nrb sensitises towards cell death

In order to investigate the role of p54nrb on tumorigenic features that have an immediate impact on cell fate, the effect of p54nrb on cell death and survival was measured. Therefore, the generated p54nrb knockdown cells of HeLa cervix carcinoma, DLD-1 colon carcinoma, and SK-MEL melanoma in comparison to their equivalent control cells were measured by flow cytometry. Thereby, cells were stained with annexin-V and propidium-iodide (Figure 11 A) or annexin-V and Sytox-Blue (Figure 11 B), to detect apoptotic and necrotic cells, and non-stained viable cells were quantified.

The knockdown of p54nrb in HeLa cells did not significantly affect the viability in comparison to the control cells (Figure 11 A and B). Hence, the cells were further stressed by the induction of apoptosis with chemotherapeutic compounds. To stimulate apoptosis, etoposide and doxorubicin were applied for activation of the intrinsic pathway, and TRAIL (human recombinant TRAIL) was used for inducing the extrinsic pathway.

Under apoptotic stimulation, the HeLa shRNA p54nrb knockdown cells showed significantly reduced viability in comparison to the stimulated control cells. P54nrb knockdown with 10 µM etoposide, 240 ng/ml TRAIL, or 10 µg/ml doxorubicin stimulation for 24 hours, led to a reduction of viability by 20 % in comparison to the stimulated control cells (Figure 11 A and B).

Also, the administration of nocodazole, an inducer of mitotic arrest, led to a reduced viability under p54nrb knockdown, which was detected by an increased apoptotic SubG1 population in comparison to the stimulated control cells. The application of 1 µg/ml nocodazole for 24 hours led to an increased SubG1 population of 10 % with p54nrb depletion (Figure 11 C).

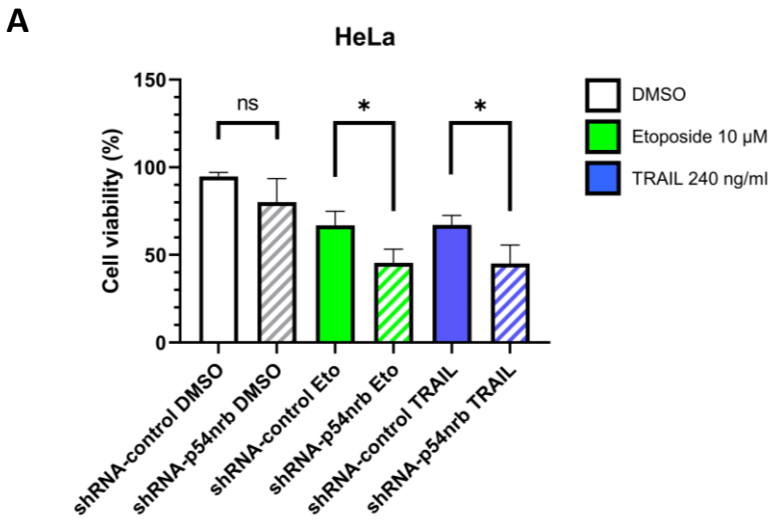

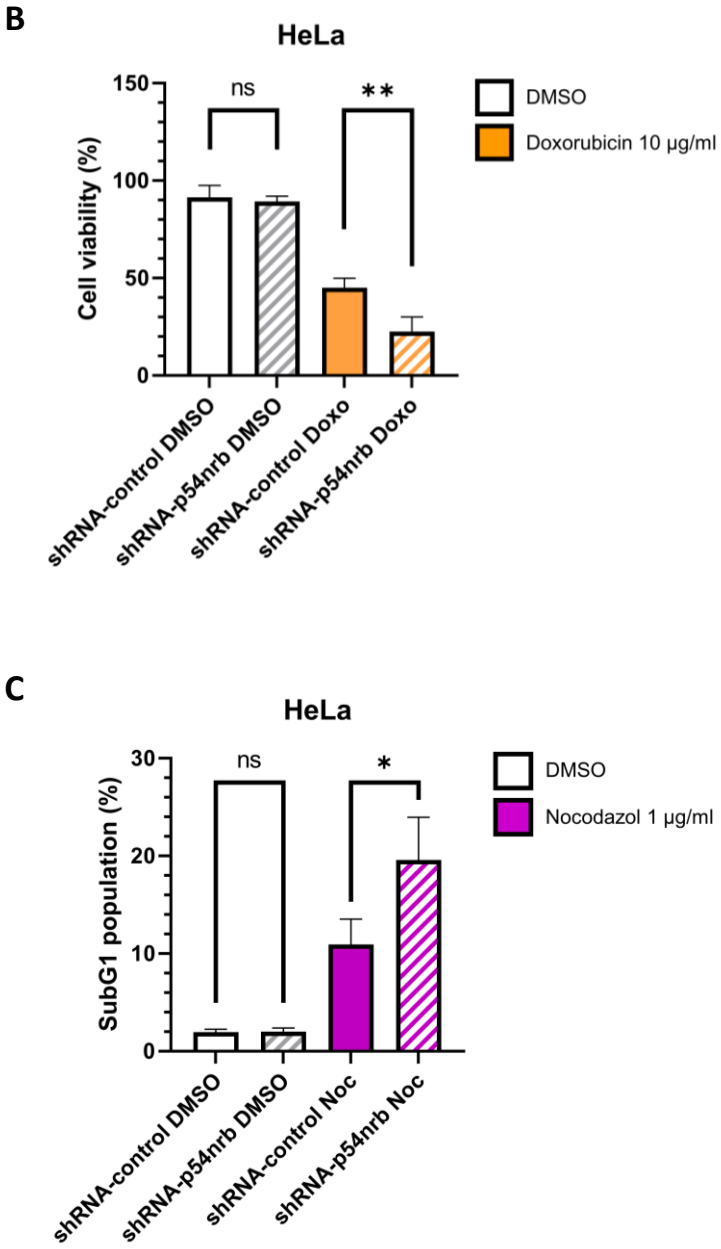

Figure 11. Cell death analysis of p54nrb depleted HeLa cells.
(A) Flow cytometry of HeLa shRNA-control and shRNA-p54nrb#3 cells at 24 h after treatment with 10 µM etoposide (Eto) and 240 ng/ml human recombinant TRAIL (TRAIL). The cell viability was measured by detection and totalling of annexin-V single positive and annexin-V and propidium-iodide double positive cells. The cells not falling to either of these categories were considered as viable cells. A significance was calculated with Student´s t test, *p<0.05, n=3. (B) Flow cytometry of HeLa shRNA-control and shRNA-p54nrb#3 cells at 24 h after treatment with 10 µg/ml Doxorubicin (Doxo). The cell viability was measured by detection and totalling of annexin-V single positive and annexin-V and Sytox Blue double positive cells. The cells not falling to either of these categories were considered as viable cells. A significance was calculated with Student´s t test, **p<0.01, n=3. (C) Flow cytometry of HeLa shRNA-control and shRNA-p54nrb#1 cells at 24 h after treatment with DMSO or 1 µg/ml Nocodazole (Noc). The percentages of the SubG1 (lower DNA content due to apoptotic DNA fragmentation) population are indicated. A significance was calculated with Student´s t test, *p<0.05, n=3 (Eichler et al., 2022).

Analog results were obtained from measurements by flow cytometry with DLD-1 colon carcinoma cells. The depletion of p54nrb alone in comparison to the control cells did not affect the viability of DLD-1 cells. However, DLD-1 cells were 10 % more susceptible to cell death under p54nrb depletion in comparison with the control cells, when stimulated with 20 µM etoposide for 24 hours (Figure 12 A).

A flow cytometry measurement of SK-MEL melanoma cells likewise showed that the depletion of p54nrb had no significant effect on viability in comparison to the control cells. SK-MEL cells, additionally stimulated with 250 nM staurosporine for 24 hours, showed 30 % more cell death under p54nrb depletion when compared with the stimulated control cells (Figure 12 B).

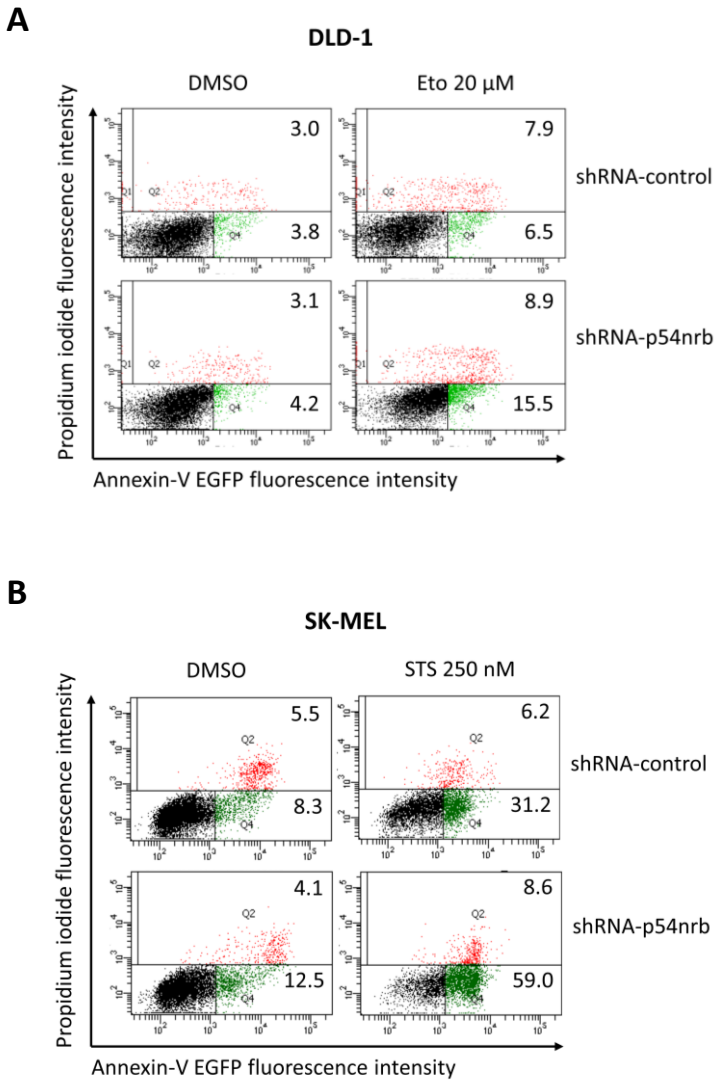

Figure 12. Cell death analysis of p54nrb depleted DLD-1 and SK-MEL cells.
(A) Flow cytometry of DLD-1 shRNA-control and shRNA-p54nrb#1 cells at 24 h after treatment with DMSO or 20 µM etoposide (Eto). Percentage of annexin-V positive (green) and propidium-iodide annexin-V double positive (red) cells are indicated. (B) Flow cytometry of SK-MEL shRNA-control and shRNA-p54nrb#1 cells at 24 h after treatment with

DMSO or 250 nM staurosporine (STS). The percentage of annexin-V positive (green) and propidium-iodide annexin-V double positive (red) cells are indicated (Eichler et al., 2022).

A minor sensitising effect towards cell death of p54nrb knockdown in HeLa cells was also measured for a shorter time of 6 hours of stimulation with a higher dose of etoposide. With depletion of p54nrb, an 11 % increase in cell death was measured by flow cytometry under stimulation with 100 µM etoposide, when compared to the stimulated control cells (Figure 13). Thus, the sensitising effect of p54nrb depletion on cell death might be restricted to a certain time period.

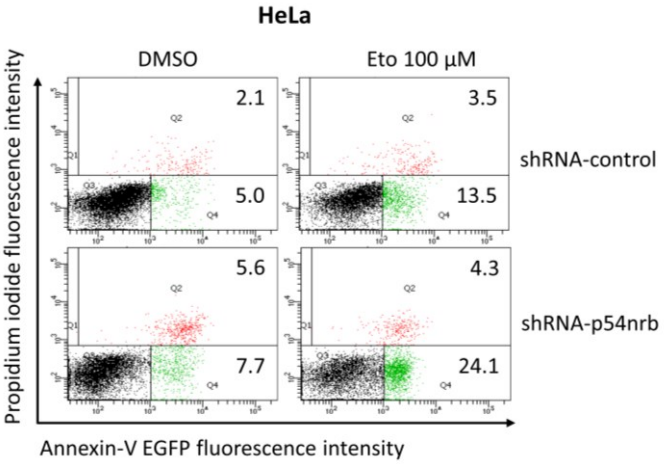

Figure 13. Cell death analysis of p54nrb depleted HeLa cells after 6 hours stimulation.
Flow cytometry of HeLa shRNA-control and shRNA-p54nrb#3 cells at 6 h after treatment with DMSO or 100 µM etoposide (Eto). The percentage of annexin-V positive (green) and propidium-iodide annexin-V double positive (red) cells are indicated (Eichler et al., 2022).

Since the proteins of the DBHS family were observed to functionally compensate each other's function by adjustment of their expression level (Knott, Bond, et al., 2016), additional experiments were made to measure the effects under transient depletion of p54nrb.

To this end, a transient p54nrb knockdown with siRNA was performed in HeLa cells (Figure 14 A) and cell death was measured by flow cytometry. A transient knockdown of p54nrb did not affect the cell viability significantly in comparison to cells transfected with control siRNA. However, administration of 60 ng/ml TRAIL over 24 hours led to increased cell death under p54nrb transient knockdown by 23 % in comparison to stimulated control cells (Figure 14 B).

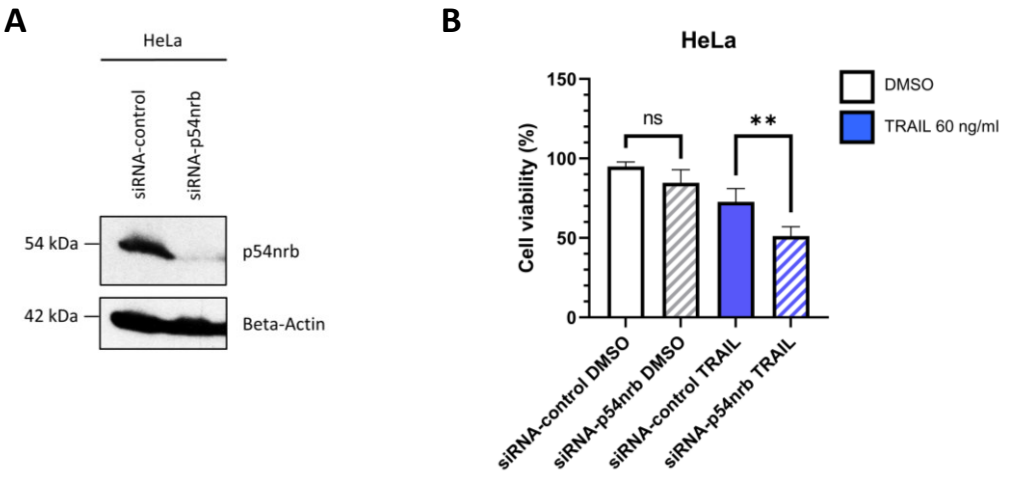

Figure 14. Cell death analysis of HeLa cells under transient p54nrb depletion.
(A) Immunoblot of the p54nrb-level in HeLa siRNA-control and siRNA-p54nrb cells. (B) Flow cytometry of HeLa siRNA-control and siRNA-p54nrb cells at 24 h after treatment with DMSO or 60 ng/ml TRAIL. The cell viability was measured by detection and totalling of annexin-V single positive and annexin-V and propidium-iodide double positive cells. The cells not falling to either of these categories were considered as viable cells. A significance was calculated with Student´s t test, **p<0.01, n=3 (Eichler et al., 2022).

3.1.4 P54nrb regulates cell death in a p53 independent manner

The tumor suppressor p53 is known to induce apoptosis in cells under high stress level. Although, in many cancer types, p53 is mutated or not expressed. To exclude a p53 dependent function of p54nrb, the p53 inhibitor pifithrin-α was applied. The administration of 30 µM pifithrin-α 1 hour prior to stimulation with 10 mM etoposide for 24 hours in p54nrb knockdown HeLa cells had no significant effect on the cell viability, compared to the cells without p53 inhibitor, as measured with flow cytometry (Figure 15). Thus, the p54nrb mediated cell death sensitisation is p53 independent in these cells.

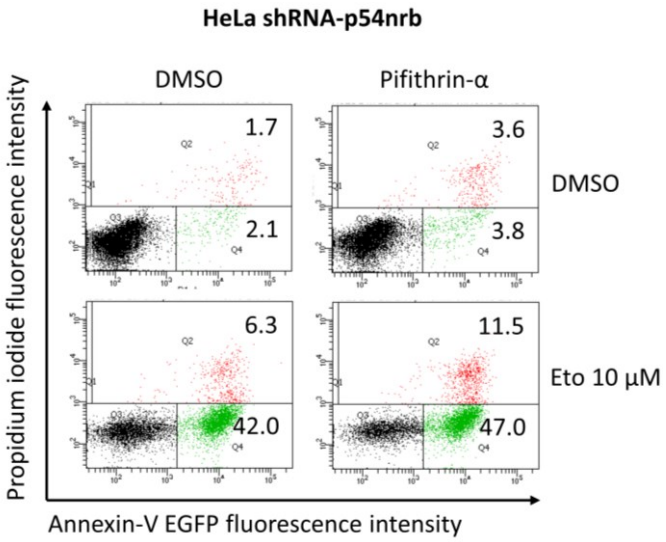

Figure 15. Cell death analysis of p54nrb depleted cells with p53 inhibitor.
Flow cytometry of HeLa shRNA-p54nrb#1 cells, 1 h prior treated with 30 µM pifithrin-α and 24 h treatment with DMSO or 10 µM etoposide (Eto). The percentage of annexin-V positive (green) and propidium-iodide annexin-V double positive (red) cells are indicated (Eichler et al., 2022).

3.1.5 P54nrb overexpression negatively affects cell death signalling

The impact of p54nrb on cell death regulation was additionally investigated by ectopic overexpression of p54nrb in shRNA-p54nrb knockdown HeLa cells with and without induction of apoptosis and subsequent measurement of the cleavage level of PARP, which is a prominent substrate downstream in the apoptotic cascade (Figure 16).

Here, the ectopic expression of the empty vector already led to a basal cleavage level of PARP. However, the ectopic overexpression of p54nrb in comparison to the empty vector in the unstimulated cells led to a reduction of the PARP cleavage ratio by about a half.

Upon stimulation with 50 µM etoposide, the cells with empty vector expression, showed about a double intense PARP cleavage level in comparison to the unstimulated empty vector expressing cells, confirming the apoptotic induction by etoposide.

An ectopic overexpression of p54nrb in the with etoposide stimulated cells led to a comparable less PARP cleavage, when compared to the empty vector expressing stimulated cells, with a reduction of the PARP cleavage ratio of about 0.5. This additionally confirms the protective role of p54nrb in cell death, which seems to act upstream of the effector caspases.

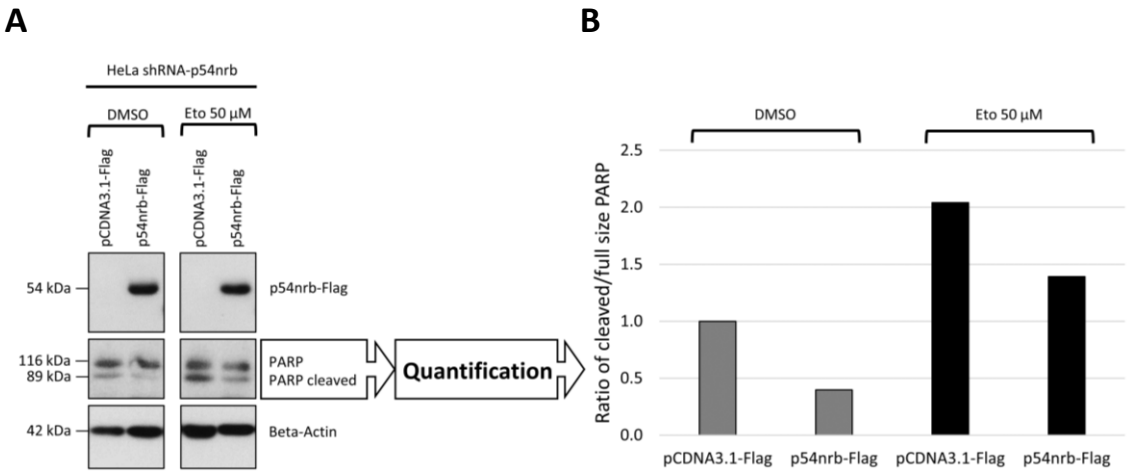

Figure 16. Effect of the p54nrb level on PARP cleavage.
(A) Immunoblot of p54nrb-Flag and PARP of HeLa shRNA-p54nrb#3 cells after ectopic overexpression of pCDNA3.1 or p54nrb-Flag plasmids for 48 h in total and a stimulation with 50 µM etoposide (Eto) for 24 h. (B) Quantification of the cleaved to full length ratio of PARP (Eichler et al., 2022).

3.1.6 Depletion of p54nrb affects the expressional level of tumorigenic proteins

P54nrb was described to have a role in transcriptional regulation (Shav-Tal & Zipori, 2002). To investigate the impact of p54nrb on the expressional regulation of tumorigenic proteins, a label free quantitative mass spectrometry of HeLa shRNA-p54nrb knockdown and control cells was performed. Proteins with significant down- or upregulation in all three biological replicates were chosen as hit (Figure 17 A) and the list of hits was further narrowed down by employing a functional annotation bioinformatics tool (Database for Annotation, Visualisation, and Integrated Discovery/DAVID) (Huang da et al., 2009).

Hereby, hits with experimentally proven relevance in key biological processes involved in cancer progression and regulation, such as cytoskeletal rearrangement, apoptosis, cell cycle regulation, and metabolic processes were selected for further investigations (Figure 17 B and C, Table 15 and Table 16). Out of these categories, candidates with strong relevance were chosen for further experimental validations.

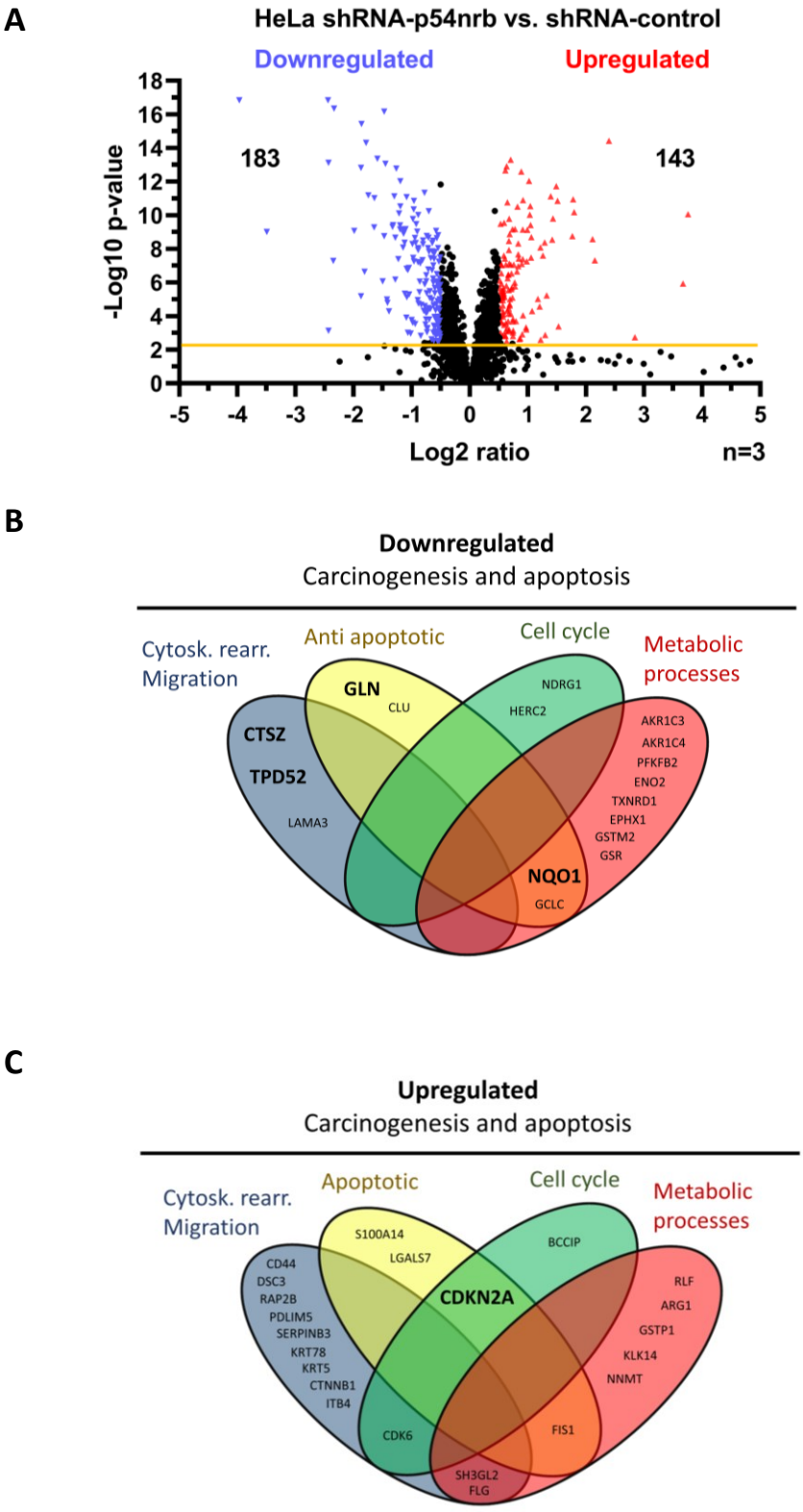

Figure 17. Identification of p54nrb dependently regulated tumorigenic proteins in HeLa cells.
(A) Volcano plot diagram of LC-MS data derived from the analysis of HeLa shRNA-control versus shRNA-p54nrb cells (n=3). Arrowheads depict 2-fold changed (X-axis) and significantly ($p<0.01$, Y-axis) upregulated (arrow up, red) and downregulated (arrow down, blue) proteins, and the total numbers of both categories are indicated on the diagram. (B) Down- and (C) up-regulated proteins ($p<0.01$, Log_2 ratio either >0.5 or <-0.5) of HeLa-shRNA-p54nrb cells compared to shRNA control cells, which exert tumor regulatory and/or apoptosis regulatory properties. Differently coloured oval diagrams represent various functional subcategories of these hits and bold written proteins were further investigated within this project (Eichler et al., 2022).

The selected candidates were validated with immunoblot detection. In HeLa cells, the proteins gelsolin (Apoptosis inhibition (Koya et al., 2000)), cathepsin-Z (Cell migration, tumor invasion, proteolysis (Wang et al., 2011; Mitrovic et al., 2017)), Tumor Protein D52 (TPD52) (Proliferation (Ummanni et al., 2008; Wang et al., 2020)), and NAD(P)H Quinone Dehydrogenase 1 (NQO1) (Metabolic processes (Zhou et al., 2019)) were confirmed being significantly downregulated. The Cyclin Dependent Kinase Inhibitor 2A (CDKN2A) (Cell cycle, tumor suppression (Liggett & Sidransky, 1998)) was significantly upregulated in HeLa shRNA-p54nrb knockdown cells (Figure 18 A and Figure 19).

The effect of p54nrb knockdown on the gelsolin and cathepsin-Z protein levels was also monitored in SK-MEL (Figure 18 B) and DLD-1 cells (Figure 18 C), whereas the protein level of TPD52 and NQO1 was not affected and the protein CDKN2A was not detectable (Figure 18 B and C).

These findings demonstrate a correlation of the protein level of p54nrb with the protein level of divers tumorigenic proteins. The expression pattern of some of these regulated proteins (TPD52 and NQO1) show a cell type dependent variability.

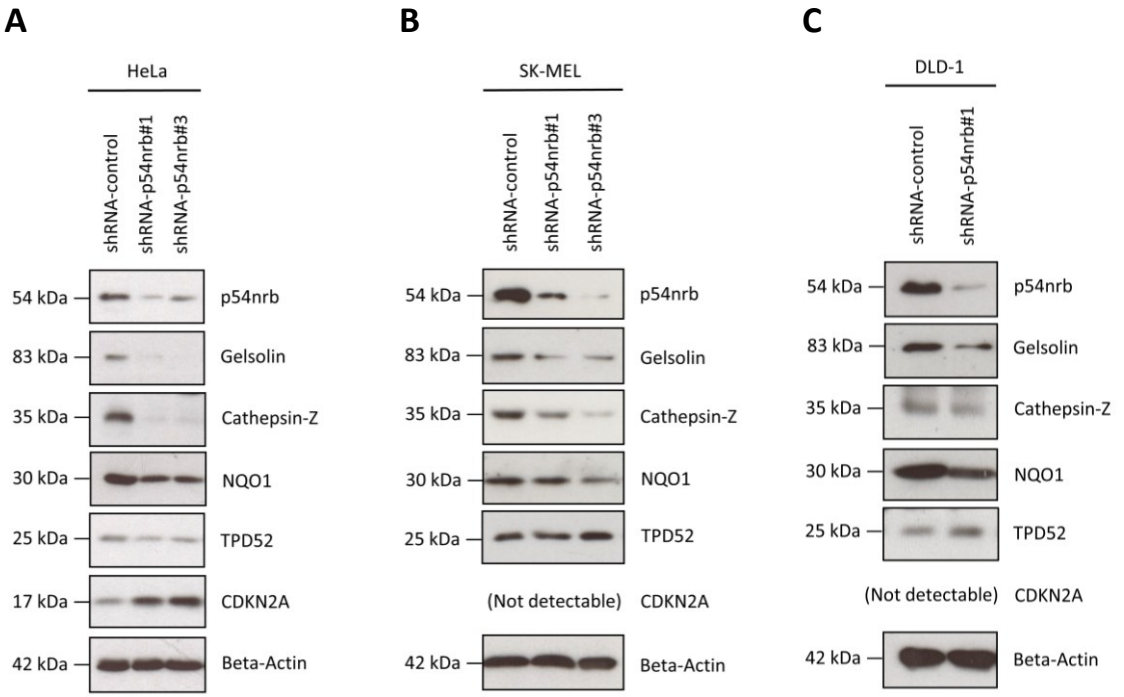

Figure 18. Altered expression level of tumorigenic proteins in p54nrb knockdown cells.
Immunoblot of the p54nrb, gelsolin, cathepsin-Z, NQO1, TPD52, and CDKN2A levels from (A) HeLa shRNA-control, shRNA-p54nrb#1, and shRNA-p54nrb#3 cells, (B) SK-MEL shRNA-control, shRNA-p54nrb#1, and shRNA-p54nrb#3 cells, and (C) DLD-1 shRNA-control and shRNA-p54nrb#1 cells. Modified from Eichler et al. (2022).

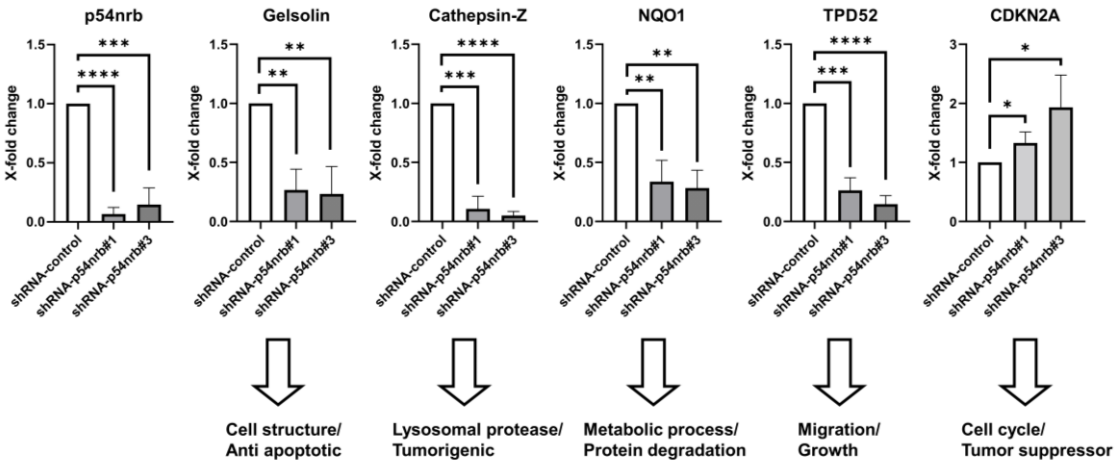

Figure 19. Quantification of the expression level of tumorigenic proteins in p54nrb depleted HeLa cells.
Quantitative analysis of immunoblots of p54nrb, Gelsolin, Cathepsin-Z, NQO1, and TPD52 from HeLa shRNA-control and shRNA-p54nrb#1 and #3 cells (Figure 18 A). Their functions in tumor/apoptosis regulatory processes are indicated under each diagram. Student´s t test was employed to test significance with *p<0.05, **p<0.01, ***p<0.001, ****p<0.0001, n=3 (Eichler et al., 2022).

3.2 Identification of p54nrb as a novel caspase-2 substrate

As presented in the chapter 3.1, p54nrb plays a role in directing tumorigenesis and cell fate. To investigate the functional role of p54nrb in cell death, further experimental approaches were performed to elucidate its mechanistic relations within the apoptotic cascade.

3.2.1 P54nrb is cleaved upon apoptotic induction in a caspase-2 dependent manner

Originally, p54nrb was predicted as a caspase-3 substrate *in vitro* (Thiede et al., 2001). Indeed, when HeLa cells were stimulated with staurosporine, a model compound for intrinsic apoptotic induction, lower molecular weight fragments, characteristic of substrates cleaved by caspases were observed. By employing western blot, the detected fragments of p54nrb appeared approximately at the level of the protein marker bands of 51 and 48 kDa (Figure 20 A and B). The p54nrb cleavage under apoptotic stimulation with staurosporine or etoposide was also detected in DLD-1 colon carcinoma cells (Figure 22 C and D) and SK-MEL melanoma cells (Figure 20 D and E).

The application of pan-caspase inhibitor z-VAD-fmk prior to the apoptotic induction prevented the p54nrb cleavage (Figure 20 A). To confirm the prediction of p54nrb being a caspase-3 substrate, the specific caspase-3 inhibitor AQZ-1 was employed. However, this inhibitor did not

hamper the p54nrb cleavage (Figure 20 A). Instead, the administration of specific caspase-2 inhibitor z-VDVAD-fmk prevented the occurrence of p54nrb cleavage induced by staurosporine and etoposide (Figure 20 B). In accordance with this, alpha toxin, a bacterial pore forming toxin from *Staphylococcus aureus,* known to induce caspase-2 activation (Imre et al., 2012; Imre & Rajalingam, 2012), led likewise to p54nrb cleavage (Figure 20 C).

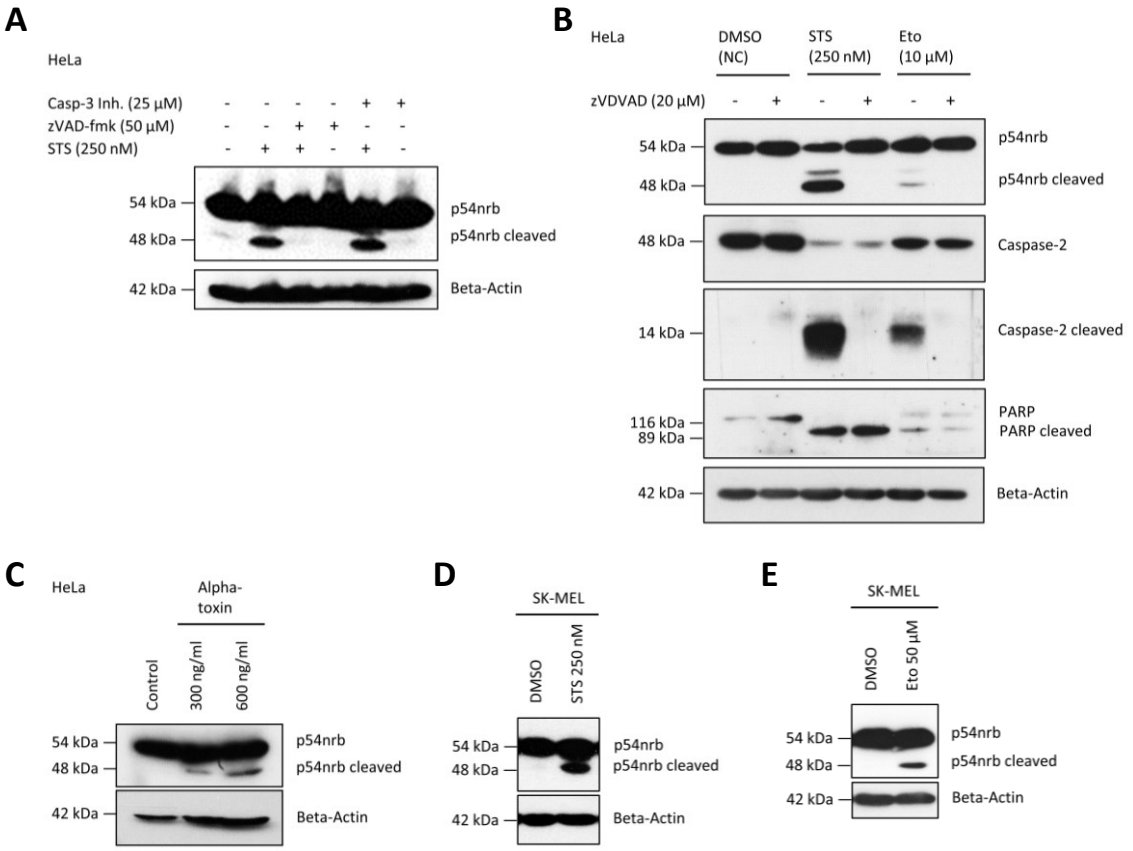

Figure 20. P54nrb cleavage upon apoptotic stimulation and caspase inhibition.
(A) Immunoblot of p54nrb cleavage in HeLa cells treated with a general caspase inhibitor (50 µM Z-VAD-fmk) or a non-peptide caspase-3 inhibitor (25 µM AQZ1) 1 h prior to 24 h treatment with 250 nM staurosporine (STS). (B) Immunoblot of p54nrb cleavage, caspase-2 activation, and PARP cleavage in HeLa cells at 24 h after treatment with DMSO or 20 µM Z-VDVAD-fmk (-1 h) and 250 nM staurosporine (STS) or 10 µM etoposide (Eto). (C) Immunoblot of p54nrb cleavage in HeLa cells at 24 h after treatment with 300 and 600 ng/ml alpha toxin. (D) Immunoblot of p54nrb cleavage in SK-MEL cells at 24 h after treatment with 250 nM staurosporine (STS). (E) Immunoblot of p54nrb cleavage in SK-MEL cells at 24 h after treatment with 50 µM etoposide (Eto). Figures from Eichler et al. (2022), except E.

The following aim was to confirm caspase-2 dependency with several approaches. First, ectopic overexpression of active caspase-2 and caspase-3 in HeLa cells was performed. Supporting the previous findings, caspase-2 overexpression led to p54nrb cleavage in a concentration dependent way (Figure 21). On the other hand, overexpression of the effector caspase-3 did not cause p54nrb cleavage (Figure 21). Likewise, the overexpression of effector caspase-7 did not

lead to p54nrb cleavage (Figure 21 B). Moreover, ectopic expression of inactive caspase-2, with a mutation at cysteine 303 of its active centre, did not result in p54nrb cleavage (Figure 21 B). This proves that the p54nrb cleavage is dependent on caspase-2 activity.

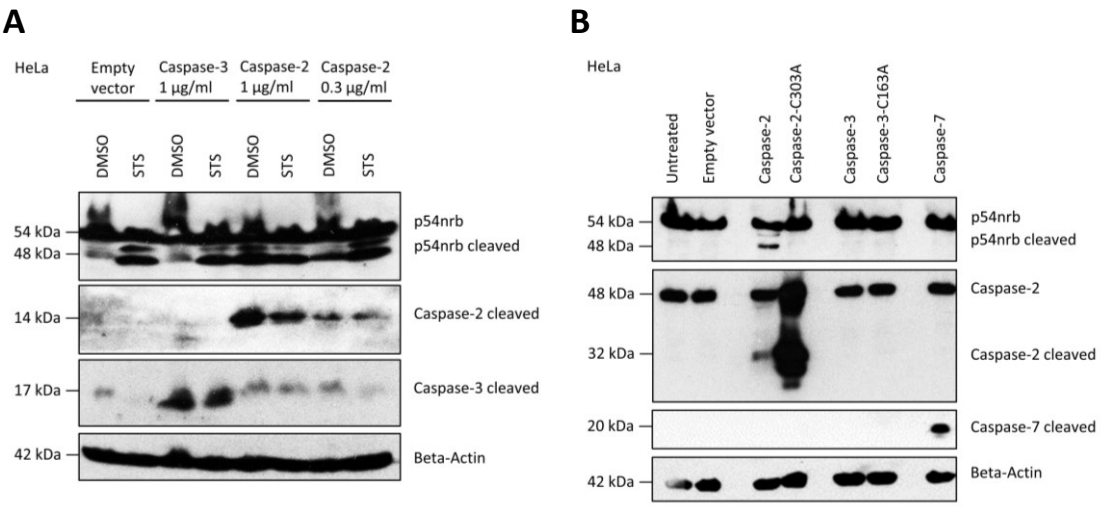

Figure 21. P54nrb cleavage upon ectopic expression of caspase-2.
(A) Immunoblot of p54nrb cleavage and caspase expression in HeLa cells. HeLa cells were transfected either with 300 or 1000 ng/ml pcDNA3-caspase-2-Flag or pcDNA3-caspase-3-myc. After 24 hthe cells were treated either with DMSO or 250 nM staurosporine (STS) for further 24 h. (B) Immunoblot of p54nrb cleavage in HeLa cells at 48 h after ectopic expression of 1 µg/ml pcDNA3-Flag, pcDNA3-caspase-2-Flag, pcDNA3-caspase-2-C303A-Flag, pcDNA3-caspase-3-myc, pcDNA3-caspase-3-C163A-myc and pcDNA3-caspase-7-Flag (Eichler et al., 2022).

A second approach to confirm caspase-2 dependency was the application a genetic depletion of caspase-2. To this end, stable shRNA knockdown of caspase-2 in HeLa cells (Figure 22 A and B) and CRISPR-Cas-9 caspase-2 depletion in DLD-1 cells (Figure 22 C and D) was generated. Under induction of apoptosis with either staurosporine or etoposide, the p54nrb cleavage was diminished in both caspase-2 depleted cells lines, in HeLa (Figure 22 A and B) and in DLD-1 cells (Figure 22 C and D).

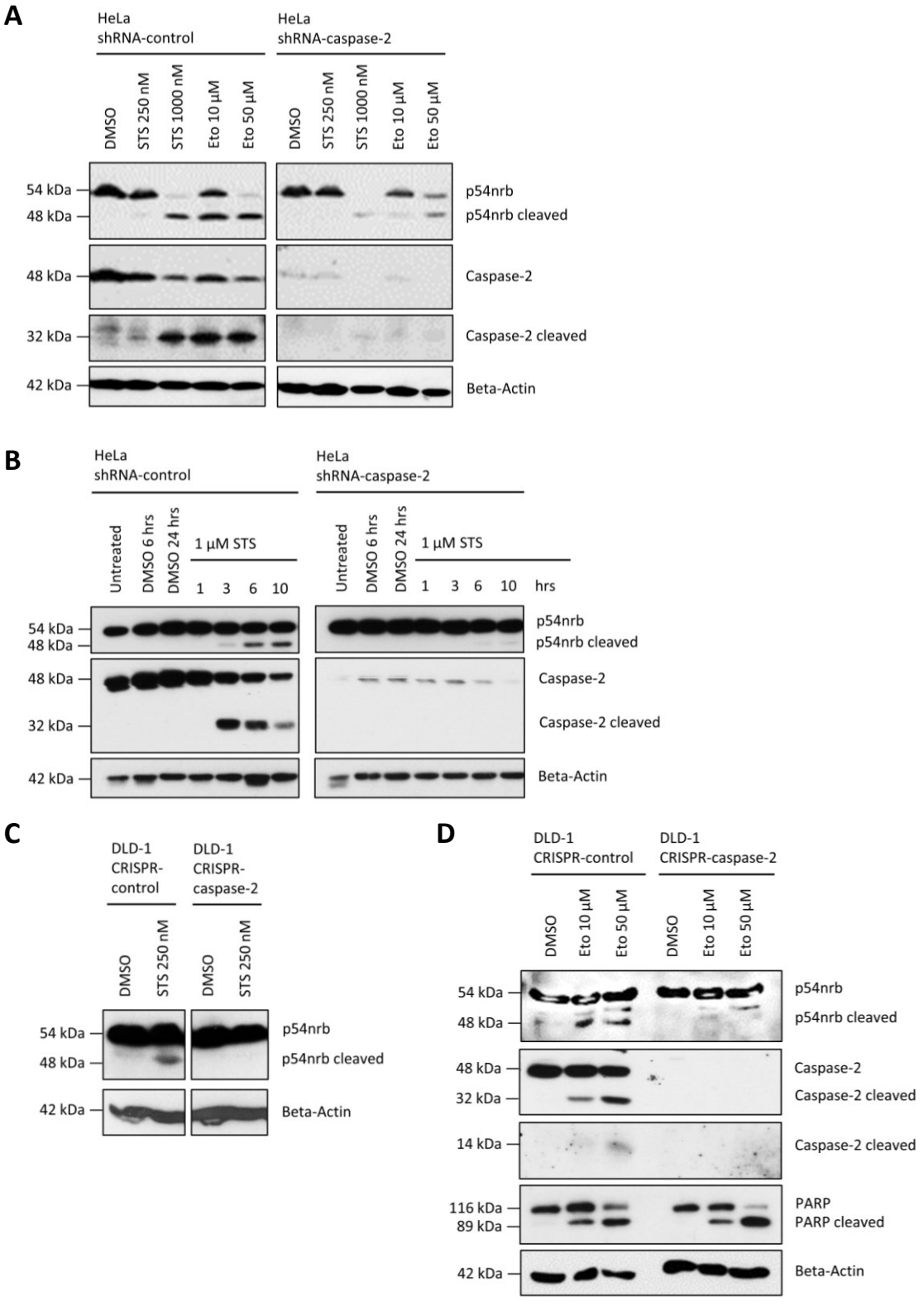

Figure 22. Caspase-2 depletion prevents p54nrb cleavage under apoptotic induction.
(A) Immunoblot of p54nrb cleavage and caspase-2 activation in HeLa shRNA-control and shRNA-caspase-2 cells, 24 h after treatment with DMSO, 250 nM or 1µM staurosporine (STS), or 10 µM etoposide (Eto). (B) Immunoblot of p54nrb cleavage and caspase-2 activation in HeLa shRNA-control and shRNA-caspase-2 cells with 1 µM staurosporine stimulation with different incubation times as indicated. (C) Immunoblot of p54nrb cleavage in DLD-1 CRISPR-control and DLD-1 CRISPR–caspase-2 cells, 24 h after treatment with DMSO or 250 nM staurosporine (STS). (D) Immunoblot of p54nrb cleavage, caspase-2 activation, and PARP cleavage in DLD-1 CRISPR-control and DLD-1 CRISPR–caspase-2 cells, 24 h after treatment with DMSO, 10 µM, or 50 µM etoposide (Eto) (Eichler et al., 2022).

In order to confirm the interaction between caspase-2 and p54nrb, an endogenous immunoprecipitation of p54nrb was performed. The subsequent immunoblot detection proved a simultaneous precipitation of caspase-2 with p54nrb. In contrast, a co-precipitation of caspase-3 with p54nrb could not be confirmed (Figure 23). This demonstrated an interaction of p54nrb with caspase-2.

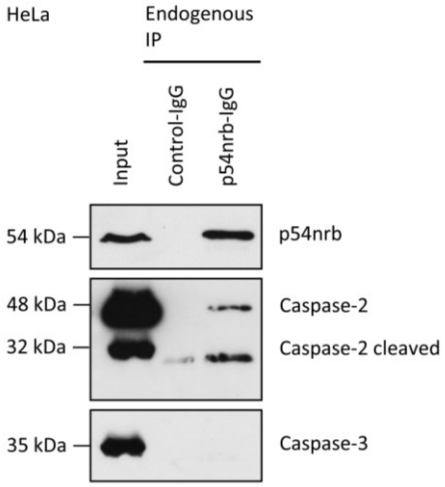

Figure 23. Endogenous co-precipitation of caspase-2 with p54nrb.
Immunoblot of p54nrb, caspase-2, and caspase-3 after endogenous immunoprecipitation of p54nrb from HeLa cells (Eichler et al., 2022).

To exclude intermediate factors in the interaction and to prove the proteolytic function of caspase-2 on p54nrb, an *in vitro* cleavage assay was carried out. Recombinant p54nrb and active recombinant caspase-2 or active recombinant caspase-3 were co-incubated, and p54nrb cleavage was subsequently detected via immunoblot. The presence of active caspase-2 caused a p54nrb cleavage in a concentration dependent manner. In contrast, caspase-3 resulted only in minor p54nrb cleavage only at the high concentration of 4 U (Unit) (Figure 24). With this, a direct correlation of caspase-2 activity and cleavage of p54nrb was verified.

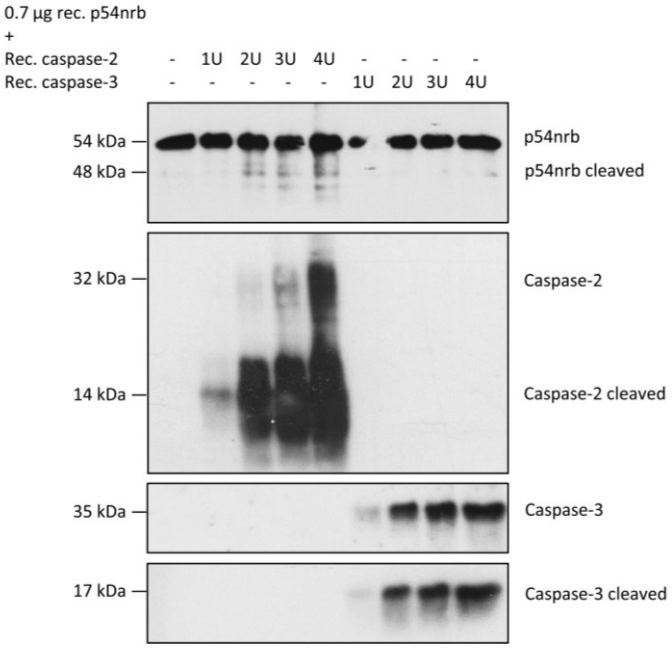

Figure 24. In vitro cleavage of p54nrb by caspase-2.
Immunoblot of p54nrb, caspase-2, and caspase-3 after an *in vitro* caspase cleavage assay with recombinant p54nrb and human recombinant active caspase-2 or caspase-3 after 6 h incubation at 37 °C (Eichler et al., 2022).

3.2.2 Caspase-2 co-localisation with p54nrb in the nucleus

Since caspase-2 has a unique subcellular localisation in the nucleus, which implicates a compartment specific role (Ando et al., 2017), a subcellular fractionation approach was applied to further determine the interaction of p54nrb with caspase-2. Herewith, p54nrb's localisation in the nucleus could be demonstrated and the localisation of caspase-2 was validated in the nucleus, as well as in the cytoplasmic fraction by employing subcellular fractionation and immunoblot detection (Figure 25). In addition, a confocal microscopy of stained HeLa cells further confirmed the nuclear localisation of p54nrb (Figure 26).

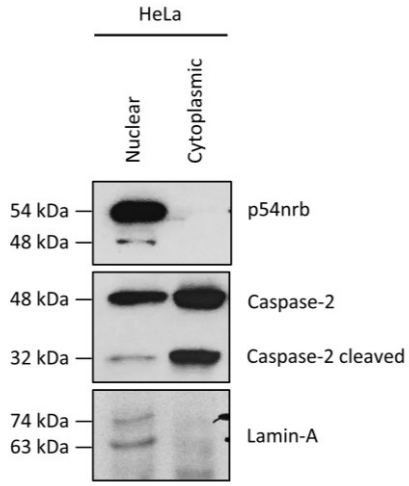

Figure 25. Subcellular distribution of p54nrb and caspase-2.
Immunoblot of p54nrb and caspase-2 of a nuclear and cytoplasmic fraction of HeLa cells. Lamin-A was detected as nuclear marker (Eichler et al., 2022).

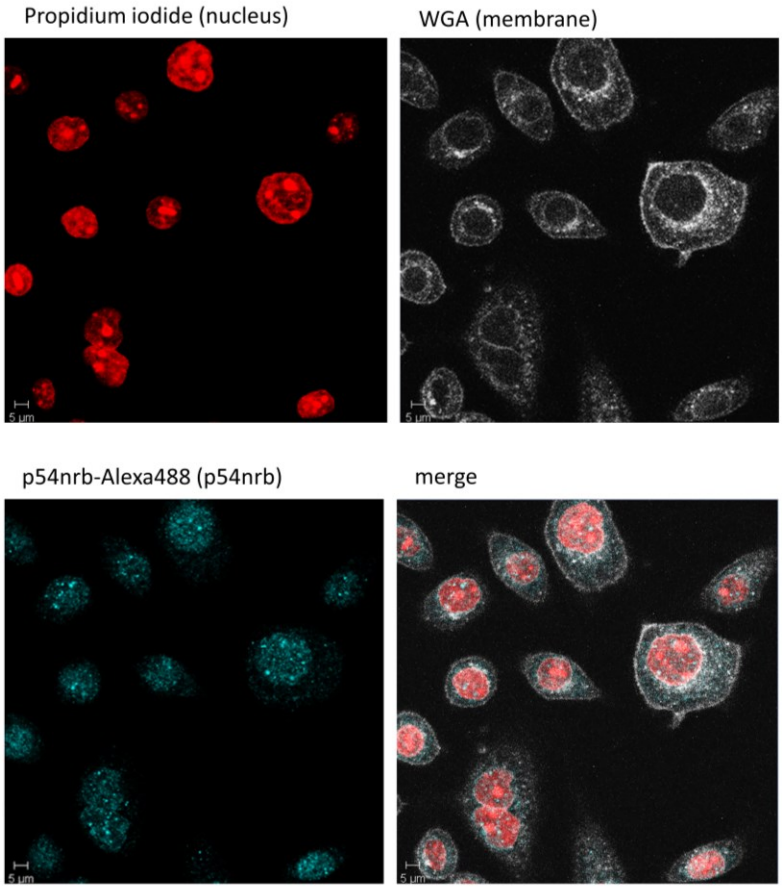

Figure 26. Confocal microscopy of p54nrb.
Fluorescence microscopy of HeLa cells stained with 1 µg/ml propidium iodide (red), 5 µg/ml Wheat Germ Agglutinin (WGA) (white), and 2 ng/µl Anti-p54nrb-Alexa-488 (cyan). Scale bar: 5 µm.

Additionally, confocal microscopy of HeLa cells with staining of p54nrb (green) and caspase-2 (red) revealed a co-localisation in the nucleus in a dot-like manner (yellow) (Figure 27).

The co-localisation of p54nrb and caspase-2 was monitored endogenously (Figure 27 A), as well as with ectopic overexpression of caspase-2 (Figure 27 B and C). This provides a further proof, that p54nrb and caspase-2 co-exist in the same location within the nucleus.

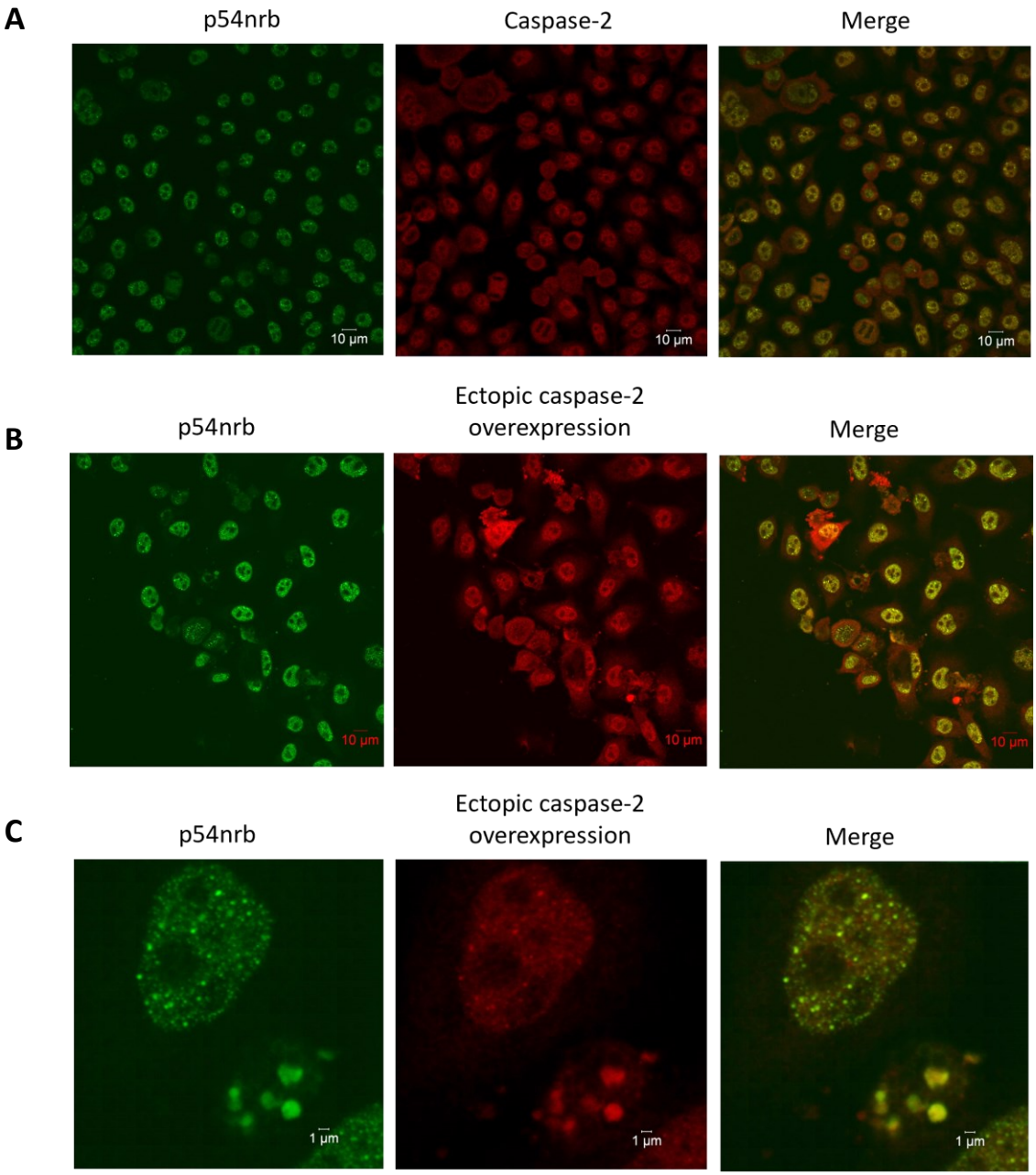

Figure 27. Confocal microscopy of the co-localisation of p54nrb and caspase-2.
Fluorescence microscopy of HeLa cells (A) without and (B) with 1 µg/ml caspase-2 (pCDNA3.1-Caspae-2-Flag) overexpression for 24 h, stained with 2 ng/µl Anti-p54nrb-Alexa-488 (green) and Anti-caspase-2-Alexa-647 (red). 10 µm scale is indicated. (C) Single cell close-up from caspase-2 overexpressing cells. 1 µm scale is indicated (Eichler et al., 2022).

3.2.3 Caspase-2 cleaves p54nrb at aspartate D422

Since caspases cleave their substrates at aspartate (D) residues of specific tetra motifs following the pattern of DXXD (X = any amino acid) (Fava et al., 2012), the sequence of p54nrb was analysed to find potential cleavage sites which can result in the fragment sizes of 48 and 51 kDa. Two potential cleavage sites were found in the amino acid sequence of p54nrb at the aspartate residue D58 and D422 (Figure 28 A).

For validation, a point mutation in the p54nrb encoding amino acid sequence was administrated, at aspartate D58 or D422, where the codons encoding aspartate residues (D) were exchanged to the codons of asparagine (N). These p54nrb mutants were ectopically overexpressed in p54nrb depleted HeLa cells and additionally treated with etoposide. The etoposide treatment resulted in p54nrb cleavage in the cells overexpressing wildtype p54nrb and p54nrb-D/N58, but not in the cells with p54nrb-D/N422 overexpression (Figure 28 B). This proves that the p54nrb cleavage occurs at the aspartate residue D422.

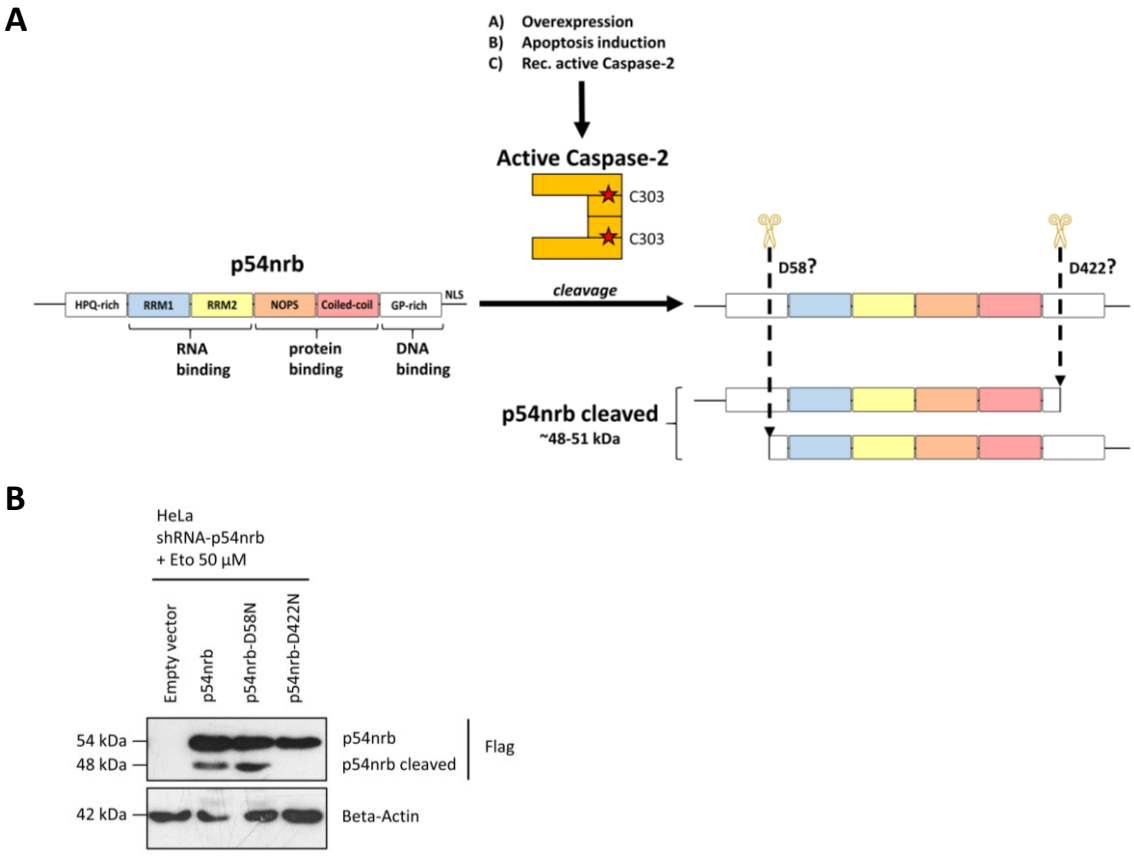

Figure 28. Caspase-2 cleaves p54nrb at D422.
(A) Graphical illustration of p54nrb cleavage by activated caspase-2 via either overexpression, apoptotic induction, or recombinant caspase-2 protein. The active site of the caspase-2 dimer is marked with red stars. The location of the

putative cleavage sites in the p54nrb protein domains are marked with arrows and its anticipated cleavage fragments are shown. Modified from Eichler et al. (2022). (B) Immunoblot of p54nrb cleavage in HeLa shRNA-p54nrb#1 cells after ectopic expression of pcDNA3-Flag, pFlag-p54nrb, pFlag-p54nrb-D/N58, and pFlag-p54nrb-D/N422 (1 µg/ml plasmid) for 24 h and further 24 h treatment with 50 µM etoposide (Eto) (Eichler et al., 2022).

3.2.4 Caspase-2 is dispensable in the apoptotic pathway

It is known that caspase-2 knockout does not generally inhibit apoptosis upon cell death induction (Bouchier-Hayes & Green, 2012). Therefore, caspase-2 does not exclusively exert an apoptotic function but can act as a feedback enhancer or might even act outside the classical apoptotic cascade, exerting non-apoptotic functions. Caspase-2's minor role in the apoptotic pathway could be demonstrated in this study by detection of unaffected PARP cleavage under apoptotic stimulation with etoposide, staurosporine, and doxorubicin in shRNA-caspase-2 depleted HeLa cells. Detected by immunoblot, the processing of PARP is not affected in the caspase-2 depleted cells, compared to the control cells (Figure 29 A). Also, in CRISPR-caspase-2 depleted DLD-1 cells the PARP cleavage is not reduced in comparison to the control cells under stimulation with etoposide or staurosporine (Figure 29 B).

This implicates, that p54nrb cleavage by caspase-2 is dispensable for the apoptotic cascade and might serve as a pro-apoptotic feedback loop or takes place in the exertion of caspase-2's non-apoptotic functions.

A

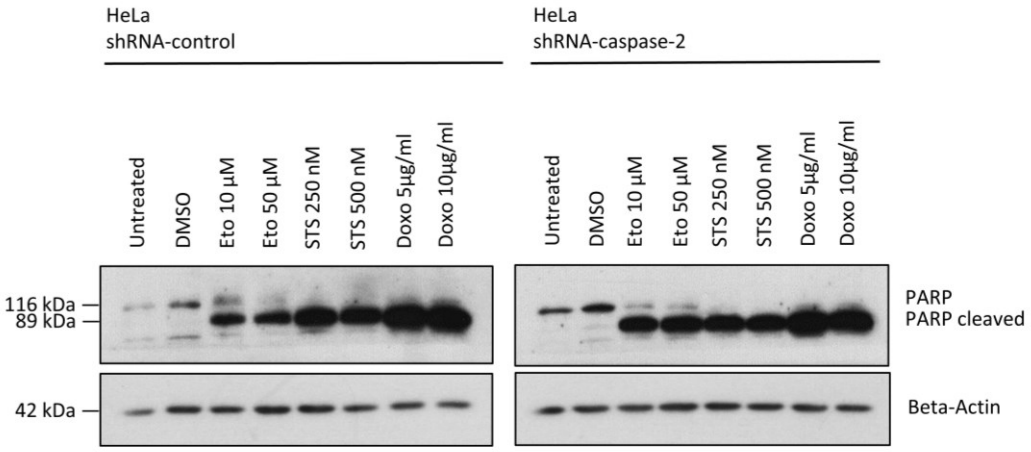

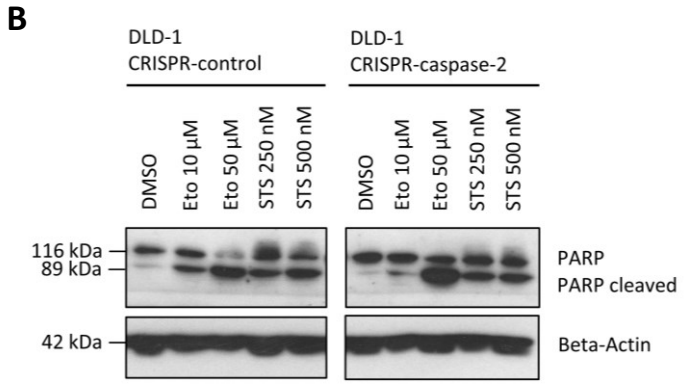

Figure 29. Caspase-2 depletion does not inhibit PARP cleavage under apoptotic induction.
(A) Immunoblot of PARP cleavage in HeLa shRNA-control and shRNA-caspase-2 cells, 24 h after stimulation as with DMSO, 10 or 50 µM etoposide (Eto), 250 or 500 nM staurosporine (STS), or 5 or 10 µg/ml doxorubicin (Doxo). (B) Immunoblot of PARP cleavage in DLD-1 CRISPR-control and CRISPR-caspase-2 cells after 24 h stimulation with DMSO, 10 or 50 µM etoposide (Eto), or 250 or 500 nM staurosporine (STS) (Eichler et al., 2022).

3.2.5 P54nrb cleavage is p53 independent

It is known that caspase-2 activity also leads to cleavage of the endogenous inhibitor of p53, MDM2, which subsequently leads to stabilisation of p53 and mediation of cell cycle arrest and apoptosis (Lim, Dorstyn, et al., 2021). To examine if the p54nrb cleavage occurs independent of p53 signalling, two experiments were performed.

In HeLa cells, treated with the p53 inhibitor pifithrin-α prior to stimulation with staurosporine, etoposide, or doxorubicin, the execution of p54nrb cleavage and the activation of apoptosis were not affected (Figure 30 A). RKO cells, expressing wildtype p53, stimulated with etoposide, staurosporine, or doxorubicin showed p54nrb cleavage (Figure 30 B). In comparison, DLD-1 cells, expressing mutated p53, likewise showed p54nrb cleavage upon apoptotic stimulation (Figure 22 C and D). These data show, that the process of p54nrb cleavage occurs in a p53 independent manner.

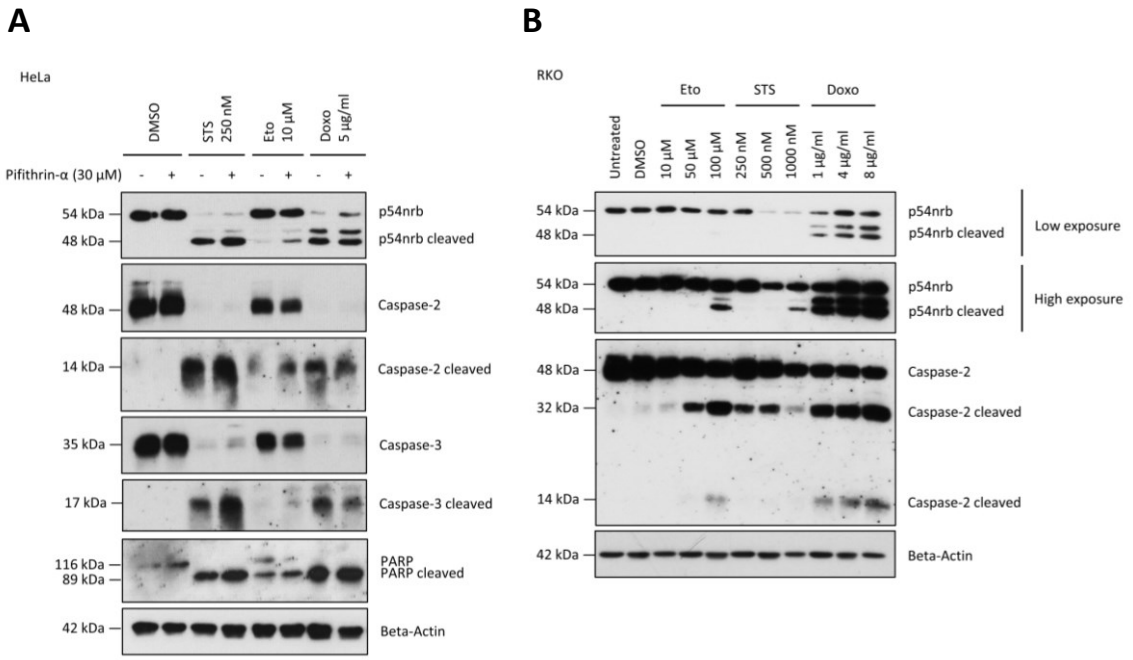

Figure 30. P53 independent cleavage of p54nrb.
(A) Immunoblot of p54nrb, caspase-2, caspase-3, and PARP cleavage in HeLa cells treated with 30 µM pifithrin-α (-1 h) and treated with DMSO, 250 nM staurosporine (STS), 10 µM etoposide (Eto), or 5 µg/ml doxorubicin (Doxo). (B) Immunoblot of p54nrb and caspase-2 cleavage in RKO cells treated with DMSO, Eto (10, 50, and 100 µM), STS (250, 500, and 1000 nM), or Doxo (1, 4, and 8 µg/ml) for 24 h (Eichler et al., 2022).

3.3 P54nrb cleavage by caspase-2 disrupts its transcriptional regulatory function

The subsequent aim was to demonstrate a direct link between the cleavage of p54nrb by caspase-2 and its function in tumorigenesis, based on a potential expressional regulation of tumorigenic proteins, as p54nrb was shown to have a role in transcriptional regulation (Knott, Bond, et al., 2016).

3.3.1 P54nrb cleavage affects the protein level of cathepsin-Z and gelsolin

We hypothesised, that p54nrb cleavage results in the loss of its regulatory function, which in turn would result in the same effect as a depletion of p54nrb. To validate this hypothesis, HeLa cells were stimulated with various compounds to induce apoptosis and the cleavage of p54nrb, and the protein level of cathepsin-Z and gelsolin were detected via immunoblot (Figure 31). The protein level of both, cathepsin-Z and gelsolin, were reduced when p54nrb was cleaved. Furthermore, the protein level correlated with the level of full length p54nrb. The level of

cathepsin-Z was reduced only under strong p54nrb cleavage (Figure 31 A), whereas the level of gelsolin was already reduced under slight p54nrb cleavage (Figure 31 B).

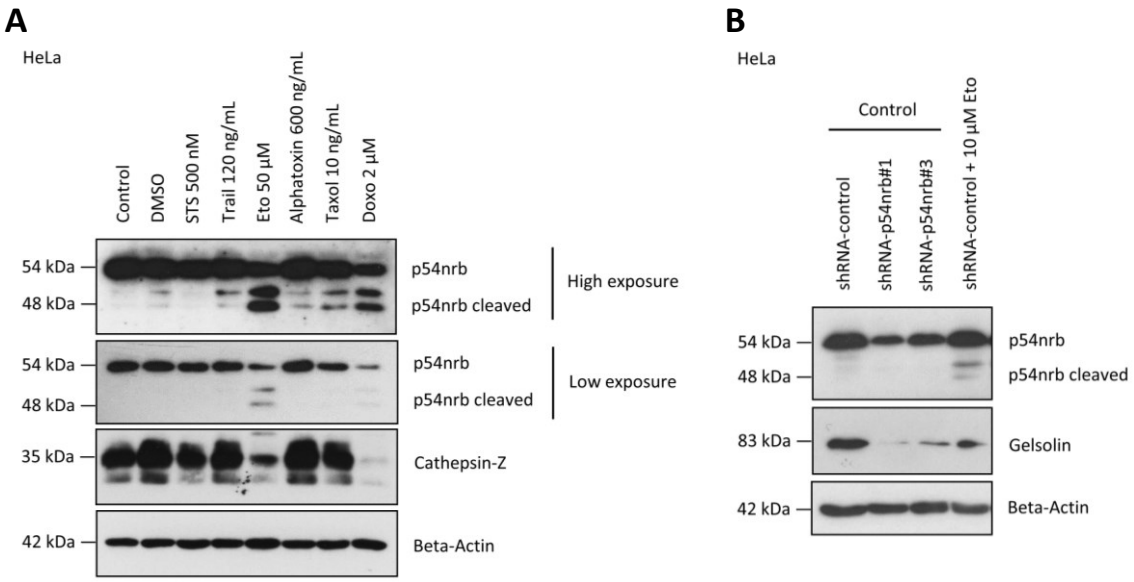

Figure 31. P54nrb cleavage level affects the level of cathepsin-Z and gelsolin.
(A) Immunoblot of p54nrb cleavage and cathepsin-Z in HeLa cells, 24 h after treatment with DMSO, 500 nM staurosporine (STS), 120 ng/ml TRAIL, 50 µM etoposide (Eto), 600 ng/ml alpha toxin, 10 ng/ml taxol, and 2 µM doxorubicin (Doxo) (Eichler et al., 2022). (B) Immunoblot of p54nrb cleavage and gelsolin in HeLa shRNA-control, shRNA-p54nrb#1, and #3 cells, and shRNA-control cells with 10 µM etoposide stimulation for 24 h.

3.3.2 P54nrb interacts with cathepsin-Z and gelsolin DNA

The multipurpose scaffold protein p54nrb was previously demonstrated to have a role in transcriptional regulation (Knott, Bond, et al., 2016). P54nrb contains a putative DNA binding site at the C-terminus. The cleavage of p54nrb at aspartate D422 is located in the same region (Figure 28). Therefore, it was investigated whether p54nrb regulates the transcription via interaction with the DNA sequences of the cathepsin-Z and gelsolin genes or their translation via interaction with their mRNA.

An endogenous precipitation of p54nrb from HeLa cells was performed with a subsequent ribonucleoprotein or chromatin immunoprecipitation. The co-precipitated nucleic acids, either DNA (Figure 32 -1) or RNA (Figure 32 -2), were isolated. RNA was transcribed into cDNA and analysed in comparison with isolated DNA by running a PCR, using primers to amplify a fragment of the cathepsin-Z or gelsolin encoding sequences.

An amplified fragment of the cathepsin-Z and gelsolin encoding sequences in the isolates of co-precipitated DNA was detected with agarose gel electrophoresis (Figure 32 B-1). In contrast, no amplification from the cDNA derived from the cathepsin-Z or gelsolin encoding mRNA sequences (Figure 32 B-2).

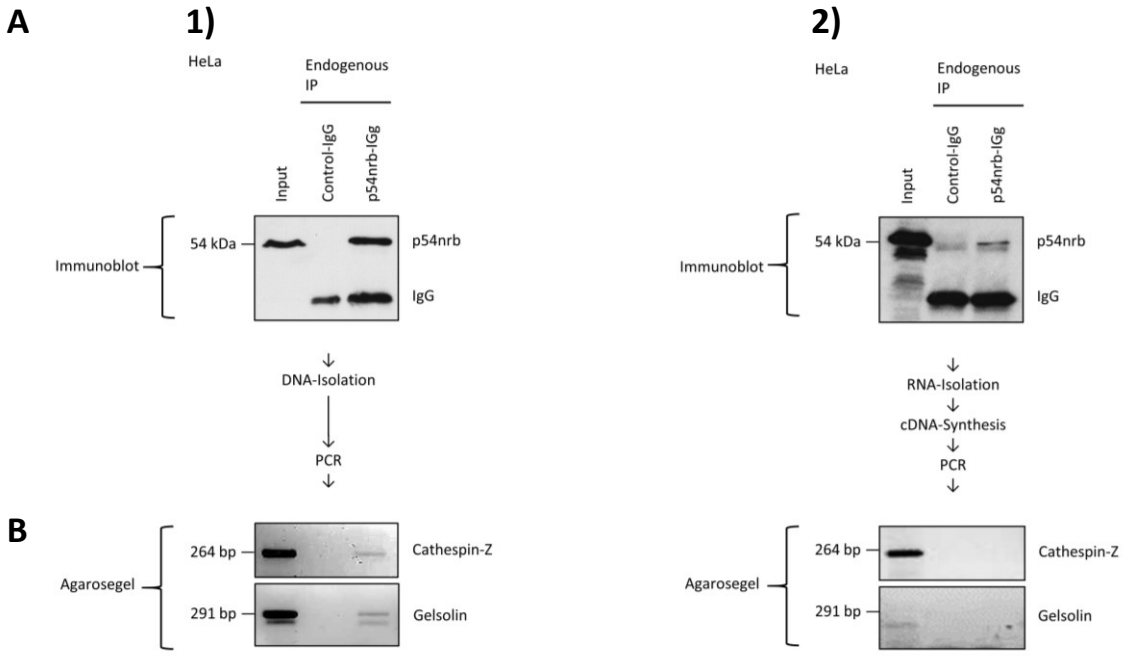

Figure 32. Endogenous co-precipitation of p54nrb binding nucleic acids.
(A) Endogenous immunoprecipitation (eIP) of p54nrb, validated by immunoblot, linked with (1) chromatin (ChIP) or (2) ribonucleoprotein (RIP) co-immunoprecipitation and a subsequent isolation of DNA or RNA (coupled with cDNA-synthesis). (B) Validation of co-precipitated nucleic acids of cathepsin-Z or gelsolin encoding sequences by PCR with the isolates of the eIP, and the subsequent agarose gel electrophoretic detection (Eichler et al., 2022).

The direct binding of p54nrb to the gelsolin encoding DNA sequence was further confirmed by a newly designed *in vitro* assay. To this end, recombinant p54nrb was incubated with plasmid DNA, containing the coding sequence of gelsolin. After immunoprecipitation of p54nrb (Figure 33 A), DNA isolation was performed with a subsequent PCR to amplify a fragment of the gelsolin encoding gene (Figure 33 B). The amplified fragment of the gelsolin encoding sequence was detected with agarose gel electrophoresis. The result is in accordance with the previous findings and points out the regulatory interaction of p54nrb on DNA level with the gelsolin encoding sequence.

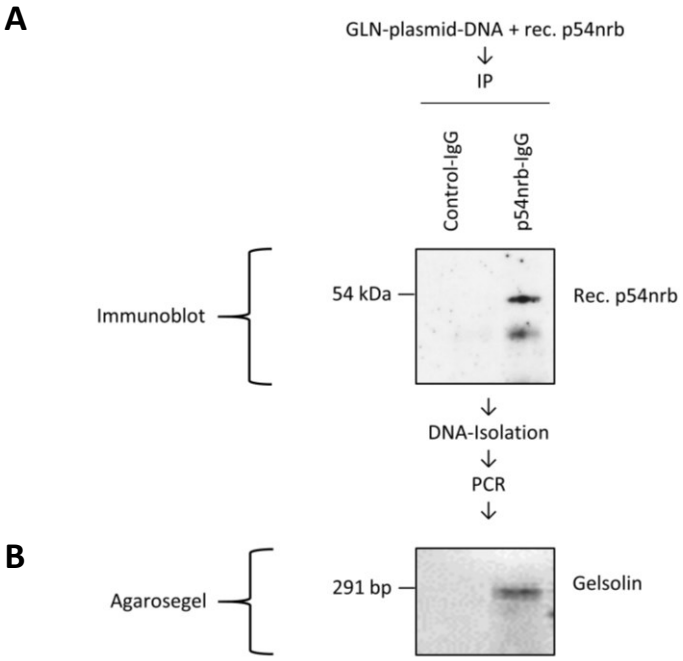

Figure 33. In vitro binding assay of recombinant p54nrb and gelsolin DNA.
In vitro p54nrb/DNA binding assay. 0.5 µg human recombinant p54nrb (Origene, Rockville, MD USA) and 100 ng plasmid, containing the coding sequence of gelsolin (Ch-gelsoln) [#37262] [Addgene]) were incubated at 37 °C for 18 h. Immunoprecipitation (IP) was performed by employing either p54nrb antibody or the same amount and species of IgG as control. P54nrb was detected by immunoblot (A). Next, the DNA was isolated as described (see ChIP assay). and the co-precipitation of the gelsolin DNA was confirmed by PCR, employing gelsolin-specific primers and the subsequent agarose gel electrophoresis detection (B) (Eichler et al., 2022).

4 Discussion

4.1 Identification of p54nrb as a novel caspase-2 substrate

Caspase-2 is the evolutionary most conserved, yet strongly understudied member of the caspase family. To understand the mechanistic and functional role of caspase-2, the identification of novel caspase-2 specific substrates is fundamental. Although around 250 caspase-2 substrates are catalogued based on their sequence in the MEROPS database, so far, only a dozen of them were experimentally confirmed (Brown-Suedel & Bouchier-Hayes, 2020).

In this study, p54nrb was identified as a direct and specific substrate of caspase-2. Induction of apoptosis with staurosporine or chemotherapeutic compounds, such as etoposide or doxorubicin led to caspase-2 activation and subsequent cleavage of p54nrb to smaller fragments, in a similar pattern as other caspase substrates (Julien & Wells, 2017). Consequently, a specific enzymatic inhibition or genetic depletion of caspase-2 prevented the cleavage of p54nrb. In line with these findings, ectopic overexpression of active caspase-2 or administration of recombinant active caspase-2 *in vitro* likewise led to p54nrb cleavage. A physical interaction of p54nrb with caspase-2 was shown by means of co-immunoprecipitation and visualised by confocal fluorescence microscopy. Furthermore, a specific cleavage site in p54nrb was identified at the aspartate residue D422 and the functional impact was confirmed by alteration of the amino acid residue through point mutation.

As shown, upon apoptotic stimulation in HeLa cells, two p54nrb fragments occurred at a lower molecular weight with sizes of approximately 48 kDa and 51 kDa. A caspase-2 specific cleavage resulting in the 48 kDa fragment of p54nrb could be confirmed. On the other hand, the 51 kDa fragment appeared after treatment with apoptotic stimuli and consequential caspase-2 activation in the cells, but it was not consistently detectable, for example *in vitro* with recombinant protein.

Previous studies by Thiede et al. (2001) and Schmidt et al. (2007) described an *in vitro* cleavage of p54nrb by caspase-3. They observe a cleavage into five fragments of 48, 32, 28, 26, and 22 kDa in cis-platin stimulated Jurkat-T-cells. They identified cleavage sites of p54nrb at D231, D286, and D422 by *in vitro* transcription of p54nrb mutants and employing recombinant caspase-3. In contrast, within our studies the ectopic overexpression of effector caspase-3 or -7 did not result in p54nrb cleavage, and our *in vitro* cleavage assay of p54nrb with recombinant caspase-3 could also not confirm the results of Schmidt et al. (2007). To be mentioned, Schmidt et al. (2007) used

a high concentration of 20 Units of recombinant enzyme, whereas employing less than 4 Units of recombinant caspase-2 in our study already resulted in cleavage of the recombinant p54nrb protein. Notably, the 51 kDa fragment could not be confirmed in our *in vitro* cleavage assay, as well as in cells ectopically expressing p54nrb upon cell death induction. Since the *in vitro* assay with caspase-2 only led to a 48 kDa fragment, a second cleavage by caspase-2 or caspase-3 resulting in the occurrence of the 51 kDa fragment is unlikely. But the non-physiological condition of the *in vitro* setup can lead to artificial results. Therefore, putative other cleavage relevant factors, in addition to the caspase activity should be considered.

A cleavage at the aspartate residue D58 of p54nrb could be excluded from this study. Additionally, no further putative caspase cleavage sites with the classic amino acid sequence pattern DXXD (X = any amino acid) (Thornberry et al., 1997) or even single aspartate residues, which could result in the sizes of 51 and 48 kDa could be identified. Therefore, endogenous post translational modifications, as observed for Bid (Zha et al., 2000; Degli Esposti et al., 2003) or alternative splicing variants (Pavao et al., 2001) can be envisaged for the generation of the 51 kDa fragment. Also, cleavage by non-aspartate proteases, as it has been observed for the caspase-3 substrate acinus (Fischer et al., 2003) cannot be excluded.

An off-target effect of the shRNAs, which seems to affect the occurrence of the 51 kDa fragment needs also further consideration (Caffrey et al., 2011; Song et al., 2015). A comparison with different expression manipulating techniques, such as CRISPR-Cas9 for depletion could help to rule out off-target effects, since in comparison to the shRNA modified HeLa cells, in the DLD-1 CRISPR-Cas9-Control cells the 51 kDa fragment of p54nrb was detected.

Notably, the occurrence of the 51 kDa fragment also seems to depend on the cell type and on the cell death stimulus, since it was not detected in cell death stimulated SK-MEL cells or upon treatment with alpha-toxin in HeLa cells. This matter is also in accordance with the observation of a cell type and condition dependence on the caspase-2 activity and function (Vigneswara & Ahmed, 2020). It is possible that an involvement of the caspase-2 activation platform PIDDosome or other caspase-2 regulating conditions have a relevant influence on the processing of p54nrb by caspase-2, depending on the cell type and stimulus. Those context dependent conditions are not replicable with an *in vitro* assay.

4.1.1 A compartment specific role of caspase-2

It has been observed that the functional diversity of caspase-2 depends on many factors, including cell type, activating stimulus, and subcellular localisation, which determines the enzymes access to different subsets of proteolytic targets (Brown-Suedel & Bouchier-Hayes, 2020). Among the known caspase-2 substrates with compartment specific functions are the nuclear protein MDM2 and golgin-160 in the Golgi apparatus.

DNA damage induced cleavage of MDM2 by caspase-2 can control p53 stability in a feedback-loop manner, and thereby regulates cell cycle arrest, whereas full length MDM2 leads to p53 degradation (Oliver et al., 2011). This demonstrates a p53-dependent role of caspase-2 in cell cycle control in the nucleus. The protein golgin-160 is involved in regulating the Golgi structure and protein shuttling. It is cleaved by caspase-2, but also by caspase-3 and -7 upon apoptotic stimulation at an early stage of apoptosis, leading to Golgi body degradation. However, it was also observed that the golgin-160 fragment can further translocate into the nucleus exerting a pro-survival effect (Mancini et al., 2000; Hicks & Machamer, 2002; Sbodio et al., 2006). Thus, golgin-160 is another compartment specific substrate of caspase-2 which may direct the fate of the cell.

The experimental identification of the nuclear protein p54nrb as a substrate of caspase-2 affirms a compartment specific role of caspase-2, due to the predominant nuclear localisation of both interacting proteins (Colussi et al., 1998; Bouchier-Hayes & Green, 2012). The nuclear localisation of caspase-2 as a pro-enzyme may provide a pole position for cleaving specific nuclear substrates, especially at an early time point. In comparison, caspase-3 requires activation in the cytoplasm prior to its shuttling to the nucleus for cleaving its nuclear substrates (Kamada et al., 2005). To be mentioned, in contrast to the *in vitro* analysis of Thiede et al. (2001) and Schmidt et al. (2007), in terms of p54nrb processing, specific cleavage by other effector caspases could not be experimentally confirmed, making p54nrb an exclusive caspase-2 substrate.

Noteworthy, caspase-2 can trigger cytochrome-C release while being localised in the nucleus (Paroni et al., 2002). This implicates a signal transmission out of the nucleus via nuclear caspase-2 substrates (Paroni et al., 2002). Meanwhile, it is tempting to speculate that the distinct localisation of caspase-2 and its substrate specificity might be mainly essential for its proposed non-apoptotic functions (Vigneswara & Ahmed, 2020) and the herein identified substrate

p54nrb, as a multifunctional scaffold with a transcription regulating function has great potential in conducting it, as demonstrated in this study.

4.2 The caspase-2—p54nrb axis exerts a tumor suppressor function

Evasion of apoptosis is a hallmark of tumors, and therefore, since discovery of apoptotic signalling, caspases have been of great therapeutical interest (Fulda, 2010). However, the role of the unique caspase family member caspase-2 in apoptosis is questionable since knockout does not universally inhibit apoptotic signalling or causes an overt phenotype (Bergeron et al., 1998; O'Reilly et al., 2002). Besides its questionable role in directing apoptosis, other studies could indicate potential non-apoptotic functions of caspase-2, such as tumor suppression, cell cycle control, DNA repair, and ageing (Dorstyn & Kumar, 2009; Brown-Suedel & Bouchier-Hayes, 2020). The underlying mechanisms to the non-apoptotic functions of caspase-2 were not characterised so far. For this reason, the current thesis focused on elucidating the direct downstream substrates of caspase-2, which might mediate its tumor suppressor function.

4.2.1 P54nrb is a transcriptional regulator of tumorigenic proteins

In this study, p54nrb was discovered as an exclusive substrate of caspase-2. The multifunctional nuclear protein p54nrb has been reported to be relevant in different regulatory steps of gene expression, starting from DNA unwinding (Straub et al., 2000), and continuing with the activation, elongation, and termination of transcription (Hallier et al., 1996; Basu et al., 1997; Emili et al., 2002; Ishitani et al., 2003; Hall-Pogar et al., 2007; Kaneko et al., 2007; Yadav et al., 2014). Furthermore, p54nrb is involved in mRNA processing and splicing (Peng et al., 2002; Kameoka et al., 2004; Liang & Lutz, 2006; Lu & Sewer, 2015), retention of defective RNA (Hu et al., 2015), and even repair of DNA (Bladen et al., 2005; Li et al., 2009). Hence, p54nrb was observed in many biological key processes, such as cell proliferation, apoptosis, and migration (Feng et al., 2020). Moreover, p54nrb is overexpressed in several tumors, such as melanoma, cervix carcinoma, and breast cancer. Accordingly, high levels of p54nrb have been linked to the overall poor survival of patients (Feng et al., 2020). An overexpression of p54nrb in cancer cells could be validated in this study by evaluating expression data from the database called oncomine.org.

A further goal of this study was to unravel the functional connection of p54nrb and caspase-2. Based on the knowledge of p54nrb being involved in transcriptional regulation, a part of this project was the identification of proteins, which were altered at the expression level in dependency of p54nrb. Therefore, a quantitative mass spectrometry of p54nrb depleted cells in comparison to control HeLa cells was employed. Proteins with significantly altered expression were selected according to their relevance in tumorigenesis.

Thereby, among the potential p54nrb regulated proteins was CDKN2A (cyclin-dependent kinase inhibitor 2 A), based on its upregulation in p54nrb knockdown cells. CDKN2A is long known to act as a tumor suppressor, as it is frequently mutated or deleted, especially in melanoma cells (Liggett & Sidransky, 1998). Low CDKN2A expression levels have also been observed in cervix carcinoma (Luan et al., 2021). In colorectal cancer, methylation of the CDKN2A promoter and loss of transcription has been commonly observed (Shima et al., 2011). The CDKN2A gene encodes two proteins, which both act as tumor suppressors and affect cell proliferation, senescence, anoikis, and growth (Rocco & Sidransky, 2001).

Another chosen candidate was gelsolin, which is a protein well known for its critical role in regulating dynamic changes in the actin cytoskeleton, relevant for cell motility and growth, but also implied in apoptosis (Koya et al., 2000). In addition, in cervical carcinoma and melanoma gelsolin was observed to be overexpressed (Liao et al., 2011; Mazurkiewicz et al., 2021).

A further identified candidate was cathepsin-Z (CTSZ), also known as cathepsin-X or cathepsin-P. Cathepsin-Z has a role in cancer, as high expression levels of this gene is linked with tumor malignancy (Rumpler et al., 2003; Vizin et al., 2012). Independent of its catalytic activity, cathepsin-Z can regulate cell migration and adhesion, as well as invasion and metastasis. It is involved in EMT (Epithelial-mesenchymal transition) regulation (Wang et al., 2011) and integrin mediated interactions with the extracellular matrix (Akkari et al., 2014).

Another identified candidate was NQO1 (NAD(P)H: Quinone Oxidoreductase 1), a flavoprotein, which catalyses the reduction of quinone substrates and thereby protects cells from oxidative stress (Dinkova-Kostova & Talalay, 2010). An overexpression of NQO1 was observed in cancer cells of breast, colon, cervix, lung, pancreas, and in melanoma (Oh & Park, 2015; K. Zhang et al., 2018).

A further candidate was TPD52 (Tumor protein D52), also called PrLZ (prostate leucine zipper), which is commonly overexpressed in different types of cancer, including breast and prostate, but also in colorectal (Petrova et al., 2008; J. Li et al., 2017) and cervix carcinoma (Safi et al.,

2021). The expression of this gene correlates with poor survival of patients and could reflect an early event in tumor progression (Lewis et al., 2007; Byrne et al., 2014).

The expressional alterations of these proteins upon knockdown of p54nrb in HeLa cells were validated by western blot. The documented expression levels in cancers of the tumorigenic proteins partially correlates with the expression level of p54nrb. This further underlines our hypothesised regulatory connection of those targets with p54nrb.

A p54nrb dependent expression of gelsolin and cathepsin-Z was also detected in SK-MEL and DLD-1 cells. Surprisingly, CDKN2A could not be detected in SK-MEL and DLD-1 cells. Whereas the levels of TPD52 and NQO1 were not affected by knockdown of p54nrb and therefore pointing to a tumor cell specific phenomenon.

4.2.1.1 P54nrb directly regulates gelsolin and cathepsin-Z expression

Another finding in this study was the proof of a direct expressional regulation of gelsolin and cathepsin-Z by p54nrb. By stimulating HeLa cells with apoptotic inducers leading to p54nrb cleavage, a reduced protein level of gelsolin and cathepsin-Z could be detected. This clearly shows, that p54nrb cleavage, equally to a genetic depletion, leads to a reduced level of the gelsolin and cathepsin-Z proteins.

In this study, a caspase-2 cleavage site in p54nrb could be identified at the aspartate residue D422, which is situated in the proline-rich region at the C-terminal site of the protein. This proline-rich region (amino acids 404-432) is postulated to mediate mainly protein-protein interactions which are relevant for the activation of transcription (Yang et al., 1993). The preceding helix-turn-helix motifs (amino acids 289-310 and 320-341) in combination with the charged region close by, is characteristic for a DNA-binding domain found in octamer-binding proteins (Yang et al., 1993). These data lead to the presumption that cleavage by caspase-2 at D422 disrupts the transcriptional regulatory function of p54nrb on gelsolin and cathepsin-Z through interruption of the contact of p54nrb with the gelsolin and cathepsin-Z encoding sequences caused by loss of its DNA-binding domain.

Indeed, by employing an endogenous ChIP assay, as well as a novel *in vitro* ChIP approach, a direct interaction of p54nrb with the gelsolin and cathepsin-Z encoding DNA was confirmed, thus underlying the direct transcriptional regulation of both genes by p54nrb.

A potential direct regulation of NQO1 by p54nrb requires further investigations on both, DNA and RNA levels. Experimental data from others have demonstrated that NQO1 gene expression depends on several cis-elements (Jaiswal, 2000), which represent potential p54nrb target sequences, in a similar way to the reported interaction of p54nrb with the IAP proximal enhancer element (IPE) (Basu et al., 1997). Alternatively, an indirect gene regulation via p54nrb through targeting other transcriptions factors, like Nrf2 or c-Jun (Hallier et al., 1996; Jaiswal, 2000), as well as a direct regulation of the translation by interaction with the NQO1 encoding mRNA through its RNA recognition motifs can be postulated (Dong et al., 1993; Hallier et al., 1996).

To date, there is no data available, demonstrating a relationship between p54nrb and TPD52 expression. So far, the current literature demonstrates, that TPD52 overexpression in cervical cancer correlates with its gene amplification value (Byrne et al., 2005) indicating that TPD52 is not primarily regulated by transcriptional regulation. In line with this study, other groups described a regulation of TPD52 by radiation induced overexpression of the microRNA miR-15a-3p in cervical cancer, resulting in enhanced apoptosis and inhibition of cell proliferation (Wu et al., 2018). Therefore, an indirect regulation of TPD52 by p54nrb via miR-15a-3p decay mediated through paraspeckles, is feasible (Pisani & Baron, 2019). Also, a direct regulation of TPD52 by p54nrb on the mRNA level through binding via its RNA recognition motifs cannot be excluded and needs further investigation (Dong et al., 1993; Hallier et al., 1996).

The direct interaction of p54nrb with the CDKN2A gene or mRNA was not further investigated in this study. However, previous studies confirmed a direct activation of the CDKN2A gene by p54nrb in mouse fibroblasts, relevant for the regulation of gating the circadian clock to the cell cycle which consequently affects wound healing processes (Kowalska et al., 2013). It is therefore tempting to speculate that a direct interaction of p54nrb with the CDKN2A encoding gene may also occur in human cells.

4.2.2 P54nrb negatively affects cell death

Since p54nrb cleavage by caspase-2 was detected in response to apoptotic stimulation, the functional consequences from loss of p54nrb upon cell death induction were monitored by flow cytometry. A clear sensitising effect towards cell death could be measured in p54nrb knockdown in cells stimulated with apoptotic inducers. However, p54nrb knockdown alone did not show a toxic effect and caspase-2 was observed to be dispensable for apoptotic signalling, as confirmed in this study by unaffected cleavage of PARP upon apoptotic stimulation in caspase-2 knockdown

cells. This let us assume, that under apoptotic stimulation the caspase-2—p54nrb axis possibly may act as a positive feedback loop to enhance the apoptotic signalling, in a similar fashion as the caspase-2—MDM2 axis (Oliver et al., 2011). In this scenario, the altered expression of tumorigenic proteins, regulated by p54nrb leads to loss of cell death protection and consequently to a sensitisation towards cell death upon apoptotic stimuli or exceeding cell stress.

Targeting transcriptional regulators through catalytic cleavage during the execution of cell death has a delayed effect due to the longer signalling process, when compared to a direct targeting of enzymes or scaffold proteins (Fischer et al., 2003; Dudgeon et al., 2009). Based on this, the cleavage of p54nrb by caspase-2 during the apoptotic cascade seems redundant for the fast execution of apoptosis. Instead, a predominant effect on the cell in a more substantial manner, as a slow feedback loop and in long term survival of tumors, seems plausible (Hat et al., 2016).

In this context, there are several reports in the literature of caspase-2 exerting non-apoptotic functions, such as tumor suppression. However, the underlying mechanisms are largely unknown (Puccini, Dorstyn, et al., 2013). The newly identified caspase-2 substrate p54nrb may contribute to the observed tumor suppressor function of caspase-2. Hereby, the cleavage of p54nrb by caspase-2 might not be lethal, as measured by flow cytometry with p54nrb knockdown cells, but leads to loss of the regulatory function of p54nrb on tumorigenic genes. The role of p54nrb as a regulator of several tumorigenic genes is in complete agreement with the observed overexpression of p54nrb in tumors and with its postulated role in malignancy (Feng et al., 2020). In line with that, the caspase-2 level is often reduced in tumors (Fava et al., 2012). According to this assumption, caspase-2 may act as a cellular stress sensor, a function of caspase-2 which is also discussed in the literature (Fava et al., 2012; Vigneswara & Ahmed, 2020).

The results of this study let us assume, that the observed effects of p54nrb on cell death are probably mediated through the regulation of tumorigenic genes. Hereinafter, the known apoptosis related features of the tumorigenic candidates are shortly discussed.

For instance, it has been demonstrated that full length gelsolin exerts an inhibitory effect on apoptosis and blocks caspase-3 activation by regulating the mitochondrial membrane potential, which leads to blockage of cytochrome-C release in Jurkat T-lymphocytes (Koya et al., 2000). However, the functional role of gelsolin in cancer has been shown to be cell type dependent, as gelsolin has a tumor suppressive role in colon cancer (Chen et al., 2019), but seems pro-tumorigenic in cervical carcinoma (Liao et al., 2011).

Furthermore, overexpression of NQO1 has been reported to exert an oncogenic function through protection of SIRT6 from ubiquitin-proteasome degradation, thereby leading to an enhanced SIRT6/AKT/XIAP signalling in hepatocellular carcinoma (Zhou et al., 2019).

TPD52 knockdown has been shown to induce caspase-3 and -9 activation, mainly through loss of the mitochondrial membrane potential, subsequently leading to apoptotic cell death in prostate cancer cells (Ummanni et al., 2008). Similarly, an increased cell death rate was observed upon TPD52 knockdown in several breast cancer lines (Shehata et al., 2008; Roslan et al., 2014).

The gene product p16 of CDKN2A (p16INK4A) regulates cell cycle arrest by blocking CDK4 and CDK6 activity via CCND1 (Cyclin D 1), whereas the gene product p14 (p14ARF) can inhibit MDM2, resulting in p53 stabilisation (Sekulic et al., 2008). The constitutively increased level of p53 leads to the activation of the cell death signalling cascade. In addition, it could be demonstrated that the gene product p14 of CDKN2A regulates cell cycle arrest and subsequently induce apoptosis in a p53 independent manner (Eymin et al., 2003). A p53 independent cell death regulation by CDKN2A, which represents a target of p54nrb regulation goes in accordance with the measured p53 independence of p54nrb.

4.2.3 P54nrb enhances tumor growth

The ability to grow independently from growth factors, such as a solid surface is considered as a hallmark of carcinogenesis (Mori et al., 2009). In this study it could be demonstrated that the p54nrb protein level in SK-MEL melanoma and DLD-1 colon carcinoma cells significantly affects the anchorage independent growth potential. These findings are in accordance with previous studies demonstrating a reduced migration and proliferation of melanoma cells upon knockdown of p54nrb (Schiffner et al., 2011). The altered expression of tumorigenic proteins, caused by knockdown of p54nrb, underscores the gene regulatory function of p54nrb, possibly relevant for the alteration in cell growth ability. The impact of the p54nrb dependently regulated proteins on growth is discussed in the following.

For instance, it was demonstrated, that the actin-regulatory protein gelsolin has an impact on prostate cancer proliferation, mobility, migration, and growth, as postulated from experiments with knockdown of gelsolin (Chen et al., 2017). Similarly, Litwin et al. (2012) measured reduced migratory potential of melanoma cells with gelsolin downregulation. Thereby, the gelsolin mediated migration is dependent on the extracellular matrix proteins (Mazurkiewicz et al., 2021).

In HeLa cells, gelsolin downregulation led to reduced MMP2 and vimentin levels, and upregulated E-cadherin and fibronectin, indicating a crucial role of gelsolin in EMT driven tumor migration and invasion (Liao et al., 2011). Comparable effects were found in colorectal cancer, where gelsolin is required for invasion as observed by Zhuo et al. (2012).

Also, cathepsin-Z was previously linked to growth behaviour. Cathepsin-Z overexpression in hepatocytes results in enhanced growth, as measured by employing soft agar assay by Wang et al. (2011), via modulation of EMT and extracellular matrix remodelling. Besides, cathepsin-Z is involved in the regulation of adhesion and migration via cleavage of integrin receptors (Lechner et al., 2006; Lines et al., 2012) and profilin-1 (Pecar Fonovic et al., 2013). Noteworthy, also a catalytically independent interaction of cathepsin-Z with integrins and extracellular matrix was observed (Akkari et al., 2014).

A p54nrb dependent regulation of NQO1 and TPD52 in SK-MEL and DLD-1 cells could not be confirmed in this study. Nevertheless, they still might contribute to growth, proliferation, and metastatic potential, as indicated by their increased expression levels in these tumors, when compared to healthy tissue.

For instance, an overexpression of TPD52 leads to a significant increase in anchorage-independent growth in breast cancer cells, as shown by Shehata et al. (2008). Other studies on pancreatic cancer proved a direct functional link of TPD52 to proliferation, migration, and invasion, mainly through a deactivation of the Akt pathway (Ummanni et al., 2008; Wang et al., 2020).

Although CDKN2A (p16INK4/p14ARF) was not detectable in SK-MEL and DLD-1 cells in this study, it can affect tumor growth. CDKN2A expression is known to be significantly reduced in melanoma A375 cells and consequently, overexpression of CDKN2A negatively affects proliferation and migration of the tumor cells (Bai et al., 2016). Similarly, loss of p16 seems to be an early cause of tumor progression as suggested by results from precancerous lesion analysis (Rocco & Sidransky, 2001). Interestingly, a study by Plath et al. (2000) revealed a novel function of p16 in regulating anoikis (anchorage dependent cell death) through the α5-integrin level in cancer cells from different sources, including the pancreas, liver, skin, and canine kidney. Hereby, mechanistically, α5-integrin binds to the fibronectin receptor, which consequently signals cell death (Frisch & Ruoslahti, 1997).

In this study, melanoma cells showed the most striking effect on growth upon p54nrb knockdown. One of the most prominent oncogenic factors of melanoma is mutations in the

retinoblastoma protein signalling pathway, which is crucial for mediation of cell cycle arrest. Mutations in p16 and its downstream target CDK4 were found in SK-MEL-29 cells (Wolfel et al., 1995) and in three melanoma families (Zuo et al., 1996; Soufir et al., 1998). Therefore, an elevation in the expression of these oncogenic factors could exhibit strong effects on tumor development.

Astonishingly, in p54nrb knockdown HeLa cells, no significant effects were measured on anchorage independent growth. An explanation could be that HeLa cells might grow too aggressively to be affected in growth by the absence of an anchorage, as measured by soft-agar assay. By using a transwell assay on cervical cancer cells, Luan et al. (2021) could demonstrate a negative effect of CDKN2A on invasion, mediated by suppressing LDHA through the inhibition of the AKT-mTOR pathway (Luan et al., 2021). Also, different expression patterns of p54nrb regulated tumorigenic proteins between the three measured cell lines may explain the differences in the cell growth properties.

In this study CDKN2A was neither detectable in DLD-1 colon carcinoma control cells, nor upon knockdown of p54nrb. Although the CDKN2A/p16 gene is present in DLD-1 cells as measured by Okamoto et al. (1994), our used DLD-1 cell line might differ in its CDKN2A expression.

The hypothesis of p54nrb acting as a regulator of proteins with relevance in cell growth is further in accordance with the observation of an enhanced growth of caspase-2 knockout MEF cells in an soft agar assay, which is dependent on its catalytic function (Ren et al., 2012).

4.2.4 The caspase-2—p54nrb axis acts p53 independent

P53 is a well-known tumor suppressor, which also is an indirect target of caspase-2 through MDM2 cleavage, which in turn leads to p53 stabilisation (Lim, Dorstyn, et al., 2021). However, in many tumors, p53 is abolished or mutated (Muller & Vousden, 2013). In addition, caspase-2 can bypass p53 in a cell and context dependent manner (Sidi et al., 2008). In fact, p53 driven caspase-2 activation via PIDDosome does even facilitate carcinogenesis in hepatocellular carcinoma (Sladky et al., 2020). Overexpression of MDM2 is considered as a prognostic marker in melanoma cells, associated with better clinical outcomes. Therefore, it seems evident that MDM2 cleavage in melanoma most likely does not account for a tumor suppressive function (Polsky et al., 2002). This raises the possibility of an alternative mechanism for how caspase-2

may control tumorigenesis in cells lacking functional p53 (Brown-Suedel & Bouchier-Hayes, 2020).

The data of this study clearly demonstrate, that p54nrb cleavage by caspase-2 occurs independent of p53, since p54nrb cleavage and cell death were not affected in HeLa cells treated with the p53-inhibitor pifithrin-α. Further, no effect on p54nrb cleavage was observed in p53 mutated DLD-1 cells, when compared to wildtype p53 expressing RKO cells.

Together, these data identified p54nrb as a novel caspase-2 substrate which navigates tumor survival and cell death sensitivity in a p53 independent manner.

4.3 Open questions and future perspectives

A prominent problem in cancer therapy is the development of drug resistant metastasis (Mansoori et al., 2017). In this study, a novel substrate of caspase-2, p54nrb, was identified. In accordance, an overexpression of p54nrb was measured in several cancer types and knockdown of p54nrb caused tumor cells to lose their resistance to stressors and led to cell death susceptibility. In contrast, knockdown of p54nrb itself was not lethal. Thus, p54nrb may represent a novel cell type specific target for cancer therapy and represents a potent biomarker. The exact functional relevance and clinical applicability of this axis warrants further experimental investigation. For example, measuring the effect of an expressional compensation of the tumorigenic protein levels in p54nrb knockdown cells. Future investigations on p54nrb's gene regulation and correlated consequences for tumorigenesis in other p54nrb overexpressing cancers would also be of interest and could be compared with non-cancerous cells.

For investigation of an *in vivo* relevance of the tumor cell death susceptibility upon chemotherapeutic treatment with depletion of p54nrb, monitoring for example mouse models like xenografts or GEMM (Genetically engineered mouse model) could offer an appropriate method. In this context the investigation of effects of p54nrb on treatment with other commonly used chemotherapeutical drugs is also of interest to solidify the clinical relevance.

Furthermore, as presented in this study, p54nrb can regulate the expression of cathepsin-Z and gelsolin directly by interaction with their DNA sequence. Whether p54nrb may additionally regulate the expression of other candidate targets such as NQO1, TPD52, and CDKN2A need further investigation.

Additionally, the identification of the exact sequence motifs of the gelsolin and cathepsin-Z encoding genes, which are bound by p54nrb is of further interest. Binding assays, like EMSA (Electrophoretic mobility shift), DPI-ELISA (DNA-protein-interaction enzyme-linked immunosorbent assay) (Brand et al., 2010), or reporter gene assays are valid approaches for investigating this issue. Also, a binding assay for monitoring interaction of p54nrb cleavage fragments with cathepsin-Z and gelsolin genes would address the question, whether p54nrb cleavage rather interrupts completely the binding to the DNA or inactivates a transactivation activity.

It needs to be mentioned, that the mass-spectrometric analysis of p54nrb dependently regulated tumorigenic proteins had to be narrowed down to only a small number of candidates in order to be able to confirm their regulation by additional experiments. However, the list of expressional altered tumorigenic proteins includes further interesting candidates, which definitely deserve future investigations.

In this study p54nrb cleavage was shown to alter the expression of gelsolin and cathepsin-Z. However, this does not exclude alternative functions by the p54nrb fragments. Analysing the effect of an ectopic overexpression of p54nrb fragments could give answers to other functions by the p54nrb fragments after the cleavage.

As previously introduced, p54nrb's function is often regulated by interaction with other proteins. Especially known are dimerisation with other proteins of the DBHS family. It is of further interest to investigate a relevance of p54nrb interacting proteins, specifically in the context of p54nrb's regulation function on tumorigenic proteins and to also address the question if other DBHS proteins are putative caspase-2 substrates.

5 Summary

5.1 Summary (English short version)

Caspase-2 is the evolutionary most conserved member of the caspase family and was shown to be involved in genotoxic stress induced apoptosis, control of aneuploidy, and ageing related metabolic changes. However, its role in apoptosis seems redundant due to the observation, that knockout does not inhibit apoptotic signalling exclusively. Instead, knockout of caspase-2 leads to tumor susceptibility *in vivo*, which led to the assumption, that caspase-2 has non-apoptotic functions and can act as a tumor suppressor. The underlying mechanism of the tumor suppressor activity of caspase-2 has not been clarified so far. Furthermore, caspase-2, has a prominent, and as pro-enzyme exclusive localisation in the nucleus and other subcellular compartments, implicating a distinct and location specific role.

In this study, a novel caspase-2 specific substrate, termed p54nrb, was identified. P54nrb is harbouring a caspase-2 specific cleavage site at the aspartate residue D422, and cleavage of p54nrb leads apparently to disruption of its putative DNA binding domain at the C-terminus.

P54nrb is a nuclear multifunctional RNA and DNA binding protein, known for roles in transcriptional regulation, DNA unwinding and repair, RNA splicing, and retention of defective RNA. Overexpression of p54nrb has been observed in several human cancers, such as cervix carcinoma, melanoma, and colon carcinoma.

Data from this study revealed, that depletion of p54nrb in tumor cell lines results in a loss of resistance to drug induced cell death and to reduced capability of anchorage independent growth, which is functionally equivalent to a reduced tumorigenic potential. Meanwhile, p54nrb depletion alone is not cytotoxic.

The investigation of p54nrb dependent gene regulations by high resolution quantitative proteomics uncovered an altering expression of multiple tumorigenic genes. For two of these candidates, the tumorigenic protease cathepsin-Z and the anti-apoptotic gelsolin, p54nrb dependent expression was detected universally in all three investigated tumor cell lines, cervix carcinoma, melanoma, and colon carcinoma. Additionally, a direct interaction of p54nrb with the cathepsin-Z and gelsolin encoding DNA, but not with their corresponding mRNA, could be demonstrated.

Conjointly, this study unveils a novel mechanistic feature of caspase-2 as a tumor suppressor. The caspase-2—p54nrb axis (Figure 34) can orchestrate the levels of several tumorigenic

proteins and thereby determine the cell death susceptibility and long-term tumor survival. These findings might be of great value for future therapeutic interventions and for overcoming drug resistance of tumors.

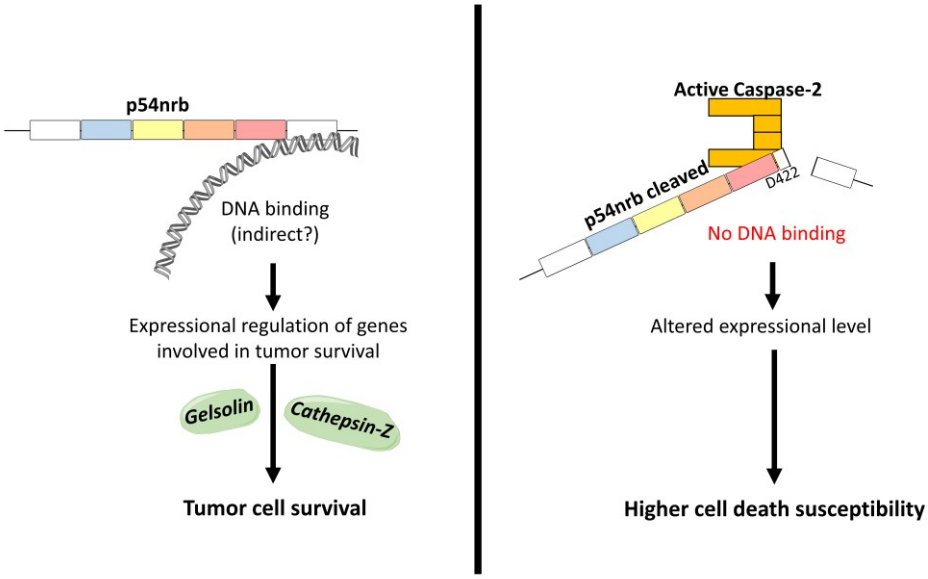

Figure 34. The caspase-2—p54nrb axis.
Schematic illustration of p54nrb's regulatory function on the gene expression of tumorigenic proteins with and without active caspase-2 and its subsequent effects on the tumor cell survival. Modified from Eichler et al. (2022).

5.2 Zusammenfassung (Ausführliche deutsche Version)

Apoptose ist eine Form des programmierten Zelltods und ist in multizellulären Organismen essentiell für die embryonale Entwicklung, sowie im adulten Zustand notwendig für die Zellhomöostase. Dabei werden redundante oder fehlerhafte Zellen entfernt, ohne umliegende gesunde Zellen zu schädigen. Der Prozess der Apoptose ist durch das Schrumpfen der Zelle, welche sich dabei von den umliegenden Zellen löst, charakterisiert. In der Zelle kondensiert die DNS und wird zusammen mit anderen Zellbestandteilen sukzessive abgebaut. Dabei bilden sich charakteristische Membranbläschen und apoptotische Körperchen, welche anschließend durch Makrophagen erkannt und verdaut werden. Damit unterscheidet sich die Apoptose entscheidend von der Nekrose, welche durch nicht-physiologische Prozesse wie einem Trauma oder einer Infektion auftritt. Die Nekrose ist gekennzeichnet durch ein Anschwellen der Zelle mit anschließender Ruptur der Zellmembran, was häufig mit der Einleitung von Entzündungsreaktionen im umliegenden Gewebe verbunden ist.

Da der programmierte Zelltod essentiell für multizelluläre Organismen ist, erfordert er eine komplexe Regulation. Eine Fehlregulation führt in den meisten Fällen zur Entstehung von Krankheiten, wie beispielsweise zu Autoimmunität, neurodegenerativen Krankheiten, aber auch zur Entstehung von Krebszellen, oftmals verbunden mit Resistenzen gegenüber chemotherapeutischen Substanzen. Um Krebs erfolgreich behandeln zu können sind bessere Kenntnisse zur Regulation des programmierten Zelltods eine wesentliche Voraussetzung für die Entwicklung effizienter Tumortherapeutika, insbesondere zur Überwindung von Resistenzentwicklungen.

Derzeit wird zwischen einem guten Dutzend verschiedener Signalwege des programmierten Zelltods unterschieden. Die bekannteste Form ist die Apoptose. Die apoptotische Signalkaskade ist abhängig von einer Enzymgruppe, genannt Caspasen, welche kaskadenhaft aktiviert werden. Diese Cysteinproteasen erkennen und schneiden spezifische Proteinsubstrate an selektiven Aminosequenzen hinter einem Aspartat. Apoptotische Caspasen werden in Initiator- und Effektor-Caspasen untergruppiert. Initiator-Caspasen werden in der apoptotischen Kaskade zuerst aktiviert. Dies geschieht über eine Rekrutierung zu spezifischen Aktivierungs-Plattformen. Effektor-Caspasen wiederum können nur von aktiven Initiator-Caspasen aktiviert werden. Neben den apoptotischen Caspasen, gibt es auch inflammatorische Caspasen, welche an Entzündungsprozessen, aber nicht an der Apoptose, beteiligt sind.

Die Caspase-2 gilt als das in der Evolution am höchsten konservierte Mitglied der Caspasen-Familie. Bedingt durch ihren verhältnismäßig unscheinbaren Knockout-Phänotyp wurde dieser Caspase jedoch für lange Zeit wenig Beachtung geschenkt. Bemerkenswerterweise zeigt die Caspase-2 charakteristische Besonderheiten, wie die Präsenz einer CARD-Domäne (Caspase Rekrutierungsdomäne), welche typisch für Initiator-Caspasen sind. Zugleich weist diese aber auch eine Aktivität als Effektor-Caspase auf, welche spezifische Substrate spaltet.

Der Caspase-2 konnte eine Rolle in durch genotoxischen Stress induziertem Zelltod, bei der Kontrolle von Aneuploidie, sowie bei alterungsbedingten metabolischen Veränderungen nachgewiesen werden. Im programmierten Zelltod scheint die Caspase-2 jedoch eher eine redundante Rolle zu spielen, da ein Caspase-2 Knockout die Zelltod Signalwege nicht ausschließlich beeinträchtigt. Anstelle dessen führt ein Knockout der Caspase-2 in Mäusen, welche konstitutiv Onkogene exprimieren, zu einer erhöhten Anfälligkeit gegenüber Aneuploidie und einer beschleunigten Tumorgenese, was zu der Annahme führte, dass die Caspase-2 eine nicht-apoptotische Funktion als Tumorsuppressor innehat. Die zugrundeliegenden Mechanismen sind derzeit jedoch noch nicht bekannt.

Zudem ist die Caspase-2, einzig unter den Caspasen, im Zellkern und anderen Zellkompartimenten, wie beispielsweise dem Golgi-Apparat, lokalisiert. Dies weist auf eine lokalisationsspezifische Rolle der Caspase-2, durch die Kontrolle über Kompartiment spezifische Substrate, hin. Bislang konnten nur wenige Substrate der Caspase-2 identifiziert werden, von welchen wiederum weniger als ein Dutzend experimentell ausreichend bestätigt sind.

Ziel dieser Arbeit war die experimentelle Untersuchung der Funktion der Caspase-2 als Tumorsuppressor. Als Zellkulturmodelle dienten hierbei Tumorzelllinien von Zervix (HeLa), Kolon (DLD-1) und Haut (SK-MEL-28). Ein besonderer Fokus stellte dabei die Identifizierung von neuen Caspase-2 Substraten dar.

In dieser Arbeit wurde p54nrb, oder auch NonO genannt, als ein bisher unbekanntes Substrat der Caspase-2 identifiziert. Tumorzelllinien zeigten unter Stimulierung mit Apoptose induzierenden Substanzen, wie Etoposid, Staurosporin und Doxorubizin, eine proteolytische Spaltung des Proteins p54nrb, welche für Caspase Substrate charakteristisch ist. Eine Caspase-2 spezifische Spaltung konnte mittels ektopischer Caspase-2 Überexpression, sowie genetischer Caspase-2 Depletion und enzymatischer Caspase-2 Inhibition bestätigt werden. Die Durchführung eines *in-vitro* Assays mit rekombinantem p54nrb und rekombinanter aktiver Caspase-2 bestätigte eine Caspase-2 vermittelte p54nrb Spaltung.

Eine Zellkompartiment spezifische physikalische Interaktion von Caspase-2 und p54nrb wurde anhand der Ergebnisse von Ko-Immunopräzipitations-Experimenten mit p54nrb und Caspase-2 postuliert und konnte mit einer fluoreszenzmikroskopisch beobachteten Ko-Lokalisation belegt werden. P54nrb ist ein nukleäres Protein und Caspase-2 ist als einzige Caspase auch als Pro-Enzym im Zellkern lokalisiert. Dies wurde in dieser Arbeit mittels biochemischer Zellfraktionierung bestätigt. Die Ergebnisse unterstreichen die Hypothese einer Zellkompartiment spezifischen Funktion der Caspase-2.

P54nrb gehört zur Familie der DBHS-Proteine, dessen Struktur aus konservierten Elementen und individuellen C- und N-Termini Strukturen besteht. P54nrb ist ein multifunktionelles RNS- und DNS-Bindeprotein. Es ist an Prozessen, wie der transkriptionellen Regulation, der DNS Entwindung und Reparatur, dem RNS Spleißen, sowie beim Rückstau von defekter RNS, beteiligt. Eine Überexpression von p54nrb konnte bei verschiedenen humanen Krebsarten nachgewiesen werden, wie beispielsweise bei Zervixkarzinomen, Melanomen, sowie bei Kolorektal-karzinomen. Diese Befunde wurden in dieser Arbeit anhand von *in silico* Analysen von mRNA-Expressions-Messungen aus der Online Datenbank Oncomine.org validiert.

In dieser Arbeit wurde eine Spaltung von p54nrb zu zwei kleineren Fragmenten, mit den Größen 48 und 51 kDa, detektiert. Innerhalb der Aminosäuresequenz von p54nrb konnten die beiden Aspartate, D58 und D422, als potentielle Spaltstellen identifiziert werden. Durch die Generierung von p54nrb-Aspartat/Asparagin-Mutanten konnte gezeigt werden, dass die Spaltung von p54nrb durch die Caspase-2 an der spezifischen Schnittstelle des Aspartats D422 stattfindet und tatsächlich zur Bildung des 48 kDa Fragments führt.

Desweiteren konnte in dieser Arbeit gezeigt werden, dass die Depletion von p54nrb in Tumorzelllinien, durch einen stabilen lentiviralen Knockdown, zum Verlust der Resistenz gegenüber Stressoren führt. So wurde eine Zelltod-Sensitivierung mittels Durchflusszytometrie nachgewiesen. Im Vergleich zu den Kontroll-Zellen führte die Depletion von p54nrb unter Zelltod Stimulation mit chemotherapeutischen Substanzen zu einer verringerten Lebensfähigkeit, welche anhand von Annexin-V und Propidium-Iodid-Färbungen gezeigt werden konnte. Die Depletion von p54nrb alleine, ohne zusätzlichem Stressor, zeigte hingegen keinen zytotoxischen Effekt.

Ebenfalls konnte gezeigt werden, dass eine Depletion von p54nrb zu einem reduzierten onkogenen Potential von verschiedenen Tumorzelllinien führt. Mittels 3D-Soft-Agar Assays konnte ein verringertes Wachstum und eine verringerte Kolonienbildung von p54nrb depletierten DLD-1 und SK-MEL-28 Zellen im Vergleich zu Kontroll-Zellen bestätigt werden. Eine

Depletion von p54nrb in HeLa Zellen hatte jedoch keinen Effekt auf das mittels 3D-Soft-Agar Assay gemessene Kolonien-Wachstum.

Aufgrund der bekannten Funktion von p54nrb in der transkriptionellen Regulation, wurde dessen Auswirkungen auf die Regulation von bekannten onkogenen Proteinen untersucht. Mit Hilfe hochauflösender Massenspektrometrie von p54nrb depletierten HeLa Zellen im Vergleich zu Kontroll-Zellen wurden Proteine mit einer signifikant veränderten Expression ermittelt. Anschließend wurden diese mittels des bioinformatischen Programmes DAVID (Database for Annotation, Visualisation and Integrated Discovery) klassifiziert und Proteine mit einer nachgewiesenen Rolle in onkogenen Schlüsselfunktionen ausgewählt. Aus dieser Auswahl wurden wiederum die fünf Kandidaten Gelsolin, Cathepsin-Z, NQO1, TPD52 und CDKN2A mittels Western Blot Analyse validiert.

In p54nrb depletierten HeLa Zellen ist das Protein Gelsolin, welches vor allem für die Aufrechterhaltung des mitochondrialen Membranpotentials verantwortlich ist und damit eine anti-apoptotische Funktion innehat, herabreguliert. Ebenso herabreguliert ist die Expression von Cathepsin-Z, welches an der Modellierung der extrazellulären Matrix beteiligt ist und damit die Adhäsion und Migration von Zellen maßgeblich beeinflussen kann.

Eine Herabregulierung konnte außerdem für das Tumor Protein D52 (TPD52), welches eine Rolle in der Proliferation hat, gezeigt werden. Desweiteren ist die Expression von NAD(P)H Quinone Dehydrogenase 1 (NQO1) nachweislich herabreguliert. Dem zum Metabolismus beitragenden Enzym NQO1 wurde eine onkogene Funktion zugesprochen, da es möglicherweise an der Stabilisierung von XIAP beteiligt ist. Hochreguliert ist in p54nrb depletierten HeLa Zellen hingegen das Protein CDKN2A (Cyclin Dependent Kinase Inhibitor 2A), welches an der Regulation des Zellzyklus beteiligt ist und dadurch letztlich Einfluss auf die Zellproliferation hat.

Gelsolin und Cathepsin-Z waren in sämtlichen der untersuchten drei Zelllinien (HeLa, DLD-1 und SK-MEL-28) p54nrb-abhängig reguliert, während TPD52 und NQO1 nur in HeLa Zellen eine Abhängigkeit von p54nrb zeigten. CDKN2A konnte hingegen nur in HeLa Zellen detektiert werden. Die Unterschiede in den von p54nrb regulierten onkogenen Proteinen zwischen den einzelnen Zelltypen weist auf eine Zelltyp Abhängigkeit hin. Diese ist auch eine mögliche Erklärung für die unterschiedlichen Effekte einer p54nrb Depletion zwischen den verschiedenen Zelltypen, wie sie anhand des Kolonien-Wachstums Assays gemessen wurde.

Zusätzlich konnte mit Hilfe von Protein-DNS und -RNS Ko-Immunopräzipitationen gezeigt werden, dass p54nrb an die DNS-Sequenz von Cathepsin-Z und Gelsolin und nicht an die für

Cathepsin-Z und Gelsolin kodierenden mRNS-Sequenzen bindet. Ein in dieser Arbeit konzipierter und durchgeführter *in-vitro* Assay belegte zusätzlich die Interaktion von p54nrb mit der doppelsträngigen Gensequenz von Gelsolin.

Basierend auf der Beobachtung, dass p54nrb mit der Gensequenzen von Cathepsin-Z, als auch der von Gelsolin interagiert und mit der Spaltung von p54nrb eine verminderte Expression beider Genprodukte gemessen wurde, kann vermutet werden, dass die Spaltung von p54nrb am D422 durch Caspase-2 zum Verlust der Interaktion mit den Gensequenzen führt. Diese Erklärung deckt sich zudem mit der Lokalisation der am C-Terminus von p54nrb postulierten DNS-Bindedomäne.

Zusammengefasst, tragen die Ergebnisse dieser Arbeit maßgeblich zur besseren Kenntnis der Mechanismen der Tumorsuppressor-Funktion der Caspase-2, in Verbindung mit dessen Substrat p54nrb, bei. Durch Spaltung von p54nrb durch die Caspase-2 am Aspartat D422 wird der Spiegel des „Full-length“ Proteins vermindert. Der Proteinspiegel von p54nrb wiederum korreliert mit dem Expressionsspiegel verschiedener onkogener Proteine. P54nrb agiert hierbei als transkriptioneller Regulator und interagiert hierzu mit der DNS-Sequenz von Gelsolin und Cathepsin-Z. Folgend beeinflussen die Expressionsspiegel der onkogenen Proteine wiederum die Zelltodsensitivität und das Überleben der Tumorzellen.

Damit stellt die hier identifizierte Caspase-2—p54nrb Achse (Abbildung 35) ein potentielles therapeutisches Modell der modernen Tumortherapie dar, insbesondere zur Bewältigung von Tumorresistenzen.

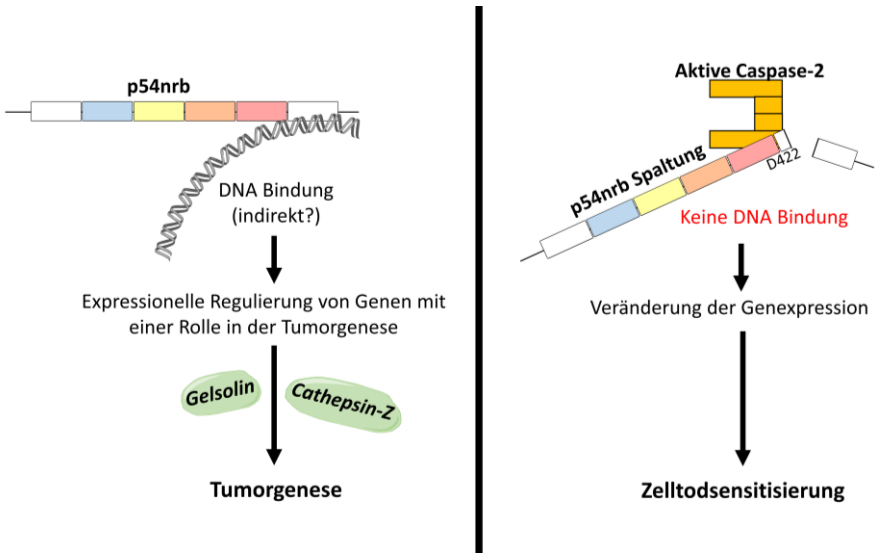

Abbildung 35. Die Caspase-2—p54nrb Achse.
Schematische Illustration der genregulatorischen Funktion von p54nrb mit und ohne aktiver Caspase-2 und die dadurch erfolgenden Effekte auf das Überleben von Tumorzellen. Die Spaltung von p54nrb durch die Caspase-2 führt zum Verlust der Genregulation der Onkoproteine Gelsolin und Cathepsin-Z. Modifiziert von Eichler et al. (2022).

6 References

Aachoui, Y., Sagulenko, V., Miao, E. A., & Stacey, K. J. (2013). Inflammasome-mediated pyroptotic and apoptotic cell death, and defense against infection. *Curr Opin Microbiol*, *16*(3), 319-326. https://doi.org/10.1016/j.mib.2013.04.004

Akkari, L., Gocheva, V., Kester, J. C., Hunter, K. E., Quick, M. L., Sevenich, L., Wang, H. W., Peters, C., Tang, L. H., Klimstra, D. S., Reinheckel, T., & Joyce, J. A. (2014). Distinct functions of macrophage-derived and cancer cell-derived cathepsin Z combine to promote tumor malignancy via interactions with the extracellular matrix. *Genes Dev*, *28*(19), 2134-2150. https://doi.org/10.1101/gad.249599.114

Albershardt, T. C., Salerni, B. L., Soderquist, R. S., Bates, D. J., Pletnev, A. A., Kisselev, A. F., & Eastman, A. (2011). Multiple BH3 mimetics antagonize antiapoptotic MCL1 protein by inducing the endoplasmic reticulum stress response and up-regulating BH3-only protein NOXA. *J Biol Chem*, *286*(28), 24882-24895. https://doi.org/10.1074/jbc.M111.255828

Amantana, A., London, C. A., Iversen, P. L., & Devi, G. R. (2004). X-linked inhibitor of apoptosis protein inhibition induces apoptosis and enhances chemotherapy sensitivity in human prostate cancer cells. *Mol Cancer Ther*, *3*(6), 699-707. https://www.ncbi.nlm.nih.gov/pubmed/15210856

Amarante-Mendes, G. P., & Griffith, T. S. (2015). Therapeutic applications of TRAIL receptor agonists in cancer and beyond. *Pharmacol Ther*, *155*, 117-131. https://doi.org/10.1016/j.pharmthera.2015.09.001

Andersen, J. L., Johnson, C. E., Freel, C. D., Parrish, A. B., Day, J. L., Buchakjian, M. R., Nutt, L. K., Thompson, J. W., Moseley, M. A., & Kornbluth, S. (2009). Restraint of apoptosis during mitosis through interdomain phosphorylation of caspase-2. *EMBO J*, *28*(20), 3216-3227. https://doi.org/10.1038/emboj.2009.253

Andersen, J. S., Lyon, C. E., Fox, A. H., Leung, A. K., Lam, Y. W., Steen, H., Mann, M., & Lamond, A. I. (2002). Directed proteomic analysis of the human nucleolus. *Curr Biol*, *12*(1), 1-11. https://doi.org/10.1016/s0960-9822(01)00650-9

Ando, K., Kernan, J. L., Liu, P. H., Sanda, T., Logette, E., Tschopp, J., Look, A. T., Wang, J., Bouchier-Hayes, L., & Sidi, S. (2012). PIDD death-domain phosphorylation by ATM controls prodeath versus prosurvival PIDDosome signaling. *Mol Cell*, *47*(5), 681-693. https://doi.org/10.1016/j.molcel.2012.06.024

Ando, K., Parsons, M. J., Shah, R. B., Charendoff, C. I., Paris, S. L., Liu, P. H., Fassio, S. R., Rohrman, B. A., Thompson, R., Oberst, A., Sidi, S., & Bouchier-Hayes, L. (2017). NPM1 directs PIDDosome-dependent caspase-2 activation in the nucleolus. *J Cell Biol*, *216*(6), 1795-1810. https://doi.org/10.1083/jcb.201608095

Bai, M., Yu, N. Z., Long, F., Feng, C., & Wang, X. J. (2016). Effects of CDKN2A (p16INK4A/p14ARF) Over-Expression on Proliferation and Migration of Human Melanoma A375 Cells. *Cell Physiol Biochem*, *40*(6), 1367-1376. https://doi.org/10.1159/000453189

Baliga, B. C., Read, S. H., & Kumar, S. (2004). The biochemical mechanism of caspase-2 activation. *Cell Death Differ*, *11*(11), 1234-1241. https://doi.org/10.1038/sj.cdd.4401492

Basu, A., Dong, B., Krainer, A. R., & Howe, C. C. (1997). The intracisternal A-particle proximal enhancer-binding protein activates transcription and is identical to the RNA- and DNA-

binding protein p54nrb/NonO. *Mol Cell Biol*, *17*(2), 677-686. https://doi.org/10.1128/MCB.17.2.677

Bergeron, L., Perez, G. I., Macdonald, G., Shi, L., Sun, Y., Jurisicova, A., Varmuza, S., Latham, K. E., Flaws, J. A., Salter, J. C., Hara, H., Moskowitz, M. A., Li, E., Greenberg, A., Tilly, J. L., & Yuan, J. (1998). Defects in regulation of apoptosis in caspase-2-deficient mice. *Genes Dev*, *12*(9), 1304-1314. https://doi.org/10.1101/gad.12.9.1304

Bladen, C. L., Udayakumar, D., Takeda, Y., & Dynan, W. S. (2005). Identification of the polypyrimidine tract binding protein-associated splicing factor.p54(nrb) complex as a candidate DNA double-strand break rejoining factor. *J Biol Chem*, *280*(7), 5205-5210. https://doi.org/10.1074/jbc.M412758200

Bonzon, C., Bouchier-Hayes, L., Pagliari, L. J., Green, D. R., & Newmeyer, D. D. (2006). Caspase-2-induced apoptosis requires bid cleavage: a physiological role for bid in heat shock-induced death. *Mol Biol Cell*, *17*(5), 2150-2157. https://doi.org/10.1091/mbc.e05-12-1107

Bouchier-Hayes, L., & Green, D. R. (2012). Caspase-2: the orphan caspase. *Cell Death Differ*, *19*(1), 51-57. https://doi.org/10.1038/cdd.2011.157

Brand, L. H., Kirchler, T., Hummel, S., Chaban, C., & Wanke, D. (2010). DPI-ELISA: a fast and versatile method to specify the binding of plant transcription factors to DNA in vitro. *Plant Methods*, *6*, 25. https://doi.org/10.1186/1746-4811-6-25

Brinkmann, V., Reichard, U., Goosmann, C., Fauler, B., Uhlemann, Y., Weiss, D. S., Weinrauch, Y., & Zychlinsky, A. (2004). Neutrophil extracellular traps kill bacteria. *Science*, *303*(5663), 1532-1535. https://doi.org/10.1126/science.1092385

Brown-Suedel, A. N., & Bouchier-Hayes, L. (2020). Caspase-2 Substrates: To Apoptosis, Cell Cycle Control, and Beyond. *Front Cell Dev Biol*, *8*, 610022. https://doi.org/10.3389/fcell.2020.610022

Bruelle, C., Bedard, M., Blier, S., Gauthier, M., Traish, A. M., & Vincent, M. (2011). The mitotic phosphorylation of p54(nrb) modulates its RNA binding activity. *Biochem Cell Biol*, *89*(4), 423-433. https://doi.org/10.1139/O11-030

Bucur, O., Gaidos, G., Yatawara, A., Pennarun, B., Rupasinghe, C., Roux, J., Andrei, S., Guo, B., Panaitiu, A., Pellegrini, M., Mierke, D. F., & Khosravi-Far, R. (2015). A novel caspase 8 selective small molecule potentiates TRAIL-induced cell death. *Sci Rep*, *5*, 9893. https://doi.org/10.1038/srep09893

Butt, A. J., Harvey, N. L., Parasivam, G., & Kumar, S. (1998). Dimerization and autoprocessing of the Nedd2 (caspase-2) precursor requires both the prodomain and the carboxyl-terminal regions. *J Biol Chem*, *273*(12), 6763-6768. https://doi.org/10.1074/jbc.273.12.6763

Byrne, J. A., Balleine, R. L., Schoenberg Fejzo, M., Mercieca, J., Chiew, Y. E., Livnat, Y., St Heaps, L., Peters, G. B., Byth, K., Karlan, B. Y., Slamon, D. J., Harnett, P., & Defazio, A. (2005). Tumor protein D52 (TPD52) is overexpressed and a gene amplification target in ovarian cancer. *Int J Cancer*, *117*(6), 1049-1054. https://doi.org/10.1002/ijc.21250

Byrne, J. A., Frost, S., Chen, Y., & Bright, R. K. (2014). Tumor protein D52 (TPD52) and cancer-oncogene understudy or understudied oncogene? *Tumour Biol*, *35*(8), 7369-7382. https://doi.org/10.1007/s13277-014-2006-x

Caffrey, D. R., Zhao, J., Song, Z., Schaffer, M. E., Haney, S. A., Subramanian, R. R., Seymour, A. B., & Hughes, J. D. (2011). siRNA off-target effects can be reduced at concentrations that match their individual potency. *PLoS One*, *6*(7), e21503. https://doi.org/10.1371/journal.pone.0021503

Cao, S., Moss, W., O'Grady, T., Concha, M., Strong, M. J., Wang, X., Yu, Y., Baddoo, M., Zhang, K., Fewell, C., Lin, Z., Dong, Y., & Flemington, E. K. (2015). New Noncoding Lytic Transcripts Derived from the Epstein-Barr Virus Latency Origin of Replication, oriP, Are Hyperedited, Bind the Paraspeckle Protein, NONO/p54nrb, and Support Viral Lytic Transcription. *J Virol*, *89*(14), 7120-7132. https://doi.org/10.1128/JVI.00608-15

Carneiro, B. A., & El-Deiry, W. S. (2020). Targeting apoptosis in cancer therapy. *Nat Rev Clin Oncol*, *17*(7), 395-417. https://doi.org/10.1038/s41571-020-0341-y

Chaabane, W., User, S. D., El-Gazzah, M., Jaksik, R., Sajjadi, E., Rzeszowska-Wolny, J., & Los, M. J. (2013). Autophagy, apoptosis, mitoptosis and necrosis: interdependence between those pathways and effects on cancer. *Arch Immunol Ther Exp (Warsz)*, *61*(1), 43-58. https://doi.org/10.1007/s00005-012-0205-y

Chan, F. K., Shisler, J., Bixby, J. G., Felices, M., Zheng, L., Appel, M., Orenstein, J., Moss, B., & Lenardo, M. J. (2003). A role for tumor necrosis factor receptor-2 and receptor-interacting protein in programmed necrosis and antiviral responses. *J Biol Chem*, *278*(51), 51613-51621. https://doi.org/10.1074/jbc.M305633200

Chaudhary, P. M., Eby, M., Jasmin, A., Bookwalter, A., Murray, J., & Hood, L. (1997). Death receptor 5, a new member of the TNFR family, and DR4 induce FADD-dependent apoptosis and activate the NF-kappaB pathway. *Immunity*, *7*(6), 821-830. https://doi.org/10.1016/s1074-7613(00)80400-8

Chen, C. C., Chiou, S. H., Yang, C. L., Chow, K. C., Lin, T. Y., Chang, H. W., You, W. C., Huang, H. W., Chen, C. M., Chen, N. C., Chou, F. P., & Chou, M. C. (2017). Secreted gelsolin desensitizes and induces apoptosis of infiltrated lymphocytes in prostate cancer. *Oncotarget*, *8*(44), 77152-77167. https://doi.org/10.18632/oncotarget.20414

Chen, L. L., & Carmichael, G. G. (2009). Altered nuclear retention of mRNAs containing inverted repeats in human embryonic stem cells: functional role of a nuclear noncoding RNA. *Mol Cell*, *35*(4), 467-478. https://doi.org/10.1016/j.molcel.2009.06.027

Chen, Q., Kang, J., & Fu, C. (2018). The independence of and associations among apoptosis, autophagy, and necrosis. *Signal Transduct Target Ther*, *3*, 18. https://doi.org/10.1038/s41392-018-0018-5

Chen, Z., Li, K., Yin, X., Li, H., Li, Y., Zhang, Q., Wang, H., & Qiu, Y. (2019). Lower Expression of Gelsolin in Colon Cancer and Its Diagnostic Value in Colon Cancer Patients. *J Cancer*, *10*(5), 1288-1296. https://doi.org/10.7150/jca.28529

Cheung, H. H., Lynn Kelly, N., Liston, P., & Korneluk, R. G. (2006). Involvement of caspase-2 and caspase-9 in endoplasmic reticulum stress-induced apoptosis: a role for the IAPs. *Exp Cell Res*, *312*(12), 2347-2357. https://doi.org/10.1016/j.yexcr.2006.03.027

Chi, S., Kitanaka, C., Noguchi, K., Mochizuki, T., Nagashima, Y., Shirouzu, M., Fujita, H., Yoshida, M., Chen, W., Asai, A., Himeno, M., Yokoyama, S., & Kuchino, Y. (1999). Oncogenic Ras triggers cell suicide through the activation of a caspase-independent cell death program in human cancer cells. *Oncogene*, *18*(13), 2281-2290. https://doi.org/10.1038/sj.onc.1202538

Cho, Y. S., Challa, S., Moquin, D., Genga, R., Ray, T. D., Guildford, M., & Chan, F. K. (2009). Phosphorylation-driven assembly of the RIP1-RIP3 complex regulates programmed necrosis and virus-induced inflammation. *Cell*, *137*(6), 1112-1123. https://doi.org/10.1016/j.cell.2009.05.037

Colussi, P. A., Harvey, N. L., & Kumar, S. (1998). Prodomain-dependent nuclear localization of the caspase-2 (Nedd2) precursor. A novel function for a caspase prodomain. *J Biol Chem*, *273*(38), 24535-24542. https://doi.org/10.1074/jbc.273.38.24535

Cookson, B. T., & Brennan, M. A. (2001). Pro-inflammatory programmed cell death. *Trends Microbiol*, *9*(3), 113-114. https://doi.org/10.1016/s0966-842x(00)01936-3

Dadsena, S., King, L. E., & Garcia-Saez, A. J. (2021). Apoptosis regulation at the mitochondria membrane level. *Biochim Biophys Acta Biomembr*, *1863*(12), 183716. https://doi.org/10.1016/j.bbamem.2021.183716

David, K. K., Andrabi, S. A., Dawson, T. M., & Dawson, V. L. (2009). Parthanatos, a messenger of death. *Front Biosci (Landmark Ed)*, *14*(3), 1116-1128. https://doi.org/10.2741/3297

Dawar, S., Lim, Y., Puccini, J., White, M., Thomas, P., Bouchier-Hayes, L., Green, D. R., Dorstyn, L., & Kumar, S. (2017). Caspase-2-mediated cell death is required for deleting aneuploid cells. *Oncogene*, *36*(19), 2704-2714. https://doi.org/10.1038/onc.2016.423

Degli Esposti, M., Ferry, G., Masdehors, P., Boutin, J. A., Hickman, J. A., & Dive, C. (2003). Post-translational modification of Bid has differential effects on its susceptibility to cleavage by caspase 8 or caspase 3. *J Biol Chem*, *278*(18), 15749-15757. https://doi.org/10.1074/jbc.M209208200

Degterev, A., Huang, Z., Boyce, M., Li, Y., Jagtap, P., Mizushima, N., Cuny, G. D., Mitchison, T. J., Moskowitz, M. A., & Yuan, J. (2005). Chemical inhibitor of nonapoptotic cell death with therapeutic potential for ischemic brain injury. *Nat Chem Biol*, *1*(2), 112-119. https://doi.org/10.1038/nchembio711

Dekkers, M. P., Nikoletopoulou, V., & Barde, Y. A. (2013). Cell biology in neuroscience: Death of developing neurons: new insights and implications for connectivity. *J Cell Biol*, *203*(3), 385-393. https://doi.org/10.1083/jcb.201306136

Dinkova-Kostova, A. T., & Talalay, P. (2010). NAD(P)H:quinone acceptor oxidoreductase 1 (NQO1), a multifunctional antioxidant enzyme and exceptionally versatile cytoprotector. *Arch Biochem Biophys*, *501*(1), 116-123. https://doi.org/10.1016/j.abb.2010.03.019

Distler, U., Kuharev, J., Navarro, P., & Tenzer, S. (2016). Label-free quantification in ion mobility-enhanced data-independent acquisition proteomics. *Nat Protoc*, *11*(4), 795-812. https://doi.org/10.1038/nprot.2016.042

Distler, U., Kuharev, J., & Tenzer, S. (2014). Biomedical applications of ion mobility-enhanced data-independent acquisition-based label-free quantitative proteomics. *Expert Rev Proteomics*, *11*(6), 675-684. https://doi.org/10.1586/14789450.2014.971114

Dixon, S. J., Lemberg, K. M., Lamprecht, M. R., Skouta, R., Zaitsev, E. M., Gleason, C. E., Patel, D. N., Bauer, A. J., Cantley, A. M., Yang, W. S., Morrison, B., 3rd, & Stockwell, B. R. (2012). Ferroptosis: an iron-dependent form of nonapoptotic cell death. *Cell*, *149*(5), 1060-1072. https://doi.org/10.1016/j.cell.2012.03.042

Dong, B., Horowitz, D. S., Kobayashi, R., & Krainer, A. R. (1993). Purification and cDNA cloning of HeLa cell p54nrb, a nuclear protein with two RNA recognition motifs and extensive

homology to human splicing factor PSF and Drosophila NONA/BJ6. *Nucleic Acids Res*, *21*(17), 4085-4092. https://doi.org/10.1093/nar/21.17.4085

Dorstyn, L., & Kumar, S. (2009). Putative functions of caspase-2. *F1000 Biol Rep*, *1*, 96. https://doi.org/10.3410/B1-96

Dorstyn, L., Puccini, J., Wilson, C. H., Shalini, S., Nicola, M., Moore, S., & Kumar, S. (2012). Caspase-2 deficiency promotes aberrant DNA-damage response and genetic instability. *Cell Death Differ*, *19*(8), 1288-1298. https://doi.org/10.1038/cdd.2012.36

Droin, N., Beauchemin, M., Solary, E., & Bertrand, R. (2000). Identification of a caspase-2 isoform that behaves as an endogenous inhibitor of the caspase cascade. *Cancer Res*, *60*(24), 7039-7047. https://www.ncbi.nlm.nih.gov/pubmed/11156409

Duan, H., & Dixit, V. M. (1997). RAIDD is a new 'death' adaptor molecule. *Nature*, *385*(6611), 86-89. https://doi.org/10.1038/385086a0

Dudgeon, C., Qiu, W., Sun, Q. H., Zhang, L., & Yu, J. (2009). Transcriptional Regulation of Apoptosis. *Essentials of Apoptosis, Second Edition*, 239-260. https://doi.org/10.1007/978-1-60327-381-7_10

Eichler, M., Aksi, E., Pfeilschifter, J., & Imre, G. (2021). Application of pseudotyped virus particles to monitor Ebola virus and SARS-CoV-2 viral entry in human cell lines. *STAR Protoc*, *2*(4), 100818. https://doi.org/10.1016/j.xpro.2021.100818

Eichler, M., Distler, U., Nasrullah, U., Krishnan, A., Kaulich, M., Husnjak, K., Eberhardt, W., Rajalingam, K., Tenzer, S., Pfeilschifter, J., & Imre, G. (2022). The caspase-2 substrate p54nrb exhibits a multifaceted role in tumor cell death susceptibility via gene regulatory functions. *Cell Death Dis*, *13*(4), 386. https://doi.org/10.1038/s41419-022-04829-2

Elmore, S. (2007). Apoptosis: a review of programmed cell death. *Toxicol Pathol*, *35*(4), 495-516. https://doi.org/10.1080/01926230701320337

Emili, A., Shales, M., McCracken, S., Xie, W., Tucker, P. W., Kobayashi, R., Blencowe, B. J., & Ingles, C. J. (2002). Splicing and transcription-associated proteins PSF and p54nrb/nonO bind to the RNA polymerase II CTD. *RNA*, *8*(9), 1102-1111. https://doi.org/10.1017/s1355838202025037

Eymin, B., Leduc, C., Coll, J. L., Brambilla, E., & Gazzeri, S. (2003). p14ARF induces G2 arrest and apoptosis independently of p53 leading to regression of tumours established in nude mice. *Oncogene*, *22*(12), 1822-1835. https://doi.org/10.1038/sj.onc.1206303

Fadeel, B., Orrenius, S., & Zhivotovsky, B. (1999). Apoptosis in human disease: a new skin for the old ceremony? *Biochem Biophys Res Commun*, *266*(3), 699-717. https://doi.org/10.1006/bbrc.1999.1888

Fava, L. L., Bock, F. J., Geley, S., & Villunger, A. (2012). Caspase-2 at a glance. *J Cell Sci*, *125*(Pt 24), 5911-5915. https://doi.org/10.1242/jcs.115105

Feng, P., Li, L., Deng, T., Liu, Y., Ling, N., Qiu, S., Zhang, L., Peng, B., Xiong, W., Cao, L., Zhang, L., & Ye, M. (2020). NONO and tumorigenesis: More than splicing. *J Cell Mol Med*, *24*(8), 4368-4376. https://doi.org/10.1111/jcmm.15141

Feng, S., Yang, Y., Mei, Y., Ma, L., Zhu, D. E., Hoti, N., Castanares, M., & Wu, M. (2007). Cleavage of RIP3 inactivates its caspase-independent apoptosis pathway by removal of kinase domain. *Cell Signal*, *19*(10), 2056-2067. https://doi.org/10.1016/j.cellsig.2007.05.016

Fischer, U., Janicke, R. U., & Schulze-Osthoff, K. (2003). Many cuts to ruin: a comprehensive update of caspase substrates. *Cell Death Differ*, *10*(1), 76-100. https://doi.org/10.1038/sj.cdd.4401160

Fox, A. H., Bond, C. S., & Lamond, A. I. (2005). P54nrb forms a heterodimer with PSP1 that localizes to paraspeckles in an RNA-dependent manner. *Mol Biol Cell*, *16*(11), 5304-5315. https://doi.org/10.1091/mbc.e05-06-0587

Fox, A. H., Lam, Y. W., Leung, A. K., Lyon, C. E., Andersen, J., Mann, M., & Lamond, A. I. (2002). Paraspeckles: a novel nuclear domain. *Curr Biol*, *12*(1), 13-25. https://doi.org/10.1016/s0960-9822(01)00632-7

Frisch, S. M., & Francis, H. (1994). Disruption of epithelial cell-matrix interactions induces apoptosis. *J Cell Biol*, *124*(4), 619-626. https://doi.org/10.1083/jcb.124.4.619

Frisch, S. M., & Ruoslahti, E. (1997). Integrins and anoikis. *Curr Opin Cell Biol*, *9*(5), 701-706. https://doi.org/10.1016/s0955-0674(97)80124-x

Fuchs, T. A., Abed, U., Goosmann, C., Hurwitz, R., Schulze, I., Wahn, V., Weinrauch, Y., Brinkmann, V., & Zychlinsky, A. (2007). Novel cell death program leads to neutrophil extracellular traps. *J Cell Biol*, *176*(2), 231-241. https://doi.org/10.1083/jcb.200606027

Fulda, S. (2010). Evasion of apoptosis as a cellular stress response in cancer. *Int J Cell Biol*, *2010*, 370835. https://doi.org/10.1155/2010/370835

Fulda, S. (2015). Promises and Challenges of Smac Mimetics as Cancer Therapeutics. *Clin Cancer Res*, *21*(22), 5030-5036. https://doi.org/10.1158/1078-0432.CCR-15-0365

Fulda, S., & Debatin, K. M. (2002). IFNgamma sensitizes for apoptosis by upregulating caspase-8 expression through the Stat1 pathway. *Oncogene*, *21*(15), 2295-2308. https://doi.org/10.1038/sj.onc.1205255

Garibaldi, F., Falcone, E., Trisciuoglio, D., Colombo, T., Lisek, K., Walerych, D., Del Sal, G., Paci, P., Bossi, G., Piaggio, G., & Gurtner, A. (2016). Mutant p53 inhibits miRNA biogenesis by interfering with the microprocessor complex. *Oncogene*, *35*(29), 3760-3770. https://doi.org/10.1038/onc.2016.51

Garufi, A., Ubertini, V., Mancini, F., D'Orazi, V., Baldari, S., Moretti, F., Bossi, G., & D'Orazi, G. (2015). The beneficial effect of Zinc(II) on low-dose chemotherapeutic sensitivity involves p53 activation in wild-type p53-carrying colorectal cancer cells. *J Exp Clin Cancer Res*, *34*, 87. https://doi.org/10.1186/s13046-015-0206-x

Green, D. R., & Llambi, F. (2015). Cell Death Signaling. *Cold Spring Harb Perspect Biol*, *7*(12). https://doi.org/10.1101/cshperspect.a006080

Grimm, S., Stanger, B. Z., & Leder, P. (1996). RIP and FADD: two "death domain"-containing proteins can induce apoptosis by convergent, but dissociable, pathways. *Proc Natl Acad Sci U S A*, *93*(20), 10923-10927. https://doi.org/10.1073/pnas.93.20.10923

Guo, Y., Srinivasula, S. M., Druilhe, A., Fernandes-Alnemri, T., & Alnemri, E. S. (2002). Caspase-2 induces apoptosis by releasing proapoptotic proteins from mitochondria. *J Biol Chem*, *277*(16), 13430-13437. https://doi.org/10.1074/jbc.M108029200

Hacker, G. (2000). The morphology of apoptosis. *Cell Tissue Res*, *301*(1), 5-17. https://doi.org/10.1007/s004410000193

Hall-Pogar, T., Liang, S., Hague, L. K., & Lutz, C. S. (2007). Specific trans-acting proteins interact with auxiliary RNA polyadenylation elements in the COX-2 3'-UTR. *RNA*, *13*(7), 1103-1115. https://doi.org/10.1261/rna.577707

Hallier, M., Tavitian, A., & Moreau-Gachelin, F. (1996). The transcription factor Spi-1/PU.1 binds RNA and interferes with the RNA-binding protein p54nrb. *J Biol Chem*, *271*(19), 11177-11181. https://doi.org/10.1074/jbc.271.19.11177

Han, C., Zhao, R., Kroger, J., Qu, M., Wani, A. A., & Wang, Q. E. (2013). Caspase-2 short isoform interacts with membrane-associated cytoskeleton proteins to inhibit apoptosis. *PLoS One*, *8*(7), e67033. https://doi.org/10.1371/journal.pone.0067033

Hasegawa, H., Yamada, Y., Tsukasaki, K., Mori, N., Tsuruda, K., Sasaki, D., Usui, T., Osaka, A., Atogami, S., Ishikawa, C., Machijima, Y., Sawada, S., Hayashi, T., Miyazaki, Y., & Kamihira, S. (2011). LBH589, a deacetylase inhibitor, induces apoptosis in adult T-cell leukemia/lymphoma cells via activation of a novel RAIDD-caspase-2 pathway. *Leukemia*, *25*(4), 575-587. https://doi.org/10.1038/leu.2010.315

Hat, B., Kochanczyk, M., Bogdal, M. N., & Lipniacki, T. (2016). Feedbacks, Bifurcations, and Cell Fate Decision-Making in the p53 System. *PLoS Comput Biol*, *12*(2), e1004787. https://doi.org/10.1371/journal.pcbi.1004787

Hicks, S. W., & Machamer, C. E. (2002). The NH2-terminal domain of Golgin-160 contains both Golgi and nuclear targeting information. *J Biol Chem*, *277*(39), 35833-35839. https://doi.org/10.1074/jbc.M206280200

Ho, L. H., Taylor, R., Dorstyn, L., Cakouros, D., Bouillet, P., & Kumar, S. (2009). A tumor suppressor function for caspase-2. *Proc Natl Acad Sci U S A*, *106*(13), 5336-5341. https://doi.org/10.1073/pnas.0811928106

Hofmann, K., Bucher, P., & Tschopp, J. (1997). The CARD domain: a new apoptotic signalling motif. *Trends Biochem Sci*, *22*(5), 155-156. https://doi.org/10.1016/s0968-0004(97)01043-8

Holler, N., Zaru, R., Micheau, O., Thome, M., Attinger, A., Valitutti, S., Bodmer, J. L., Schneider, P., Seed, B., & Tschopp, J. (2000). Fas triggers an alternative, caspase-8-independent cell death pathway using the kinase RIP as effector molecule. *Nat Immunol*, *1*(6), 489-495. https://doi.org/10.1038/82732

Hsu, H., Xiong, J., & Goeddel, D. V. (1995). The TNF receptor 1-associated protein TRADD signals cell death and NF-kappa B activation. *Cell*, *81*(4), 495-504. https://doi.org/10.1016/0092-8674(95)90070-5

Hu, S. B., Xiang, J. F., Li, X., Xu, Y., Xue, W., Huang, M., Wong, C. C., Sagum, C. A., Bedford, M. T., Yang, L., Cheng, D., & Chen, L. L. (2015). Protein arginine methyltransferase CARM1 attenuates the paraspeckle-mediated nuclear retention of mRNAs containing IRAlus. *Genes Dev*, *29*(6), 630-645. https://doi.org/10.1101/gad.257048.114

Huang da, W., Sherman, B. T., & Lempicki, R. A. (2009). Systematic and integrative analysis of large gene lists using DAVID bioinformatics resources. *Nat Protoc*, *4*(1), 44-57. https://doi.org/10.1038/nprot.2008.211

Imre, G., Berthelet, J., Heering, J., Kehrloesser, S., Melzer, I. M., Lee, B. I., Thiede, B., Dotsch, V., & Rajalingam, K. (2017). Apoptosis inhibitor 5 is an endogenous inhibitor of caspase-2. *EMBO Rep*, *18*(5), 733-744. https://doi.org/10.15252/embr.201643744

Imre, G., Heering, J., Takeda, A. N., Husmann, M., Thiede, B., zu Heringdorf, D. M., Green, D. R., van der Goot, F. G., Sinha, B., Dotsch, V., & Rajalingam, K. (2012). Caspase-2 is an initiator caspase responsible for pore-forming toxin-mediated apoptosis. *EMBO J*, *31*(11), 2615-2628. https://doi.org/10.1038/emboj.2012.93

Imre, G., Krahling, V., Eichler, M., Trautmann, S., Ferreiros, N., Aman, M. J., Kashanchi, F., Rajalingam, K., Pohlmann, S., Becker, S., Meyer Zu Heringdorf, D., & Pfeilschifter, J. (2021). The sphingosine kinase 1 activator, K6PC-5, attenuates Ebola virus infection. *iScience*, *24*(4), 102266. https://doi.org/10.1016/j.isci.2021.102266

Imre, G., & Rajalingam, K. (2012). Role for caspase-2 during pore-forming toxin-mediated apoptosis. *Cell Cycle*, *11*(20), 3709-3710. https://doi.org/10.4161/cc.22046

Irmler, M., Thome, M., Hahne, M., Schneider, P., Hofmann, K., Steiner, V., Bodmer, J. L., Schroter, M., Burns, K., Mattmann, C., Rimoldi, D., French, L. E., & Tschopp, J. (1997). Inhibition of death receptor signals by cellular FLIP. *Nature*, *388*(6638), 190-195. https://doi.org/10.1038/40657

Ishiguro, H., Uemura, H., Fujinami, K., Ikeda, N., Ohta, S., & Kubota, Y. (2003). 55 kDa nuclear matrix protein (nmt55) mRNA is expressed in human prostate cancer tissue and is associated with the androgen receptor. *Int J Cancer*, *105*(1), 26-32. https://doi.org/10.1002/ijc.11021

Ishitani, K., Yoshida, T., Kitagawa, H., Ohta, H., Nozawa, S., & Kato, S. (2003). p54nrb acts as a transcriptional coactivator for activation function 1 of the human androgen receptor. *Biochem Biophys Res Commun*, *306*(3), 660-665. https://doi.org/10.1016/s0006-291x(03)01021-0

Iwanaga, N., Kamachi, M., Aratake, K., Izumi, Y., Ida, H., Tanaka, F., Tamai, M., Arima, K., Nakamura, H., Origuchi, T., Kawakami, A., & Eguchi, K. (2005). Regulation of alternative splicing of caspase-2 through an intracellular signaling pathway in response to pro-apoptotic stimuli. *J Lab Clin Med*, *145*(2), 105-110. https://doi.org/10.1016/j.lab.2004.11.020

Jaiswal, A. K. (2000). Regulation of genes encoding NAD(P)H:quinone oxidoreductases. *Free Radic Biol Med*, *29*(3-4), 254-262. https://doi.org/10.1016/s0891-5849(00)00306-3

Julien, O., & Wells, J. A. (2017). Caspases and their substrates. *Cell Death and Differentiation*, *24*(8), 1380-1389. https://doi.org/10.1038/cdd.2017.44

Kamada, S., Kikkawa, U., Tsujimoto, Y., & Hunter, T. (2005). Nuclear translocation of caspase-3 is dependent on its proteolytic activation and recognition of a substrate-like protein(s). *J Biol Chem*, *280*(2), 857-860. https://doi.org/10.1074/jbc.C400538200

Kameoka, S., Duque, P., & Konarska, M. M. (2004). p54(nrb) associates with the 5' splice site within large transcription/splicing complexes. *EMBO J*, *23*(8), 1782-1791. https://doi.org/10.1038/sj.emboj.7600187

Kaneko, S., Rozenblatt-Rosen, O., Meyerson, M., & Manley, J. L. (2007). The multifunctional protein p54nrb/PSF recruits the exonuclease XRN2 to facilitate pre-mRNA 3' processing and transcription termination. *Genes Dev*, *21*(14), 1779-1789. https://doi.org/10.1101/gad.1565207

Kang, M. H., & Reynolds, C. P. (2009). Bcl-2 inhibitors: targeting mitochondrial apoptotic pathways in cancer therapy. *Clin Cancer Res*, *15*(4), 1126-1132. https://doi.org/10.1158/1078-0432.CCR-08-0144

Kaufmann, S. H., Desnoyers, S., Ottaviano, Y., Davidson, N. E., & Poirier, G. G. (1993). Specific proteolytic cleavage of poly(ADP-ribose) polymerase: an early marker of chemotherapy-induced apoptosis. *Cancer Res*, *53*(17), 3976-3985. https://www.ncbi.nlm.nih.gov/pubmed/8358726

Kerr, J. F., Wyllie, A. H., & Currie, A. R. (1972). Apoptosis: a basic biological phenomenon with wide-ranging implications in tissue kinetics. *Br J Cancer*, *26*(4), 239-257. https://doi.org/10.1038/bjc.1972.33

Kharade, S. S., Parekh, V. I., & Agarwal, S. K. (2018). Functional Defects From Endocrine Disease-Associated Mutations in HLXB9 and Its Interacting Partner, NONO. *Endocrinology*, *159*(2), 1199-1212. https://doi.org/10.1210/en.2017-03155

Kim, I. R., Murakami, K., Chen, N. J., Saibil, S. D., Matysiak-Zablocki, E., Elford, A. R., Bonnard, M., Benchimol, S., Jurisicova, A., Yeh, W. C., & Ohashi, P. S. (2009). DNA damage- and stress-induced apoptosis occurs independently of PIDD. *Apoptosis*, *14*(9), 1039-1049. https://doi.org/10.1007/s10495-009-0375-1

Kiraz, Y., Adan, A., Kartal Yandim, M., & Baran, Y. (2016). Major apoptotic mechanisms and genes involved in apoptosis. *Tumour Biol*, *37*(7), 8471-8486. https://doi.org/10.1007/s13277-016-5035-9

Kischkel, F. C., Hellbardt, S., Behrmann, I., Germer, M., Pawlita, M., Krammer, P. H., & Peter, M. E. (1995). Cytotoxicity-dependent APO-1 (Fas/CD95)-associated proteins form a death-inducing signaling complex (DISC) with the receptor. *EMBO J*, *14*(22), 5579-5588. https://doi.org/10.1002/j.1460-2075.1995.tb00245.x

Kischkel, F. C., Lawrence, D. A., Tinel, A., LeBlanc, H., Virmani, A., Schow, P., Gazdar, A., Blenis, J., Arnott, D., & Ashkenazi, A. (2001). Death receptor recruitment of endogenous caspase-10 and apoptosis initiation in the absence of caspase-8. *J Biol Chem*, *276*(49), 46639-46646. https://doi.org/10.1074/jbc.M105102200

Knott, G. J., Bond, C. S., & Fox, A. H. (2016). The DBHS proteins SFPQ, NONO and PSPC1: a multipurpose molecular scaffold. *Nucleic Acids Res*, *44*(9), 3989-4004. https://doi.org/10.1093/nar/gkw271

Knott, G. J., Lee, M., Passon, D. M., Fox, A. H., & Bond, C. S. (2015). Caenorhabditis elegans NONO-1: Insights into DBHS protein structure, architecture, and function. *Protein Sci*, *24*(12), 2033-2043. https://doi.org/10.1002/pro.2816

Knott, G. J., Panjikar, S., Thorn, A., Fox, A. H., Conte, M. R., Lee, M., & Bond, C. S. (2016). A crystallographic study of human NONO (p54(nrb)): overcoming pathological problems with purification, data collection and noncrystallographic symmetry. *Acta Crystallogr D Struct Biol*, *72*(Pt 6), 761-769. https://doi.org/10.1107/S2059798316005830

Kowalska, E., Ripperger, J. A., Hoegger, D. C., Bruegger, P., Buch, T., Birchler, T., Mueller, A., Albrecht, U., Contaldo, C., & Brown, S. A. (2013). NONO couples the circadian clock to the cell cycle. *Proc Natl Acad Sci U S A*, *110*(5), 1592-1599. https://doi.org/10.1073/pnas.1213317110

Kowalska, E., Ripperger, J. A., Muheim, C., Maier, B., Kurihara, Y., Fox, A. H., Kramer, A., & Brown, S. A. (2012). Distinct roles of DBHS family members in the circadian transcriptional feedback loop. *Mol Cell Biol*, *32*(22), 4585-4594. https://doi.org/10.1128/MCB.00334-12

Koya, R. C., Fujita, H., Shimizu, S., Ohtsu, M., Takimoto, M., Tsujimoto, Y., & Kuzumaki, N. (2000). Gelsolin inhibits apoptosis by blocking mitochondrial membrane potential loss and cytochrome c release. *J Biol Chem*, *275*(20), 15343-15349. https://doi.org/10.1074/jbc.275.20.15343

Kroemer, G., & Martin, S. J. (2005). Caspase-independent cell death. *Nat Med*, *11*(7), 725-730. https://doi.org/10.1038/nm1263

Krumschnabel, G., Sohm, B., Bock, F., Manzl, C., & Villunger, A. (2009). The enigma of caspase-2: the laymen's view. *Cell Death Differ*, *16*(2), 195-207. https://doi.org/10.1038/cdd.2008.170

Kumar, S. (2009). Caspase 2 in apoptosis, the DNA damage response and tumour suppression: enigma no more? *Nat Rev Cancer*, *9*(12), 897-903. https://doi.org/10.1038/nrc2745

Kumar, S., Kinoshita, M., Noda, M., Copeland, N. G., & Jenkins, N. A. (1994). Induction of apoptosis by the mouse Nedd2 gene, which encodes a protein similar to the product of the Caenorhabditis elegans cell death gene ced-3 and the mammalian IL-1 beta-converting enzyme. *Genes Dev*, *8*(14), 1613-1626. https://doi.org/10.1101/gad.8.14.1613

Kumar, S., White, D. L., Takai, S., Turczynowicz, S., Juttner, C. A., & Hughes, T. P. (1995). Apoptosis regulatory gene NEDD2 maps to human chromosome segment 7q34-35, a region frequently affected in haematological neoplasms. *Hum Genet*, *95*(6), 641-644. https://doi.org/10.1007/BF00209480

Lamkanfi, M., Declercq, W., Kalai, M., Saelens, X., & Vandenabeele, P. (2002). Alice in caspase land. A phylogenetic analysis of caspases from worm to man. *Cell Death Differ*, *9*(4), 358-361. https://doi.org/10.1038/sj.cdd.4400989

Lamkanfi, M., Declercq, W., Vanden Berghe, T., & Vandenabeele, P. (2006). Caspases leave the beaten track: caspase-mediated activation of NF-kappaB. *J Cell Biol*, *173*(2), 165-171. https://doi.org/10.1083/jcb.200509092

Lechner, A. M., Assfalg-Machleidt, I., Zahler, S., Stoeckelhuber, M., Machleidt, W., Jochum, M., & Nagler, D. K. (2006). RGD-dependent binding of procathepsin X to integrin alphavbeta3 mediates cell-adhesive properties. *J Biol Chem*, *281*(51), 39588-39597. https://doi.org/10.1074/jbc.M513439200

Leist, M., & Jaattela, M. (2001). Four deaths and a funeral: from caspases to alternative mechanisms. *Nat Rev Mol Cell Biol*, *2*(8), 589-598. https://doi.org/10.1038/35085008

Lewis, J. D., Payton, L. A., Whitford, J. G., Byrne, J. A., Smith, D. I., Yang, L., & Bright, R. K. (2007). Induction of tumorigenesis and metastasis by the murine orthologue of tumor protein D52. *Mol Cancer Res*, *5*(2), 133-144. https://doi.org/10.1158/1541-7786.MCR-06-0245

Li, H., Bergeron, L., Cryns, V., Pasternack, M. S., Zhu, H., Shi, L., Greenberg, A., & Yuan, J. (1997). Activation of caspase-2 in apoptosis. *J Biol Chem*, *272*(34), 21010-21017. https://doi.org/10.1074/jbc.272.34.21010

Li, J., Li, Y., Liu, H., Liu, Y., & Cui, B. (2017). The four-transmembrane protein MAL2 and tumor protein D52 (TPD52) are highly expressed in colorectal cancer and correlated with poor prognosis. *PLoS One*, *12*(5), e0178515. https://doi.org/10.1371/journal.pone.0178515

Li, P., Nijhawan, D., Budihardjo, I., Srinivasula, S. M., Ahmad, M., Alnemri, E. S., & Wang, X. (1997). Cytochrome c and dATP-dependent formation of Apaf-1/caspase-9 complex initiates an

apoptotic protease cascade. *Cell*, *91*(4), 479-489. https://doi.org/10.1016/s0092-8674(00)80434-1

Li, Q., Guo, H., Li, H., Zhu, Q., & Liu, Y. (2017). P54/nrb prompts rheumatoid arthritis progression mainly by transcriptionally activating NF-kappaB signaling. *Pharmazie*, *72*(5), 260-264. https://doi.org/10.1691/ph.2017.6904

Li, S., Kuhne, W. W., Kulharya, A., Hudson, F. Z., Ha, K., Cao, Z., & Dynan, W. S. (2009). Involvement of p54(nrb), a PSF partner protein, in DNA double-strand break repair and radioresistance. *Nucleic Acids Res*, *37*(20), 6746-6753. https://doi.org/10.1093/nar/gkp741

Liang, S., & Lutz, C. S. (2006). p54nrb is a component of the snRNP-free U1A (SF-A) complex that promotes pre-mRNA cleavage during polyadenylation. *RNA*, *12*(1), 111-121. https://doi.org/10.1261/rna.2213506

Liao, C. J., Wu, T. I., Huang, Y. H., Chang, T. C., Wang, C. S., Tsai, M. M., Hsu, C. Y., Tsai, M. H., Lai, C. H., & Lin, K. H. (2011). Overexpression of gelsolin in human cervical carcinoma and its clinicopathological significance. *Gynecol Oncol*, *120*(1), 135-144. https://doi.org/10.1016/j.ygyno.2010.10.005

Liggett, W. H., Jr., & Sidransky, D. (1998). Role of the p16 tumor suppressor gene in cancer. *J Clin Oncol*, *16*(3), 1197-1206. https://doi.org/10.1200/jco.1998.16.3.1197

Lim, Y., De Bellis, D., Sandow, J. J., Capalbo, L., D'Avino, P. P., Murphy, J. M., Webb, A. I., Dorstyn, L., & Kumar, S. (2021). Phosphorylation by Aurora B kinase regulates caspase-2 activity and function. *Cell Death Differ*, *28*(1), 349-366. https://doi.org/10.1038/s41418-020-00604-y

Lim, Y., Dorstyn, L., & Kumar, S. (2021). The p53-caspase-2 axis in the cell cycle and DNA damage response. *Exp Mol Med*, *53*(4), 517-527. https://doi.org/10.1038/s12276-021-00590-2

Lima, R. T., Busacca, S., Almeida, G. M., Gaudino, G., Fennell, D. A., & Vasconcelos, M. H. (2011). MicroRNA regulation of core apoptosis pathways in cancer. *Eur J Cancer*, *47*(2), 163-174. https://doi.org/10.1016/j.ejca.2010.11.005

Lin, Y., Ma, W., & Benchimol, S. (2000). Pidd, a new death-domain-containing protein, is induced by p53 and promotes apoptosis. *Nat Genet*, *26*(1), 122-127. https://doi.org/10.1038/79102

Lindsten, T., Ross, A. J., King, A., Zong, W. X., Rathmell, J. C., Shiels, H. A., Ulrich, E., Waymire, K. G., Mahar, P., Frauwirth, K., Chen, Y., Wei, M., Eng, V. M., Adelman, D. M., Simon, M. C., Ma, A., Golden, J. A., Evan, G., Korsmeyer, S. J., . . . Thompson, C. B. (2000). The combined functions of proapoptotic Bcl-2 family members bak and bax are essential for normal development of multiple tissues. *Mol Cell*, *6*(6), 1389-1399. https://doi.org/10.1016/s1097-2765(00)00136-2

Lines, K. E., Chelala, C., Dmitrovic, B., Wijesuriya, N., Kocher, H. M., Marshall, J. F., & Crnogorac-Jurcevic, T. (2012). S100P-binding protein, S100PBP, mediates adhesion through regulation of cathepsin Z in pancreatic cancer cells. *Am J Pathol*, *180*(4), 1485-1494. https://doi.org/10.1016/j.ajpath.2011.12.031

Litwin, M., Nowak, D., Mazur, A. J., Baczynska, D., Mannherz, H. G., & Malicka-Blaszkiewicz, M. (2012). Gelsolin affects the migratory ability of human colon adenocarcinoma and melanoma cells. *Life Sci*, *90*(21-22), 851-861. https://doi.org/10.1016/j.lfs.2012.03.039

Liu, L., Xie, N., Rennie, P., Challis, J. R., Gleave, M., Lye, S. J., & Dong, X. (2011). Consensus PP1 binding motifs regulate transcriptional corepression and alternative RNA splicing activities of the steroid receptor coregulators, p54nrb and PSF. *Mol Endocrinol*, *25*(7), 1197-1210. https://doi.org/10.1210/me.2010-0517

Liu, P. Y., Erriquez, D., Marshall, G. M., Tee, A. E., Polly, P., Wong, M., Liu, B., Bell, J. L., Zhang, X. D., Milazzo, G., Cheung, B. B., Fox, A., Swarbrick, A., Huttelmaier, S., Kavallaris, M., Perini, G., Mattick, J. S., Dinger, M. E., & Liu, T. (2014). Effects of a novel long noncoding RNA, lncUSMycN, on N-Myc expression and neuroblastoma progression. *J Natl Cancer Inst*, *106*(7). https://doi.org/10.1093/jnci/dju113

Lopez-Garcia, C., Sansregret, L., Domingo, E., McGranahan, N., Hobor, S., Birkbak, N. J., Horswell, S., Gronroos, E., Favero, F., Rowan, A. J., Matthews, N., Begum, S., Phillimore, B., Burrell, R., Oukrif, D., Spencer-Dene, B., Kovac, M., Stamp, G., Stewart, A., . . . Swanton, C. (2017). BCL9L Dysfunction Impairs Caspase-2 Expression Permitting Aneuploidy Tolerance in Colorectal Cancer. *Cancer Cell*, *31*(1), 79-93. https://doi.org/10.1016/j.ccell.2016.11.001

Lu, J. Y., & Sewer, M. B. (2015). p54nrb/NONO regulates cyclic AMP-dependent glucocorticoid production by modulating phosphodiesterase mRNA splicing and degradation. *Mol Cell Biol*, *35*(7), 1223-1237. https://doi.org/10.1128/MCB.00993-14

Luan, Y., Zhang, W., Xie, J., & Mao, J. (2021). CDKN2A inhibits cell proliferation and invasion in cervical cancer through LDHA-mediated AKT/mTOR pathway. *Clin Transl Oncol*, *23*(2), 222-228. https://doi.org/10.1007/s12094-020-02409-4

Mahmood, Z., & Shukla, Y. (2010). Death receptors: targets for cancer therapy. *Exp Cell Res*, *316*(6), 887-899. https://doi.org/10.1016/j.yexcr.2009.12.011

Malla, W. A., Arora, R., Khan, R. I. N., Mahajan, S., & Tiwari, A. K. (2020). Apoptin as a Tumor-Specific Therapeutic Agent: Current Perspective on Mechanism of Action and Delivery Systems. *Front Cell Dev Biol*, *8*, 524. https://doi.org/10.3389/fcell.2020.00524

Maltese, W. A., & Overmeyer, J. H. (2014). Methuosis: nonapoptotic cell death associated with vacuolization of macropinosome and endosome compartments. *Am J Pathol*, *184*(6), 1630-1642. https://doi.org/10.1016/j.ajpath.2014.02.028

Mancini, M., Machamer, C. E., Roy, S., Nicholson, D. W., Thornberry, N. A., Casciola-Rosen, L. A., & Rosen, A. (2000). Caspase-2 is localized at the Golgi complex and cleaves golgin-160 during apoptosis. *J Cell Biol*, *149*(3), 603-612. https://doi.org/10.1083/jcb.149.3.603

Maniam, S., & Maniam, S. (2021). Small Molecules Targeting Programmed Cell Death in Breast Cancer Cells. *Int J Mol Sci*, *22*(18). https://doi.org/10.3390/ijms22189722

Mansoori, B., Mohammadi, A., Davudian, S., Shirjang, S., & Baradaran, B. (2017). The Different Mechanisms of Cancer Drug Resistance: A Brief Review. *Adv Pharm Bull*, *7*(3), 339-348. https://doi.org/10.15171/apb.2017.041

Manzl, C., Krumschnabel, G., Bock, F., Sohm, B., Labi, V., Baumgartner, F., Logette, E., Tschopp, J., & Villunger, A. (2009). Caspase-2 activation in the absence of PIDDosome formation. *J Cell Biol*, *185*(2), 291-303. https://doi.org/10.1083/jcb.200811105

Markiewicz, A., Sigorski, D., Markiewicz, M., Owczarczyk-Saczonek, A., & Placek, W. (2021). Caspase-14-From Biomolecular Basics to Clinical Approach. A Review of Available Data. *Int J Mol Sci*, *22*(11). https://doi.org/10.3390/ijms22115575

Martinon, F., & Tschopp, J. (2007). Inflammatory caspases and inflammasomes: master switches of inflammation. *Cell Death Differ*, *14*(1), 10-22. https://doi.org/10.1038/sj.cdd.4402038

Mazurkiewicz, E., Makowiecka, A., Mrowczynska, E., Kopernyk, I., Nowak, D., & Mazur, A. J. (2021). Gelsolin Contributes to the Motility of A375 Melanoma Cells and This Activity Is Mediated by the Fibrous Extracellular Matrix Protein Profile. *Cells*, *10*(8). https://doi.org/10.3390/cells10081848

McCoy, F., Eckard, L., & Nutt, L. K. (2012). Janus-faced PIDD: a sensor for DNA damage-induced cell death or survival? *Mol Cell*, *47*(5), 667-668. https://doi.org/10.1016/j.molcel.2012.08.019

Mircsof, D., Langouet, M., Rio, M., Moutton, S., Siquier-Pernet, K., Bole-Feysot, C., Cagnard, N., Nitschke, P., Gaspar, L., Znidaric, M., Alibeu, O., Fritz, A. K., Wolfer, D. P., Schroter, A., Bosshard, G., Rudin, M., Koester, C., Crestani, F., Seebeck, P., . . . Colleaux, L. (2015). Mutations in NONO lead to syndromic intellectual disability and inhibitory synaptic defects. *Nat Neurosci*, *18*(12), 1731-1736. https://doi.org/10.1038/nn.4169

Mitrovic, A., Pecar Fonovic, U., & Kos, J. (2017). Cysteine cathepsins B and X promote epithelial-mesenchymal transition of tumor cells. *Eur J Cell Biol*, *96*(6), 622-631. https://doi.org/10.1016/j.ejcb.2017.04.003

Mizushima, N., & Levine, B. (2010). Autophagy in mammalian development and differentiation. *Nat Cell Biol*, *12*(9), 823-830. https://doi.org/10.1038/ncb0910-823

Momand, J., Wu, H. H., & Dasgupta, G. (2000). MDM2--master regulator of the p53 tumor suppressor protein. *Gene*, *242*(1-2), 15-29. https://doi.org/10.1016/s0378-1119(99)00487-4

Mori, S., Chang, J. T., Andrechek, E. R., Matsumura, N., Baba, T., Yao, G., Kim, J. W., Gatza, M., Murphy, S., & Nevins, J. R. (2009). Anchorage-independent cell growth signature identifies tumors with metastatic potential. *Oncogene*, *28*(31), 2796-2805. https://doi.org/10.1038/onc.2009.139

Mullard, A. (2016). Parsing clinical success rates. *Nat Rev Drug Discov*, *15*(7), 447. https://doi.org/10.1038/nrd.2016.136

Muller, P. A., & Vousden, K. H. (2013). p53 mutations in cancer. *Nat Cell Biol*, *15*(1), 2-8. https://doi.org/10.1038/ncb2641

Muzio, M., Chinnaiyan, A. M., Kischkel, F. C., O'Rourke, K., Shevchenko, A., Ni, J., Scaffidi, C., Bretz, J. D., Zhang, M., Gentz, R., Mann, M., Krammer, P. H., Peter, M. E., & Dixit, V. M. (1996). FLICE, a novel FADD-homologous ICE/CED-3-like protease, is recruited to the CD95 (Fas/APO-1) death--inducing signaling complex. *Cell*, *85*(6), 817-827. https://doi.org/10.1016/s0092-8674(00)81266-0

Nagata, S. (1997). Apoptosis by death factor. *Cell*, *88*(3), 355-365. https://doi.org/10.1016/s0092-8674(00)81874-7

Nailwal, H., & Chan, F. K. (2019). Necroptosis in anti-viral inflammation. *Cell Death Differ*, *26*(1), 4-13. https://doi.org/10.1038/s41418-018-0172-x

Nakahara, T., Kita, A., Yamanaka, K., Mori, M., Amino, N., Takeuchi, M., Tominaga, F., Hatakeyama, S., Kinoyama, I., Matsuhisa, A., Kudoh, M., & Sasamata, M. (2007). YM155, a novel small-molecule survivin suppressant, induces regression of established human

hormone-refractory prostate tumor xenografts. *Cancer Res*, *67*(17), 8014-8021. https://doi.org/10.1158/0008-5472.CAN-07-1343

Nelson, L. D., Bender, C., Mannsperger, H., Buergy, D., Kambakamba, P., Mudduluru, G., Korf, U., Hughes, D., Van Dyke, M. W., & Allgayer, H. (2012). Triplex DNA-binding proteins are associated with clinical outcomes revealed by proteomic measurements in patients with colorectal cancer. *Mol Cancer*, *11*, 38. https://doi.org/10.1186/1476-4598-11-38

Nicholson, D. W. (1999). Caspase structure, proteolytic substrates, and function during apoptotic cell death. *Cell Death Differ*, *6*(11), 1028-1042. https://doi.org/10.1038/sj.cdd.4400598

Nikoletopoulou, V., Markaki, M., Palikaras, K., & Tavernarakis, N. (2013). Crosstalk between apoptosis, necrosis and autophagy. *Biochim Biophys Acta*, *1833*(12), 3448-3459. https://doi.org/10.1016/j.bbamcr.2013.06.001

Notterman, D. A., Alon, U., Sierk, A. J., & Levine, A. J. (2001). Transcriptional gene expression profiles of colorectal adenoma, adenocarcinoma, and normal tissue examined by oligonucleotide arrays. *Cancer Res*, *61*(7), 3124-3130. https://www.ncbi.nlm.nih.gov/pubmed/11306497

Nutt, L. K., Margolis, S. S., Jensen, M., Herman, C. E., Dunphy, W. G., Rathmell, J. C., & Kornbluth, S. (2005). Metabolic regulation of oocyte cell death through the CaMKII-mediated phosphorylation of caspase-2. *Cell*, *123*(1), 89-103. https://doi.org/10.1016/j.cell.2005.07.032

O'Reilly, L. A., Ekert, P., Harvey, N., Marsden, V., Cullen, L., Vaux, D. L., Hacker, G., Magnusson, C., Pakusch, M., Cecconi, F., Kuida, K., Strasser, A., Huang, D. C., & Kumar, S. (2002). Caspase-2 is not required for thymocyte or neuronal apoptosis even though cleavage of caspase-2 is dependent on both Apaf-1 and caspase-9. *Cell Death Differ*, *9*(8), 832-841. https://doi.org/10.1038/sj.cdd.4401033

Oh, E. T., & Park, H. J. (2015). Implications of NQO1 in cancer therapy. *BMB Rep*, *48*(11), 609-617. https://doi.org/10.5483/bmbrep.2015.48.11.190

Okamoto, A., Demetrick, D. J., Spillare, E. A., Hagiwara, K., Hussain, S. P., Bennett, W. P., Forrester, K., Gerwin, B., Serrano, M., Beach, D. H., & et al. (1994). Mutations and altered expression of p16INK4 in human cancer. *Proc Natl Acad Sci U S A*, *91*(23), 11045-11049. https://doi.org/10.1073/pnas.91.23.11045

Oliver, T. G., Meylan, E., Chang, G. P., Xue, W., Burke, J. R., Humpton, T. J., Hubbard, D., Bhutkar, A., & Jacks, T. (2011). Caspase-2-mediated cleavage of Mdm2 creates a p53-induced positive feedback loop. *Mol Cell*, *43*(1), 57-71. https://doi.org/10.1016/j.molcel.2011.06.012

Olsson, M., Forsberg, J., & Zhivotovsky, B. (2015). Caspase-2: the reinvented enzyme. *Oncogene*, *34*(15), 1877-1882. https://doi.org/10.1038/onc.2014.139

Oltersdorf, T., Elmore, S. W., Shoemaker, A. R., Armstrong, R. C., Augeri, D. J., Belli, B. A., Bruncko, M., Deckwerth, T. L., Dinges, J., Hajduk, P. J., Joseph, M. K., Kitada, S., Korsmeyer, S. J., Kunzer, A. R., Letai, A., Li, C., Mitten, M. J., Nettesheim, D. G., Ng, S., . . . Rosenberg, S. H. (2005). An inhibitor of Bcl-2 family proteins induces regression of solid tumours. *Nature*, *435*(7042), 677-681. https://doi.org/10.1038/nature03579

Orrenius, S., Zhivotovsky, B., & Nicotera, P. (2003). Regulation of cell death: the calcium-apoptosis link. *Nat Rev Mol Cell Biol*, *4*(7), 552-565. https://doi.org/10.1038/nrm1150

Otto, H., Dreger, M., Bengtsson, L., & Hucho, F. (2001). Identification of tyrosine-phosphorylated proteins associated with the nuclear envelope. *Eur J Biochem*, *268*(2), 420-428. https://doi.org/10.1046/j.1432-1033.2001.01901.x

Overholtzer, M., Mailleux, A. A., Mouneimne, G., Normand, G., Schnitt, S. J., King, R. W., Cibas, E. S., & Brugge, J. S. (2007). A nonapoptotic cell death process, entosis, that occurs by cell-in-cell invasion. *Cell*, *131*(5), 966-979. https://doi.org/10.1016/j.cell.2007.10.040

Paroni, G., Henderson, C., Schneider, C., & Brancolini, C. (2002). Caspase-2 can trigger cytochrome C release and apoptosis from the nucleus. *J Biol Chem*, *277*(17), 15147-15161. https://doi.org/10.1074/jbc.M112338200

Parsons, M. J., McCormick, L., Janke, L., Howard, A., Bouchier-Hayes, L., & Green, D. R. (2013). Genetic deletion of caspase-2 accelerates MMTV/c-neu-driven mammary carcinogenesis in mice. *Cell Death Differ*, *20*(9), 1174-1182. https://doi.org/10.1038/cdd.2013.38

Passon, D. M., Lee, M., Fox, A. H., & Bond, C. S. (2011). Crystallization of a paraspeckle protein PSPC1-NONO heterodimer. *Acta Crystallogr Sect F Struct Biol Cryst Commun*, *67*(Pt 10), 1231-1234. https://doi.org/10.1107/S1744309111026212

Pavao, M., Huang, Y. H., Hafer, L. J., Moreland, R. B., & Traish, A. M. (2001). Immunodetection of nmt55/p54nrb isoforms in human breast cancer. *BMC Cancer*, *1*, 15. https://doi.org/10.1186/1471-2407-1-15

Pecar Fonovic, U., Jevnikar, Z., Rojnik, M., Doljak, B., Fonovic, M., Jamnik, P., & Kos, J. (2013). Profilin 1 as a target for cathepsin X activity in tumor cells. *PLoS One*, *8*(1), e53918. https://doi.org/10.1371/journal.pone.0053918

Peng, R., Dye, B. T., Perez, I., Barnard, D. C., Thompson, A. B., & Patton, J. G. (2002). PSF and p54nrb bind a conserved stem in U5 snRNA. *RNA*, *8*(10), 1334-1347. https://doi.org/10.1017/s1355838202022070

Perez, J. F., Chemello, M. E., Liprandi, F., Ruiz, M. C., & Michelangeli, F. (1998). Oncosis in MA104 cells is induced by rotavirus infection through an increase in intracellular Ca2+ concentration. *Virology*, *252*(1), 17-27. https://doi.org/10.1006/viro.1998.9433

Petrova, D. T., Asif, A. R., Armstrong, V. W., Dimova, I., Toshev, S., Yaramov, N., Oellerich, M., & Toncheva, D. (2008). Expression of chloride intracellular channel protein 1 (CLIC1) and tumor protein D52 (TPD52) as potential biomarkers for colorectal cancer. *Clin Biochem*, *41*(14-15), 1224-1236. https://doi.org/10.1016/j.clinbiochem.2008.07.012

Philchenkov, A., Zavelevich, M., Kroczak, T. J., & Los, M. (2004). Caspases and cancer: mechanisms of inactivation and new treatment modalities. *Exp Oncol*, *26*(2), 82-97. https://www.ncbi.nlm.nih.gov/pubmed/15273659

Pisani, G., & Baron, B. (2019). Nuclear paraspeckles function in mediating gene regulatory and apoptotic pathways. *Noncoding RNA Res*, *4*(4), 128-134. https://doi.org/10.1016/j.ncrna.2019.11.002

Pistritto, G., Trisciuoglio, D., Ceci, C., Garufi, A., & D'Orazi, G. (2016). Apoptosis as anticancer mechanism: function and dysfunction of its modulators and targeted therapeutic strategies. *Aging (Albany NY)*, *8*(4), 603-619. https://doi.org/10.18632/aging.100934

Plath, T., Detjen, K., Welzel, M., von Marschall, Z., Murphy, D., Schirner, M., Wiedenmann, B., & Rosewicz, S. (2000). A novel function for the tumor suppressor p16(INK4a): induction of

anoikis via upregulation of the alpha(5)beta(1) fibronectin receptor. *J Cell Biol*, *150*(6), 1467-1478. https://doi.org/10.1083/jcb.150.6.1467

Plati, J., Bucur, O., & Khosravi-Far, R. (2008). Dysregulation of apoptotic signaling in cancer: molecular mechanisms and therapeutic opportunities. *J Cell Biochem*, *104*(4), 1124-1149. https://doi.org/10.1002/jcb.21707

Polsky, D., Melzer, K., Hazan, C., Panageas, K. S., Busam, K., Drobnjak, M., Kamino, H., Spira, J. G., Kopf, A. W., Houghton, A., Cordon-Cardo, C., & Osman, I. (2002). HDM2 protein overexpression and prognosis in primary malignant melanoma. *J Natl Cancer Inst*, *94*(23), 1803-1806. https://doi.org/10.1093/jnci/94.23.1803

Pop, C., & Salvesen, G. S. (2009). Human caspases: activation, specificity, and regulation. *J Biol Chem*, *284*(33), 21777-21781. https://doi.org/10.1074/jbc.R800084200

Proteau, A., Blier, S., Albert, A. L., Lavoie, S. B., Traish, A. M., & Vincent, M. (2005). The multifunctional nuclear protein p54nrb is multiphosphorylated in mitosis and interacts with the mitotic regulator Pin1. *J Mol Biol*, *346*(4), 1163-1172. https://doi.org/10.1016/j.jmb.2004.12.034

Puccini, J., Dorstyn, L., & Kumar, S. (2013). Caspase-2 as a tumour suppressor. *Cell Death Differ*, *20*(9), 1133-1139. https://doi.org/10.1038/cdd.2013.87

Puccini, J., Shalini, S., Voss, A. K., Gatei, M., Wilson, C. H., Hiwase, D. K., Lavin, M. F., Dorstyn, L., & Kumar, S. (2013). Loss of caspase-2 augments lymphomagenesis and enhances genomic instability in Atm-deficient mice. *Proc Natl Acad Sci U S A*, *110*(49), 19920-19925. https://doi.org/10.1073/pnas.1311947110

Raghavendra, N. K., Shkriabai, N., Graham, R., Hess, S., Kvaratskhelia, M., & Wu, L. (2010). Identification of host proteins associated with HIV-1 preintegration complexes isolated from infected CD4+ cells. *Retrovirology*, *7*, 66. https://doi.org/10.1186/1742-4690-7-66

Read, S. H., Baliga, B. C., Ekert, P. G., Vaux, D. L., & Kumar, S. (2002). A novel Apaf-1-independent putative caspase-2 activation complex. *J Cell Biol*, *159*(5), 739-745. https://doi.org/10.1083/jcb.200209004

Ren, K., Lu, J., Porollo, A., & Du, C. (2012). Tumor-suppressing function of caspase-2 requires catalytic site Cys-320 and site Ser-139 in mice. *J Biol Chem*, *287*(18), 14792-14802. https://doi.org/10.1074/jbc.M112.347625

Ren, Z., Wang, Z., Hu, Z., Hu, X., Zhang, H., Wu, H., Hu, R., & Liu, H. (2014). Decreased expression of P54(nrb) /NonO correlates with collagen deposition and fibrosis in human aortic dissection. *Histopathology*, *65*(4), 570-580. https://doi.org/10.1111/his.12434

Rocco, J. W., & Sidransky, D. (2001). p16(MTS-1/CDKN2/INK4a) in cancer progression. *Exp Cell Res*, *264*(1), 42-55. https://doi.org/10.1006/excr.2000.5149

Rohn, J. L., & Noteborn, M. H. (2004). The viral death effector Apoptin reveals tumor-specific processes. *Apoptosis*, *9*(3), 315-322. https://doi.org/10.1023/b:appt.0000025808.48885.9c

Roos, W. P., & Kaina, B. (2006). DNA damage-induced cell death by apoptosis. *Trends Mol Med*, *12*(9), 440-450. https://doi.org/10.1016/j.molmed.2006.07.007

Roslan, N., Bieche, I., Bright, R. K., Lidereau, R., Chen, Y., & Byrne, J. A. (2014). TPD52 represents a survival factor in ERBB2-amplified breast cancer cells. *Mol Carcinog*, *53*(10), 807-819. https://doi.org/10.1002/mc.22038

Rumpler, G., Becker, B., Hafner, C., McClelland, M., Stolz, W., Landthaler, M., Schmitt, R., Bosserhoff, A., & Vogt, T. (2003). Identification of differentially expressed genes in models of melanoma progression by cDNA array analysis: SPARC, MIF and a novel cathepsin protease characterize aggressive phenotypes. *Exp Dermatol*, *12*(6), 761-771. https://doi.org/10.1111/j.0906-6705.2003.00082.x

Safi, S., Badshah, Y., Shabbir, M., Zahra, K., Khan, K., Dilshad, E., Afsar, T., Almajwal, A., Alruwaili, N. W., Al-Disi, D., Abulmeaty, M., & Razak, S. (2021). Predicting 3D Structure, Cross Talks, and Prognostic Significance of KLF9 in Cervical Cancer. *Front Oncol*, *11*, 797007. https://doi.org/10.3389/fonc.2021.797007

Sakahira, H., Enari, M., & Nagata, S. (1998). Cleavage of CAD inhibitor in CAD activation and DNA degradation during apoptosis. *Nature*, *391*(6662), 96-99. https://doi.org/10.1038/34214

Sakamaki, K., & Satou, Y. (2009). Caspases: evolutionary aspects of their functions in vertebrates. *J Fish Biol*, *74*(4), 727-753. https://doi.org/10.1111/j.1095-8649.2009.02184.x

Sasaki, H., Sheng, Y., Kotsuji, F., & Tsang, B. K. (2000). Down-regulation of X-linked inhibitor of apoptosis protein induces apoptosis in chemoresistant human ovarian cancer cells. *Cancer Res*, *60*(20), 5659-5666. https://www.ncbi.nlm.nih.gov/pubmed/11059757

Saunders, J. W., Jr. (1966). Death in embryonic systems. *Science*, *154*(3749), 604-612. https://doi.org/10.1126/science.154.3749.604

Sbodio, J. I., Hicks, S. W., Simon, D., & Machamer, C. E. (2006). GCP60 preferentially interacts with a caspase-generated golgin-160 fragment. *J Biol Chem*, *281*(38), 27924-27931. https://doi.org/10.1074/jbc.M603276200

Schiffner, S., Zimara, N., Schmid, R., & Bosserhoff, A. K. (2011). p54nrb is a new regulator of progression of malignant melanoma. *Carcinogenesis*, *32*(8), 1176-1182. https://doi.org/10.1093/carcin/bgr103

Schmidt, F., Hustoft, H. K., Strozynski, M., Dimmler, C., Rudel, T., & Thiede, B. (2007). Quantitative proteome analysis of cisplatin-induced apoptotic Jurkat T cells by stable isotope labeling with amino acids in cell culture, SDS-PAGE, and LC-MALDI-TOF/TOF MS. *Electrophoresis*, *28*(23), 4359-4368. https://doi.org/10.1002/elps.200700119

Scott, D. A., Hernandez-Garcia, A., Azamian, M. S., Jordan, V. K., Kim, B. J., Starkovich, M., Zhang, J., Wong, L. J., Darilek, S. A., Breman, A. M., Yang, Y., Lupski, J. R., Jiwani, A. K., Das, B., Lalani, S. R., Iglesias, A. D., Rosenfeld, J. A., & Xia, F. (2017). Congenital heart defects and left ventricular non-compaction in males with loss-of-function variants in NONO. *J Med Genet*, *54*(1), 47-53. https://doi.org/10.1136/jmedgenet-2016-104039

Scotto, L., Narayan, G., Nandula, S. V., Arias-Pulido, H., Subramaniyam, S., Schneider, A., Kaufmann, A. M., Wright, J. D., Pothuri, B., Mansukhani, M., & Murty, V. V. (2008). Identification of copy number gain and overexpressed genes on chromosome arm 20q by an integrative genomic approach in cervical cancer: potential role in progression. *Genes Chromosomes Cancer*, *47*(9), 755-765. https://doi.org/10.1002/gcc.20577

Sekulic, A., Haluska, P., Jr., Miller, A. J., Genebriera De Lamo, J., Ejadi, S., Pulido, J. S., Salomao, D. R., Thorland, E. C., Vile, R. G., Swanson, D. L., Pockaj, B. A., Laman, S. D., Pittelkow, M. R., Markovic, S. N., & Melanoma Study Group of Mayo Clinic Cancer, C. (2008). Malignant melanoma in the 21st century: the emerging molecular landscape. *Mayo Clin Proc*, *83*(7), 825-846. https://doi.org/10.4065/83.7.825

Shalini, S., Nikolic, A., Wilson, C. H., Puccini, J., Sladojevic, N., Finnie, J., Dorstyn, L., & Kumar, S. (2016). Caspase-2 deficiency accelerates chemically induced liver cancer in mice. *Cell Death Differ*, *23*(10), 1727-1736. https://doi.org/10.1038/cdd.2016.81

Shangary, S., & Wang, S. (2008). Targeting the MDM2-p53 interaction for cancer therapy. *Clin Cancer Res*, *14*(17), 5318-5324. https://doi.org/10.1158/1078-0432.CCR-07-5136

Shav-Tal, Y., & Zipori, D. (2002). PSF and p54(nrb)/NonO--multi-functional nuclear proteins. *FEBS Lett*, *531*(2), 109-114. https://doi.org/10.1016/s0014-5793(02)03447-6

Shehata, M., Bieche, I., Boutros, R., Weidenhofer, J., Fanayan, S., Spalding, L., Zeps, N., Byth, K., Bright, R. K., Lidereau, R., & Byrne, J. A. (2008). Nonredundant functions for tumor protein D52-like proteins support specific targeting of TPD52. *Clin Cancer Res*, *14*(16), 5050-5060. https://doi.org/10.1158/1078-0432.CCR-07-4994

Shi, J., Gao, W., & Shao, F. (2017). Pyroptosis: Gasdermin-Mediated Programmed Necrotic Cell Death. *Trends Biochem Sci*, *42*(4), 245-254. https://doi.org/10.1016/j.tibs.2016.10.004

Shi, M., Vivian, C. J., Lee, K. J., Ge, C., Morotomi-Yano, K., Manzl, C., Bock, F., Sato, S., Tomomori-Sato, C., Zhu, R., Haug, J. S., Swanson, S. K., Washburn, M. P., Chen, D. J., Chen, B. P., Villunger, A., Florens, L., & Du, C. (2009). DNA-PKcs-PIDDosome: a nuclear caspase-2-activating complex with role in G2/M checkpoint maintenance. *Cell*, *136*(3), 508-520. https://doi.org/10.1016/j.cell.2008.12.021

Shima, K., Nosho, K., Baba, Y., Cantor, M., Meyerhardt, J. A., Giovannucci, E. L., Fuchs, C. S., & Ogino, S. (2011). Prognostic significance of CDKN2A (p16) promoter methylation and loss of expression in 902 colorectal cancers: Cohort study and literature review. *Int J Cancer*, *128*(5), 1080-1094. https://doi.org/10.1002/ijc.25432

Shirley, S., & Micheau, O. (2013). Targeting c-FLIP in cancer. *Cancer Lett*, *332*(2), 141-150. https://doi.org/10.1016/j.canlet.2010.10.009

Sidi, S., Sanda, T., Kennedy, R. D., Hagen, A. T., Jette, C. A., Hoffmans, R., Pascual, J., Imamura, S., Kishi, S., Amatruda, J. F., Kanki, J. P., Green, D. R., D'Andrea, A. A., & Look, A. T. (2008). Chk1 suppresses a caspase-2 apoptotic response to DNA damage that bypasses p53, Bcl-2, and caspase-3. *Cell*, *133*(5), 864-877. https://doi.org/10.1016/j.cell.2008.03.037

Silva, J. C., Gorenstein, M. V., Li, G. Z., Vissers, J. P., & Geromanos, S. J. (2006). Absolute quantification of proteins by LCMSE: a virtue of parallel MS acquisition. *Mol Cell Proteomics*, *5*(1), 144-156. https://doi.org/10.1074/mcp.M500230-MCP200

Skulachev, V. P. (1999). Mitochondrial physiology and pathology; concepts of programmed death of organelles, cells and organisms. *Mol Aspects Med*, *20*(3), 139-184. https://doi.org/10.1016/s0098-2997(99)00008-4

Sladky, V. C., Knapp, K., Szabo, T. G., Braun, V. Z., Bongiovanni, L., van den Bos, H., Spierings, D. C., Westendorp, B., Curinha, A., Stojakovic, T., Scharnagl, H., Timelthaler, G., Tsuchia, K., Pinter, M., Semmler, G., Foijer, F., de Bruin, A., Reiberger, T., Rohr-Udilova, N., & Villunger, A. (2020). PIDDosome-induced p53-dependent ploidy restriction facilitates hepatocarcinogenesis. *EMBO Rep*, *21*(12), e50893. https://doi.org/10.15252/embr.202050893

Song, H. W., Bettegowda, A., Oliver, D., Yan, W., Phan, M. H., de Rooij, D. G., Corbett, M. A., & Wilkinson, M. F. (2015). shRNA off-target effects in vivo: impaired endogenous siRNA expression and spermatogenic defects. *PLoS One*, *10*(3), e0118549. https://doi.org/10.1371/journal.pone.0118549

Soufir, N., Avril, M. F., Chompret, A., Demenais, F., Bombled, J., Spatz, A., Stoppa-Lyonnet, D., Benard, J., & Bressac-de Paillerets, B. (1998). Prevalence of p16 and CDK4 germline mutations in 48 melanoma-prone families in France. The French Familial Melanoma Study Group. *Hum Mol Genet*, *7*(2), 209-216. https://doi.org/10.1093/hmg/7.2.209

Sperandio, S., de Belle, I., & Bredesen, D. E. (2000). An alternative, nonapoptotic form of programmed cell death. *Proc Natl Acad Sci U S A*, *97*(26), 14376-14381. https://doi.org/10.1073/pnas.97.26.14376

Straub, T., Grue, P., Uhse, A., Lisby, M., Knudsen, B. R., Tange, T. O., Westergaard, O., & Boege, F. (1998). The RNA-splicing factor PSF/p54 controls DNA-topoisomerase I activity by a direct interaction. *J Biol Chem*, *273*(41), 26261-26264. https://doi.org/10.1074/jbc.273.41.26261

Straub, T., Knudsen, B. R., & Boege, F. (2000). PSF/p54(nrb) stimulates "jumping" of DNA topoisomerase I between separate DNA helices. *Biochemistry*, *39*(25), 7552-7558. https://doi.org/10.1021/bi992898e

Sun, H., Han, L., Zhang, X., Hao, X., Zhou, X., Pan, R., Zhang, H., & He, Y. (2020). Case Report: Characterization of a Novel NONO Intronic Mutation in a Fetus With X-Linked Syndromic Mental Retardation-34. *Front Genet*, *11*, 593688. https://doi.org/10.3389/fgene.2020.593688

Sun, H., Liu, L., Lu, J., Qiu, S., Yang, C. Y., Yi, H., & Wang, S. (2010). Cyclopeptide Smac mimetics as antagonists of IAP proteins. *Bioorg Med Chem Lett*, *20*(10), 3043-3046. https://doi.org/10.1016/j.bmcl.2010.03.114

Talantov, D., Mazumder, A., Yu, J. X., Briggs, T., Jiang, Y., Backus, J., Atkins, D., & Wang, Y. (2005). Novel genes associated with malignant melanoma but not benign melanocytic lesions. *Clin Cancer Res*, *11*(20), 7234-7242. https://doi.org/10.1158/1078-0432.CCR-05-0683

Tartaglia, L. A., Ayres, T. M., Wong, G. H., & Goeddel, D. V. (1993). A novel domain within the 55 kd TNF receptor signals cell death. *Cell*, *74*(5), 845-853. https://doi.org/10.1016/0092-8674(93)90464-2

Tekedereli, I., Alpay, S. N., Akar, U., Yuca, E., Ayugo-Rodriguez, C., Han, H. D., Sood, A. K., Lopez-Berestein, G., & Ozpolat, B. (2013). Therapeutic Silencing of Bcl-2 by Systemically Administered siRNA Nanotherapeutics Inhibits Tumor Growth by Autophagy and Apoptosis and Enhances the Efficacy of Chemotherapy in Orthotopic Xenograft Models of ER (-) and ER (+) Breast Cancer. *Mol Ther Nucleic Acids*, *2*, e121. https://doi.org/10.1038/mtna.2013.45

Terry, M. R., Arya, R., Mukhopadhyay, A., Berrett, K. C., Clair, P. M., Witt, B., Salama, M. E., Bhutkar, A., & Oliver, T. G. (2015). Caspase-2 impacts lung tumorigenesis and chemotherapy response in vivo. *Cell Death Differ*, *22*(5), 719-730. https://doi.org/10.1038/cdd.2014.159

Thiede, B., Dimmler, C., Siejak, F., & Rudel, T. (2001). Predominant identification of RNA-binding proteins in Fas-induced apoptosis by proteome analysis. *J Biol Chem*, *276*(28), 26044-26050. https://doi.org/10.1074/jbc.M101062200

Thornberry, N. A., Rano, T. A., Peterson, E. P., Rasper, D. M., Timkey, T., Garcia-Calvo, M., Houtzager, V. M., Nordstrom, P. A., Roy, S., Vaillancourt, J. P., Chapman, K. T., & Nicholson, D. W. (1997). A combinatorial approach defines specificities of members of the caspase family and granzyme B. Functional relationships established for key

mediators of apoptosis. *J Biol Chem*, *272*(29), 17907-17911. https://doi.org/10.1074/jbc.272.29.17907

Tinel, A., Janssens, S., Lippens, S., Cuenin, S., Logette, E., Jaccard, B., Quadroni, M., & Tschopp, J. (2007). Autoproteolysis of PIDD marks the bifurcation between pro-death caspase-2 and pro-survival NF-kappaB pathway. *EMBO J*, *26*(1), 197-208. https://doi.org/10.1038/sj.emboj.7601473

Tinel, A., & Tschopp, J. (2004). The PIDDosome, a protein complex implicated in activation of caspase-2 in response to genotoxic stress. *Science*, *304*(5672), 843-846. https://doi.org/10.1126/science.1095432

Tiwari, M., Sharma, L. K., Vanegas, D., Callaway, D. A., Bai, Y., Lechleiter, J. D., & Herman, B. (2014). A nonapoptotic role for CASP2/caspase 2: modulation of autophagy. *Autophagy*, *10*(6), 1054-1070. https://doi.org/10.4161/auto.28528

Tsofack, S. P., Garand, C., Sereduk, C., Chow, D., Aziz, M., Guay, D., Yin, H. H., & Lebel, M. (2011). NONO and RALY proteins are required for YB-1 oxaliplatin induced resistance in colon adenocarcinoma cell lines. *Mol Cancer*, *10*, 145. https://doi.org/10.1186/1476-4598-10-145

Ummanni, R., Teller, S., Junker, H., Zimmermann, U., Venz, S., Scharf, C., Giebel, J., & Walther, R. (2008). Altered expression of tumor protein D52 regulates apoptosis and migration of prostate cancer cells. *FEBS J*, *275*(22), 5703-5713. https://doi.org/10.1111/j.1742-4658.2008.06697.x

Vakifahmetoglu-Norberg, H., & Zhivotovsky, B. (2010). The unpredictable caspase-2: what can it do? *Trends Cell Biol*, *20*(3), 150-159. https://doi.org/10.1016/j.tcb.2009.12.006

Van Opdenbosch, N., & Lamkanfi, M. (2019). Caspases in Cell Death, Inflammation, and Disease. *Immunity*, *50*(6), 1352-1364. https://doi.org/10.1016/j.immuni.2019.05.020

Vanden Berghe, T., Kaiser, W. J., Bertrand, M. J., & Vandenabeele, P. (2015). Molecular crosstalk between apoptosis, necroptosis, and survival signaling. *Mol Cell Oncol*, *2*(4), e975093. https://doi.org/10.4161/23723556.2014.975093

Vavougios, G. D., Solenov, E. I., Hatzoglou, C., Baturina, G. S., Katkova, L. E., Molyvdas, P. A., Gourgoulianis, K. I., & Zarogiannis, S. G. (2015). Computational genomic analysis of PARK7 interactome reveals high BBS1 gene expression as a prognostic factor favoring survival in malignant pleural mesothelioma. *Am J Physiol Lung Cell Mol Physiol*, *309*(7), L677-686. https://doi.org/10.1152/ajplung.00051.2015

Verhoven, B., Schlegel, R. A., & Williamson, P. (1995). Mechanisms of phosphatidylserine exposure, a phagocyte recognition signal, on apoptotic T lymphocytes. *J Exp Med*, *182*(5), 1597-1601. https://doi.org/10.1084/jem.182.5.1597

Vigneswara, V., & Ahmed, Z. (2020). The Role of Caspase-2 in Regulating Cell Fate. *Cells*, *9*(5). https://doi.org/10.3390/cells9051259

Vizin, T., Christensen, I. J., Nielsen, H. J., & Kos, J. (2012). Cathepsin X in serum from patients with colorectal cancer: relation to prognosis. *Radiol Oncol*, *46*(3), 207-212. https://doi.org/10.2478/v10019-012-0040-0

Vousden, K. H., & Lane, D. P. (2007). p53 in health and disease. *Nat Rev Mol Cell Biol*, *8*(4), 275-283. https://doi.org/10.1038/nrm2147

Walker, N. I., Harmon, B. V., Gobe, G. C., & Kerr, J. F. (1988). Patterns of cell death. *Methods Achiev Exp Pathol*, *13*, 18-54. https://www.ncbi.nlm.nih.gov/pubmed/3045494

Wang, J., Chen, L., Li, Y., & Guan, X. Y. (2011). Overexpression of cathepsin Z contributes to tumor metastasis by inducing epithelial-mesenchymal transition in hepatocellular carcinoma. *PLoS One*, *6*(9), e24967. https://doi.org/10.1371/journal.pone.0024967

Wang, L., Miura, M., Bergeron, L., Zhu, H., & Yuan, J. (1994). Ich-1, an Ice/ced-3-related gene, encodes both positive and negative regulators of programmed cell death. *Cell*, *78*(5), 739-750. https://doi.org/10.1016/s0092-8674(94)90422-7

Wang, Z., Li, Y., Fan, L., Zhao, Q., Tan, B., Liu, R., & Li, F. (2020). Silencing of TPD52 inhibits proliferation, migration, invasion but induces apoptosis of pancreatic cancer cells by deactivating Akt pathway. *Neoplasma*, *67*(2), 277-285. https://doi.org/10.4149/neo_2019_190404N295

Wegner, M., Diehl, V., Bittl, V., de Bruyn, R., Wiechmann, S., Matthess, Y., Hebel, M., Hayes, M. G., Schaubeck, S., Benner, C., Heinz, S., Bremm, A., Dikic, I., Ernst, A., & Kaulich, M. (2019). Circular synthesized CRISPR/Cas gRNAs for functional interrogations in the coding and noncoding genome. *Elife*, *8*. https://doi.org/10.7554/eLife.42549

Wei, M. C., Zong, W. X., Cheng, E. H., Lindsten, T., Panoutsakopoulou, V., Ross, A. J., Roth, K. A., MacGregor, G. R., Thompson, C. B., & Korsmeyer, S. J. (2001). Proapoptotic BAX and BAK: a requisite gateway to mitochondrial dysfunction and death. *Science*, *292*(5517), 727-730. https://doi.org/10.1126/science.1059108

Wejda, M., Impens, F., Takahashi, N., Van Damme, P., Gevaert, K., & Vandenabeele, P. (2012). Degradomics reveals that cleavage specificity profiles of caspase-2 and effector caspases are alike. *J Biol Chem*, *287*(41), 33983-33995. https://doi.org/10.1074/jbc.M112.384552

Wisniewski, J. R., Zougman, A., Nagaraj, N., & Mann, M. (2009). Universal sample preparation method for proteome analysis. *Nat Methods*, *6*(5), 359-362. https://doi.org/10.1038/nmeth.1322

Wolfel, T., Hauer, M., Schneider, J., Serrano, M., Wolfel, C., Klehmann-Hieb, E., De Plaen, E., Hankeln, T., Meyer zum Buschenfelde, K. H., & Beach, D. (1995). A p16INK4a-insensitive CDK4 mutant targeted by cytolytic T lymphocytes in a human melanoma. *Science*, *269*(5228), 1281-1284. https://doi.org/10.1126/science.7652577

Wong, R. S. (2011). Apoptosis in cancer: from pathogenesis to treatment. *J Exp Clin Cancer Res*, *30*, 87. https://doi.org/10.1186/1756-9966-30-87

Wu, Y., Huang, J., Xu, H., & Gong, Z. (2018). Over-expression of miR-15a-3p enhances the radiosensitivity of cervical cancer by targeting tumor protein D52. *Biomed Pharmacother*, *105*, 1325-1334. https://doi.org/10.1016/j.biopha.2018.06.033

Yadav, S. P., Hao, H., Yang, H. J., Kautzmann, M. A., Brooks, M., Nellissery, J., Klocke, B., Seifert, M., & Swaroop, A. (2014). The transcription-splicing protein NonO/p54nrb and three NonO-interacting proteins bind to distal enhancer region and augment rhodopsin expression. *Hum Mol Genet*, *23*(8), 2132-2144. https://doi.org/10.1093/hmg/ddt609

Yan, G., Elbadawi, M., & Efferth, T. (2020). Multiple cell death modalities and their key features (Review). *World Acad Sci J*, *2*(2), 39-48. https://doi.org/10.3892/wasj.2020.40

Yang, Y. S., Hanke, J. H., Carayannopoulos, L., Craft, C. M., Capra, J. D., & Tucker, P. W. (1993). NonO, a non-POU-domain-containing, octamer-binding protein, is the mammalian

homolog of Drosophila nonAdiss. *Mol Cell Biol*, *13*(9), 5593-5603. https://doi.org/10.1128/mcb.13.9.5593-5603.1993

Yang, Y. S., Yang, M. C., Tucker, P. W., & Capra, J. D. (1997). NonO enhances the association of many DNA-binding proteins to their targets. *Nucleic Acids Res*, *25*(12), 2284-2292. https://doi.org/10.1093/nar/25.12.2284

Zha, J., Weiler, S., Oh, K. J., Wei, M. C., & Korsmeyer, S. J. (2000). Posttranslational N-myristoylation of BID as a molecular switch for targeting mitochondria and apoptosis. *Science*, *290*(5497), 1761-1765. https://doi.org/10.1126/science.290.5497.1761

Zhang, K., Chen, D., Ma, K., Wu, X., Hao, H., & Jiang, S. (2018). NAD(P)H:Quinone Oxidoreductase 1 (NQO1) as a Therapeutic and Diagnostic Target in Cancer. *J Med Chem*, *61*(16), 6983-7003. https://doi.org/10.1021/acs.jmedchem.8b00124

Zhang, Q., Bykov, V. J. N., Wiman, K. G., & Zawacka-Pankau, J. (2018). APR-246 reactivates mutant p53 by targeting cysteines 124 and 277. *Cell Death Dis*, *9*(5), 439. https://doi.org/10.1038/s41419-018-0463-7

Zhang, Y., Padalecki, S. S., Chaudhuri, A. R., De Waal, E., Goins, B. A., Grubbs, B., Ikeno, Y., Richardson, A., Mundy, G. R., & Herman, B. (2007). Caspase-2 deficiency enhances aging-related traits in mice. *Mech Ageing Dev*, *128*(2), 213-221. https://doi.org/10.1016/j.mad.2006.11.030

Zhang, Z., & Carmichael, G. G. (2001). The fate of dsRNA in the nucleus: a p54(nrb)-containing complex mediates the nuclear retention of promiscuously A-to-I edited RNAs. *Cell*, *106*(4), 465-475. https://doi.org/10.1016/s0092-8674(01)00466-4

Zhivotovsky, B., Samali, A., Gahm, A., & Orrenius, S. (1999). Caspases: their intracellular localization and translocation during apoptosis. *Cell Death Differ*, *6*(7), 644-651. https://doi.org/10.1038/sj.cdd.4400536

Zhou, H. Z., Zeng, H. Q., Yuan, D., Ren, J. H., Cheng, S. T., Yu, H. B., Ren, F., Wang, Q., Qin, Y. P., Huang, A. L., & Chen, J. (2019). NQO1 potentiates apoptosis evasion and upregulates XIAP via inhibiting proteasome-mediated degradation SIRT6 in hepatocellular carcinoma. *Cell Commun Signal*, *17*(1), 168. https://doi.org/10.1186/s12964-019-0491-7

Zhu, Z., Zhao, X., Zhao, L., Yang, H., Liu, L., Li, J., Wu, J., Yang, F., Huang, G., & Liu, J. (2016). p54(nrb)/NONO regulates lipid metabolism and breast cancer growth through SREBP-1A. *Oncogene*, *35*(11), 1399-1410. https://doi.org/10.1038/onc.2015.197

Zhuo, J., Tan, E. H., Yan, B., Tochhawng, L., Jayapal, M., Koh, S., Tay, H. K., Maciver, S. K., Hooi, S. C., Salto-Tellez, M., Kumar, A. P., Goh, Y. C., Lim, Y. C., & Yap, C. T. (2012). Gelsolin induces colorectal tumor cell invasion via modulation of the urokinase-type plasminogen activator cascade. *PLoS One*, *7*(8), e43594. https://doi.org/10.1371/journal.pone.0043594

Zou, H., Li, Y., Liu, X., & Wang, X. (1999). An APAF-1.cytochrome c multimeric complex is a functional apoptosome that activates procaspase-9. *J Biol Chem*, *274*(17), 11549-11556. https://doi.org/10.1074/jbc.274.17.11549

Zuo, L., Weger, J., Yang, Q., Goldstein, A. M., Tucker, M. A., Walker, G. J., Hayward, N., & Dracopoli, N. C. (1996). Germline mutations in the p16INK4a binding domain of CDK4 in familial melanoma. *Nat Genet*, *12*(1), 97-99. https://doi.org/10.1038/ng0196-97

7 Appendix

7.1 Supplemental results

Table 15. List of downregulated tumorigenic proteins
LC/MS analysis data derived from analysis of HeLa shRNA-control versus shRNA-p54nrb cells (n=3). Significantly (p<0.01, Log2 ratio <-0.5) downregulated proteins (from Figure 17 B). Their functions in tumor/apoptosis regulatory processes are indicated.

Protein	Alias name	Function
6-phosphofructo-2-kinase/fructose-2,6-biphosphatase 2	PFKFB2	Metabolism
Aldo-keto reductase family 1 member C3	AKR1C3	Metabolism, growth
Aldo-keto reductase family 1 member C4, 3α-hydroxysteroid dehydrogenase	AKR1C4, 3α-HSD	Metabolism
Cathepsin-Z, -X, -P	CTSZ, CTSX	Adhesion
Clusterin	CLU	Golgi chaperone, adhesion, anti-apoptotic
Enolase 2	ENO2	Metabolism, neuronal cell survival
Epoxide hydrolase 1	EPHX1	Metabolism, detoxification
Gelsolin	GLN	Cell structure
Glutamate-cysteine ligase catalytic subunit	GCLC	Metabolism
Glutathione S-transferase Mu 2	GSTM2	Metabolism, detoxification
Glutathione-disulfide reductase	GSR	Metabolism, oxidative stress
HECT and RLD domain containing E3 Ubiquitin Protein Ligase 2	HERC2	Growth, DNA repair, centrosome assembly
Laminin subunit alpha-3	LAMA3	Basement membrane structure, migration
NAD(P)H dehydrogenase (quinone)1	NQO1	Metabolism, detoxification
NDRG1	NDRG1	Growth, DNA repair, ageing
Thioredoxin reductase 1	TXNRD1	Metabolism, oxidative stress
Tumor protein D52	TPD52	Vesicle Trafficking, exocytosis, migration

Table 16. List of upregulated tumorigenic proteins
LC/MS analysis data derived from analysis of HeLa shRNA-control versus shRNA-p54nrb cells (n=3). Significantly ($p<0.01$, Log2 ratio >0.5) upregulated proteins (from Figure 17 C). Their functions in tumor/apoptosis regulatory processes are indicated.

Protein	Alias name	Function
Arginase 1	ARG1	Metabolism
BRCA2 and CDKN1A-interacting protein	BCCIP	Cell cycle, DNA repair
Catenin beta-1	CTNNB1	Adhesion, transcription
CD44 antigen	CD44	Adhesion, migration
Cyclin-dependent kinase inhibitor 2A	CDKN2A, p16-INK4A	Cell cycle, tumor suppressor
Cyclin-dependent protein kinase 6	CDK6	Cell cycle, migration
Desmocollin-3	DSC3	Adhesion, migration
Filaggrin	FLG	Structure
Galectin-7	LGALS7	Adhesion, apoptotic
Glutathione S-transferase pi1	GSTP1	Metabolism, detoxification
Integrin subunit beta 4	ITB4	Adhesion
Kallikrein-14	KLK14	Metabolism
Keratin 5	KRT5	Cytoskeleton
Keratin type II cytoskeletal 78	KRT78	Cytoskeleton
Mitochondrial fission 1 protein	FIS1	Mitochondrial structure, Cytochrome-C release
Nicotinamide N-methyltransferase	NNMT	Metabolism
PDZ and LIM domain protein 5	PDLIM5	Cytoskeleton
Ras-related protein Rap-2b	RAP2B	Cytoskeleton, migration
S100 calcium binding protein A14	S100A14	Tumor suppressor
Serpin B3	SERPINB3	Proliferation
SH3 domain containing GRB2 like 2, Endophilin-A1	SH3GL2	Transcription, membrane structure
Zinc finger protein Rlf	RLF	Transcription

Table 17. List of exclusively downregulated proteins
LC/MS analysis data derived from analysis of HeLa shRNA-control versus shRNA-p54nrb cells (n=3). Significantly ($p<0.01$, Log2 ratio <-0.5) and exclusively downregulated proteins (15). Their attributed functions are indicated.

Protein	Alias name	Function
60S ribosomal protein L36a	RPL36A	Translation
Ankyrin repeat domain-containing protein 35	ANKRD35	Unknown
Creatine kinase S-type, mitochondrial	CKMT2	Metabolism
Glutamine-fructose-6-phosphate aminotransferase (isomerizing)	GLMS	Metabolism
Golgin subfamily A member 3	GOLGA3	Nuclear transport, Golgi apparatus localization
GRAM domain-containing protein 2B	GRAMD2B	Unknown
Histone H1t	HIST1H1T	DNA packing
Histone H3.3	H3-3A	DNA packing
Laminin subunit alpha-3	LAMA3	Basement membrane structure, migration
Putative 40S ribosomal protein S26-like	RPS26	Translation
Putative ubiquitin-conjugating enzyme E2 N-like	UBE2NL	Unknown
RNA-binding Raly-like protein	RALYL	Unknown
Sodium/potassium-transporting ATPase subunit alpha-4	ATP1A4	Metabolism
Tubulin alpha-3C chain	TUBA3C	Cytoskeleton

Table 18. List of exclusively upregulated proteins
LC/MS analysis data derived from analysis of HeLa shRNA-control vs shRNA-p54nrb cells (n=3). Significantly ($p<0.01$, Log2 ratio >0.5) and exclusively upregulated proteins (10). Their attributed functions are indicated.

Protein	Alias name	Function
Alpha-1,3/1,6-mannosyltransferase	ALG2	Metabolism
Band 4.1-like protein	EPB41L1	Cytoskeleton
Catenin beta-1	CTNNB1	Adhesion, transcription
Cationic amino acid transporter 2	SLC7A2	Metabolism
Keratin, type I cytoskeletal	K's	Growth, migration, cell integrity
Keratin, type II cytoskeletal	CK's	Growth, migration, cell integrity
L-lactate dehydrogenase C chain	LDHC	Sperm motility
Poly(rC)-binding protein	PCBP2	Translation
Putative uncharacterized protein	Unknown	Unkown
SH3 domain containing GRB2 like 2, Endophilin-A1	SH3GL2	Transcription, membrane structure

7.2 Publications

7.2.1 Publications derived from the dissertation's project

Eichler, M., Distler, U., Nasrullah, U., Krishnan, A., Kaulich, M., Husnjak, K., Eberhardt, W., Rajalingam, K., Tenzer, S., Pfeilschifter, J., & Imre, G. (2022). The caspase-2 substrate p54nrb exhibits a multifaceted role in tumor cell death susceptibility via gene regulatory functions. Cell Death Dis, 13(4), 386. https://doi.org/10.1038/s41419-022-04829-2

The publication above was written based on the project of this dissertation, hence contains the results of the present thesis. Therefore, figures and/or text passages of the present thesis might be found similarly in this publication.

7.2.2 Other publications

Eichler, M., Aksi, E., Pfeilschifter, J., & Imre, G. (2021). Application of pseudotyped virus particles to monitor Ebola virus and SARS-CoV-2 viral entry in human cell lines. STAR Protoc, 2(4), 100818. https://doi.org/10.1016/j.xpro.2021.100818

Imre, G., Krahling, V., **Eichler, M.**, Trautmann, S., Ferreiros, N., Aman, M. J., Kashanchi, F., Rajalingam, K., Pohlmann, S., Becker, S., Meyer Zu Heringdorf, D., & Pfeilschifter, J. (2021). The sphingosine kinase 1 activator, K6PC-5, attenuates Ebola virus infection. iScience, 24(4), 102266. https://doi.org/10.1016/j.isci.2021.102266

7.3 Declaration about collaborative work

Except where stated otherwise by reference or acknowledgment, the work presented was generated by myself under the supervision of my advisors during my doctoral studies. All contributions from collaborators are explicitly referenced in the thesis.